Stable isotopic study of groundwater arsenic contaminated plume at Shepley's Hill Landfill

Author: Shakib Ahmed

Boston College

The Graduate School of Arts and Sciences

Department of Earth and Environmental Sciences

STABLE ISOTOPIC STUDY OF GROUNDWATER ARSENIC CONTAMINATED PLUME AT SHEPLEY'S HILL LANDFILL

A thesis

By

SHAKIB AHMED

Submitted in partial fulfillment of the requirements

for the degree of

Master of Science

May, 2014

STABLE ISOTOPIC STUDY OF GROUNDWATER ARSENIC CONTAMINATED PLUME AT SHEPLEY'S HILL LANDFILL

A thesis by: SHAKIB AHMED

Thesis supervisor: Dr. Rudolph Hon

Abstract

In the northeast United States, arsenic (As) contamination in groundwater is frequently associated with historical landfill leachate plumes. Based on the history of Shepley's Hill Landfill (SHL) in Devens, MA, solid waste disposal activities spanned nearly a century of landfilling with little or no documentation of when or what waste material was disposed. Past geochemical investigations proved the presence of high levels of As in groundwaters within and around the SHL region. A total of 114 samples were collected from the SHL region and analyzed for their hydrogeochemistry and isotopic signature. Since the isotopic ratios of δD and $\delta^{18}O$ can potentially be influenced by the mobilization process of As, this study attempts to identify any correlations between the stable isotopic ratios and the hydrogeochemistry of SHL waters. The results of the groundwater hydrogeochemical analysis show multiple relationships between metal concentrations and As concentration levels, typical of groundwater undergoing redox reactions. The result of the stable isotope analysis show significant fractionation of stable isotope ratios away from the meteoric water line. However, the role of strong redox gradients and various redox ladder reactions involving water did not produce a significant correlation with the isotopic fractionations present within different zones of the landfill. In most cases, the fractionations stand independent of the increase/decrease in As concentration and can be attributed to either unrelated chemical reactions within groundwater or evaporation.

Table of Contents

Index of Figures

Index of Tables

Abbreviations

D – Deuterium (^2H)

δD – Can be written as δ^2H

δ^2H – Can be written as δD (deuterium)

µL – micro-litre

µg/L – micrograms per litre

As – Abbreviation for arsenic.

ACOE – Army Corps of Engineers

As (III) – Arsenious Acid: Arsenic(III)

As (V) – Insoluble arsenic: Arsenic(V)

ATC – Anion Trap Column

BC – Boston College

DEP – Department of Environmental Protection

EPA – Environmental Protection Agency

Ga – (gigaannus) unit of time equal to one billion years

gpd – gallons per day

IAEA – International Atomic Energy Agency

IC – Ion Chromatography

ICP-OES – Inductively Coupled Plasma Optical Emission Spectrometry

IRMS – Isotope Ratio Mass Spectrometer

ka – (kiloannus) unit of time equal to one thousand years

Ma – (megaannus) unit of time equal to one million years

mg/kg – milligrams per kilogram

ml – milliliter(s)

MWL – Meteoric Water Line

NaOH – Sodium hydroxide

oz – ounce

PP – push point

ppb – parts per billion

ppm – parts per million

RF – radiofrequency

SIL – System Injection Loop

SHL – Shepley's Hill Landfill

SPATIAL – Spatio-Temporal Isotope Analytics Lab

VSMOW – Vienna Standard Mean Ocean Water

WHO – World Health Organization

WMO – World Meteorological Organization

CRDS – Cavity Ring-Down Spectrometer

1. Introduction

Arsenic is a naturally present eluent occurring in soil and bedrock in various parts of the United States and around the world. It is present in more than 200 different mineral species, but is most commonly found in arsenopyrite (FeAsS) (Ryker, 2001; Ayotte et al, 2001). Initial introduction of arsenic to the surface of the earth is through volcanic action and low-temperature volatilization. Contaminated groundwaters can chemically interact with these sources of arsenic and mobilize (dissolve) the arsenic into groundwater. In areas where the soil and bedrock contain traces of arsenic, chemically altering the medium can potentially contaminate groundwater with large concentrations of arsenic. Reducing environment tends to accelerate the mobilization of arsenic into groundwater (Moore, Ficklin, & Johns, 1988; Korte & Fernando, 1991; Stuben, Berner, Chandrasekharam, & Karmakar, 2003; Gulens, Champ, & Jackson, 1973), occasionally affecting water used as municipal drinking water. When arsenic minerals in rocks such as arsenopyrite come into contact with reducing groundwater, arsenic is released into the groundwater as arsenious acid (As(III)) or As(V).

1.1 Health Hazards of Arsenic Contamination

Risk assessments done on arsenic-contaminated drinking water suggests a link between continued exposure to arsenic and negative health effects. Ingested arsenic can cause acute effects such as nausea, vomiting, and nervous system alterations (Frank, 1976; Beckett, Moore, Keogh, & Bleecker, 1986; Bolla-Wilson & Bleecker, 1987; Morton & Caron, 1989; Rodriguez, Jiménez-Capdeville, & Giordano, 2003; Ratnaike, 2003) and chronic effects such as skin thickening and discoloration, corn-like growth, and various forms of skin, bladder, and prostate cancer (Smith, et al., 1992; Hopenhayn-Rich, et al., 1996; Hsueh, Cheng, Wu, Yu, Kuo, & Chen, 1995).

Groundwater in regions around West Bengal, India and Bangladesh shows dangerous levels of arsenic concentrations and will be discussed further below.

1.2 Environmental Hazards of Arsenic Contamination

Both inorganic and organic forms of arsenic can cause adverse effects in animals. Laboratory studies of female mice exposed to drinking water containing a dose of 500 ug/L of arsenic over a course of 2 years were associated with increased incidence of tumors in their lungs, livers, gastrointestinal tracts, and skin. Exposure also affected methylation and repair of DNA, and induced cell proliferation.

Aquatic and terrestrial biota show wide range of sensitivities to arsenic species. Arsenic compounds cause acute and chronic effects in individuals, populations and communities at concentrations ranging from micrograms to milligrams per liter. The effects include behavioral consequences as well as retardation of growth, photosynthesis, and reproduction.

Anthropogenic and geological sources of arsenic and human impact are summarized in the 2nd Edition of Arsenic and Arsenic Compounds by the World Health Organization (WHO) under Environmental Health Criteria 224 (EHC 224). In 1973, EHC set out to assess information on the relationship between arsenic exposure to human health and environment, in order to provide exposure level standards. These findings have created a need to re-evaluate the arsenic standards for drinking water. For public water systems, EPA has set the arsenic standard for drinking water at 10 parts per billion (ppb) to protect consumers from chronic exposure to arsenic. This standard went into effect on January 23, 2006, lowering the safe level from the original standard of 50 ppb (50 µg/L). This re-evaluation of standards in recent years underscores the potential threat that arsenic can pose to humans through groundwater systems.

The positive detection of arsenic poses two questions: what is the main source of arsenic in that particular region, and how is it mobilized? In certain areas, where multiple arsenic sources are identified, the exact origin of arsenic contamination can be difficult to detect using standard geochemical analyses of groundwater. This project attempts to use stable isotopes alongside standard geochemical analyses to better identify the source of arsenic.

1.3 Global Arsenic Contamination

The immense scale of human tragedy around areas like West Bengal, India, and Bangladesh is slowly attracting the attention of scientists from around the world (Bagla and Kaiser, 1996). *Figure 1*shows the distribution of documented cases of As contamination in the environment and groundwater (Apello, 2008; Smedley and Kinniburgh, 2002). Some areas of detected As contamination are near regions of mineralization and associated mining activity (Appelo, 2006). Some examples include parts of the USA and Canada, northern Burkina Faso, the Lavrion area of Greece, Chattisgarh in India, the Zimapán region of Mexico, Ron Phibun District of Thailand, and parts of south-west England (Thornton, 1994; Komnitsas et al., 1995; Williams et al., 1996; Chakraborti et al., 1999; Pandey et al., 2002; Smedley et al., 2007). Other areas of high As concentrations are not associated with obvious mineralization or geothermal activity. Parts of Argentina, Chile, Mexico, USA, Hungary, Romania, Bangladesh, India, Nepal, Burma, Cambodia, Pakistan, China and Vietnam have recently been discovered to have high concentrations of As through identification of health problems and randomized groundwater testing programs (Appelo, 2006). Most of the area shows high As concentrations due to high pH conditions or under strong reducing conditions (Appelo, 2006).

Figure 1 – Documented cases of As contamination in the environment and groundwater globally.

1.4 Arsenic in New England

The most common source of arsenic found in NE groundwater is from arsenic-bearing sulfide minerals and trace amounts of arsenic in other mineral constituents. Ayotte et al. (1999) documented arsenic behavior in groundwater and it is related to aquifer type, land use, and bedrock lithogeochemistry in New England. Despite the existence of naturally occurring arsenic in groundwater systems throughout the northeastern U.S. (Ryker, 2001; Ayotte et al, 1999), elevated arsenic levels are frequently associated with historical landfill leachate plumes (Delemos, Bostick, Renshaw, Sturup, & Feng, 2006) (Keimowitz, et al., 2005). A large number of cases involving landfill arsenic contaminations have been documented in regions around New Hampshire (Peters et al., 1999; Peters & Blum, 2003; Delemos et al, 2006). These arsenic levels are shown to exceed the arsenic concentration levels set by the DEP of 20mg/kg (Doherty et al, 2001, 2002, 2003; Hon et al. 2001a, 2001b, 2001c, 2002a,

2002b). Due to increase demand for fresh water, there has been an increase in water extraction from deeper wells, elevating contact with reduced groundwater and increased contamination. Deeper groundwater chemistry of West Bengal shows similar patterns where elevated As in the groundwater is possibly related to Fe(III) reduction (Mukherjee and Fryar, 2008).

1.5 Arsenic in Massachusetts

There is evidence of elevated levels of As in central Massachusetts soils that are occurring naturally in subsurface materials. Groundwater composition analysis shows that some of these locations have concentrations of As above 1,000 µg/L (US-EPA, 2007), which is much higher than EPA standard. If untreated groundwater is distributed from these locations, the population can potentially be exposed to the contamination. Recent observations of As contaminations around Massachusetts show that the primary contributor of As is landfill leachate plumes (*Figure 2*) (Hon et al., 2003a and 2003b, Davidson, 2003, and Tedder et al., 2004).

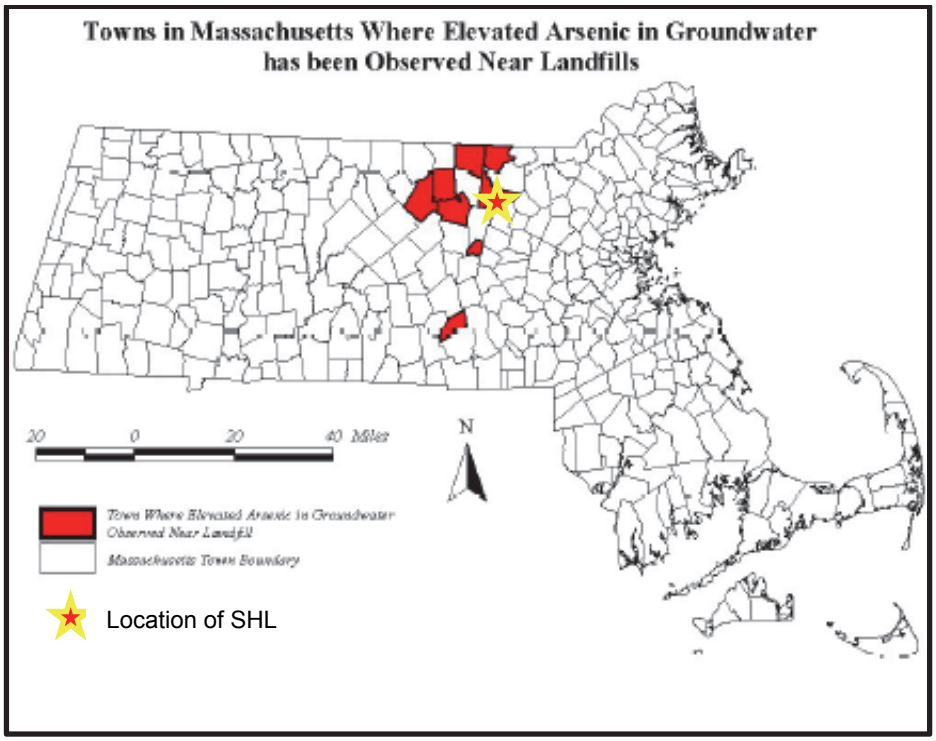

Figure 2 – Towns that observed an increase in arsenic concentration in their groundwater or municipal water supply (Mayo, 2006).

2. Background

2.1 Study Site

2.1.1 Shepley's Hill Landfill

Shepley's Hill Landfill (SHL) is a man-made, capped, and contoured landfill situated on marshland in Devens, a town in north-central Massachusetts. The landfill is located 1000 m southwest of downtown Ayer; northeast of a closed military base.

SHL has been active since early 1917 and ceased operation around 1992. Disposal of waste may have started in the late 1800s. During the last few years of landfill use, SHL received more than 6,500 tons of household waste and construction debris per year (HLA, 2000). After subsurface investigations, researchers have not found evidence of hazardous waste deposits after November 19, 1980 (HLA, 2000). There are historic records and evidence of the disposal of asbestos and building foundations within the landfill. There are also records of a landfill incinerator that shows deposited incinerator ash into the landfill. The incinerator itself was later dumped into the landfill.

Field studies done in November 1989 by the EPA indicated a presence of high concentrations of arsenic in the groundwater beneath and down-gradient (north) of the landfill. The landfill that is submerged beneath the groundwater table shows higher arsenic concentrations. So far, standard geochemical analyses of the groundwater (U.S. Army Environmental Center, 1995; Xie, 2013) (EPA, 1989) have not found evidence about the source and mobilization of these arsenic concentrations.

Among potential sources of arsenic are the waste deposits within the landfill, the peat layer deposited below the landfill, the underlying unconsolidated glacial lake sequences, and/or the bedrock. If any of these sources are the main cause of the

contamination, the role of strong redox gradients and various redox ladder reactions involving water are likely to create distinct isotopic signatures. These processes and their distinct isotopic signatures will be further discussed below.

2.1.2 Surficial Geology

Shepley's Hill Landfill is situated in the southern extend of the Nashua River watershed (*Figure 3*). The surficial geology formed after glacial retreat around 14-23 Ka (Skehan, 2001). The overburden primarily consists of Wisconsinan aged units of Glacial Lake Nashua deltaic deposits and glacial melt-water stream deposits (Harding ESE, 2002). The glacial lake deposits are mainly sand or gravelly sand with coarser materials. Subsurface studies show the fluvial materials range from sorted sands and gravels to poorly graded sands (Harding ESE, 2002).

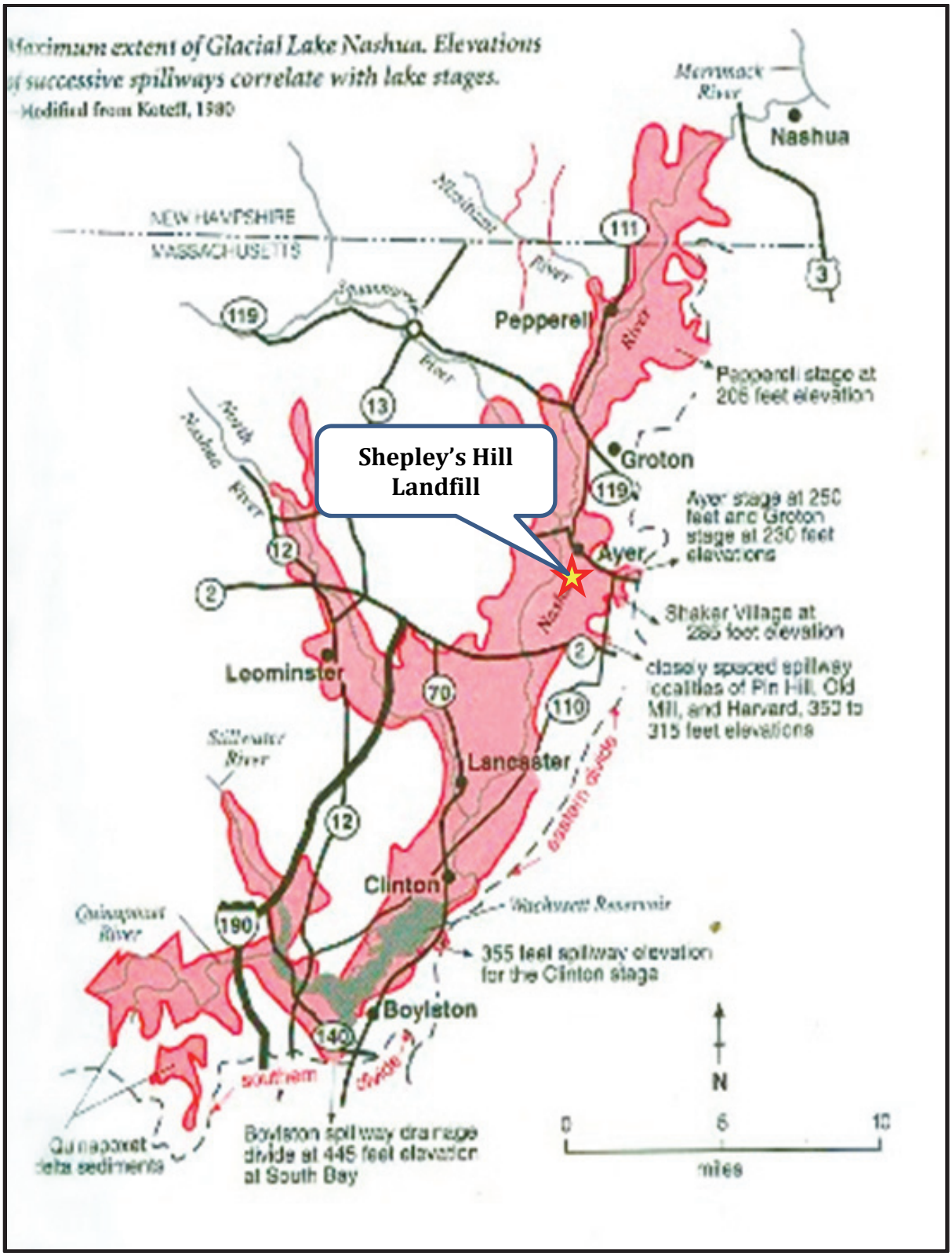

Figure 3 – Northeastern map of Glacial Lake Nashua.

2.1.3 Bedrock Geology

The fractured bedrock beneath the landfill is located within the Merrimack Belt, dominantly carrying calcareous schists, schistose rocks, and sulfidic phyllites (Robinson and Goldsmith, 1991). SHL is located above the Chelmsford Granite (Devonian) and Ayer Granodiorite (Devonian) (Kopera, 2008) (*Figure 4*). The bedrock is highly fractured with one major fault that is known to transport groundwater at greater depths. The fault zone which extends from the northwest to southeast is highlighted as a yellow line in *Figure 4*. The bedrock is exposed as small sections of outcrops along the western side of SHL which, when drilled properly, can give access to groundwater traveling through the fault.

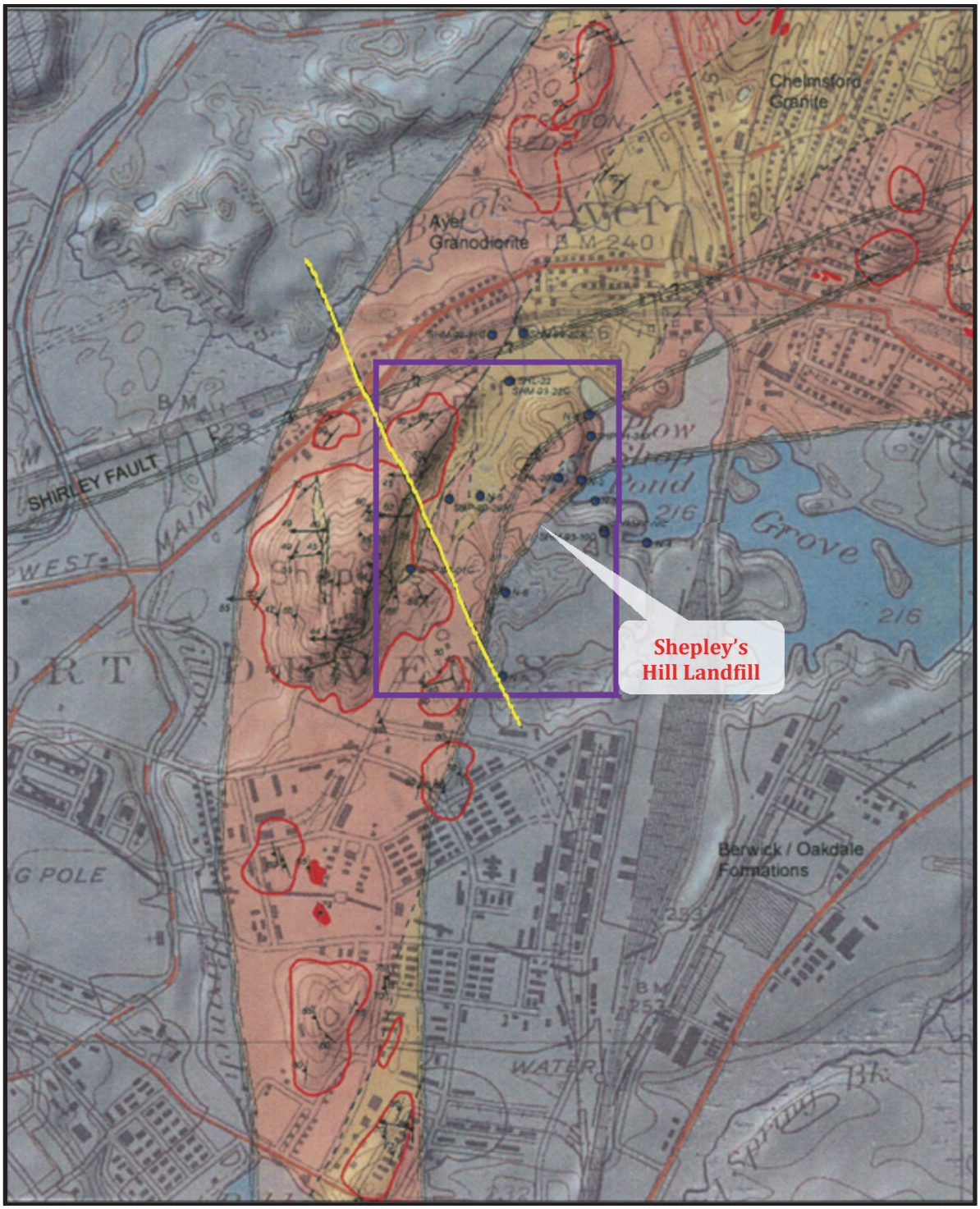

Figure 4 – Location of Shepley's Hill (purple square) above Ayer Granodiorite (orange) and Chelmsford Granite (yellow). The Oakdale formation (gray) dominates northwest and southeast of the landfill. The site resides just above a fault (highlighted in yellow). The regions outlined in red show locations where the bedrock is exposed to the surface as segmented outcrops. Map credit: Kopera, 2008.

2.1.4 Groundwater Regime

Based on a particle track model generated by HLA (2000), overall net flow of groundwater below SHL is discharged into Nonacoicus Brook, north of the landfill (*Figure 5*). A distinctly separate flow branch discharges groundwater into Plow Shop Pond. The groundwater is dominantly recharged via precipitation and southern stream runoff. The watershed is part of the Nashua River drainage and is dominantly underlain by Pleistocene glacial Lake Nashua lake-bottom sediments.

According to Brackley and Hansen (1977), the material underlying SHL has transmissivity value of around 20,000 gallons per day (gpd). In the eastern region of the landfill (including below Plow Shop Pond), the transmissivity is around 30,000 gpd. The western region transports 0 gpd to 10,000 gpd.

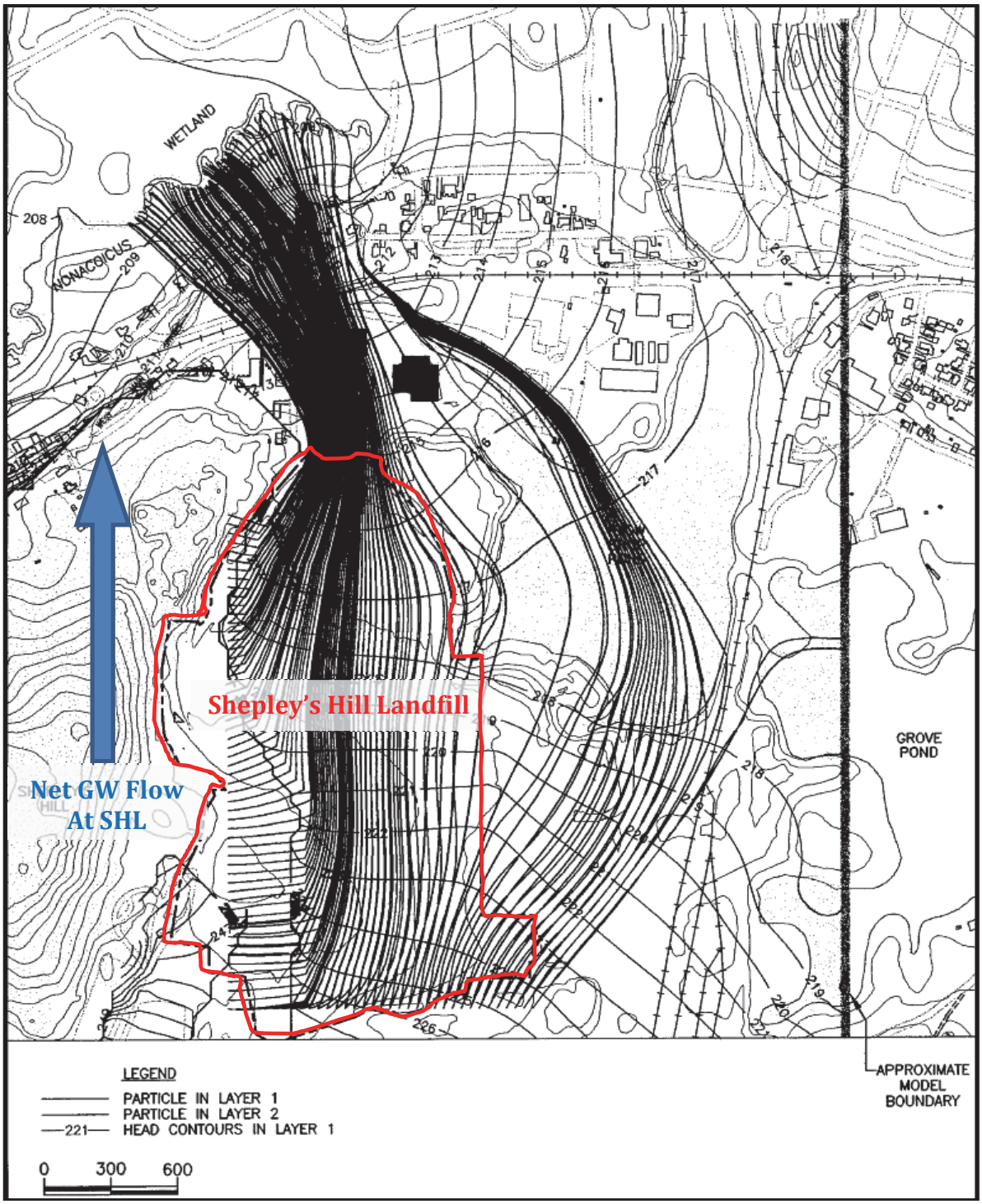

Figure 5 – Groundwater flow model based on particle tracking. Net flow of groundwater below SHL is discharged into Nonacoicus Brook, north of the landfill. Small distinct flow branch discharges groundwater into Plow Shop Pond, east of the landfill.

2.2 Arsenic in SHL Landfill Leachates

2.2.1 Origin of Arsenic in Landfills

Landfills are a threat to human health and environment due to hazardous materials (including As) that can potentially leach out of the landfill and contaminate groundwater. There were many domestic productions of household products that contained arsenic until the mid-1980s, such as wood preservatives, insecticides, and defoliants (Murunga and Zawada, 2007) that could have potentially been discarded into the landfill. Arsenic can enter a landfill due to the disposal of these household products, as well as arsenic-bearing solid residuals from drinking water treatment processes, and chromated-copper-arsenate treated timber from construction demolition (Sills et al, 2006). The landfill may also be situated on a layer of earth that already contains the naturally occurring As. Eventually, under reducing conditions, As contaminants may leach out of the landfill and potentially enter groundwater.

2.2.2 Landfill leachates at Shepley's Hill Landfill

A study by Xie (2013) shows that the highest concentration of arsenic at SHL is mainly detected in groundwater beneath the landfill (relative to surrounding groundwater) (*Figure 6*). The landfill is mainly above the groundwater table, however, the bottom 10% of the landfill comes in contact with groundwater. This portion of the landfill is undergoing chemical reduction and producing the leachate plumes in the groundwater. This plume comes in contact with a layer of peat that is situated directly below the landfill. Since the plume comes in contact with multiple mediums, it is difficult to indicate the main cause of the arsenic contamination. EPA has distributed methane vents throughout the landfill indicating the presence of methanogenic processes below the landfill.

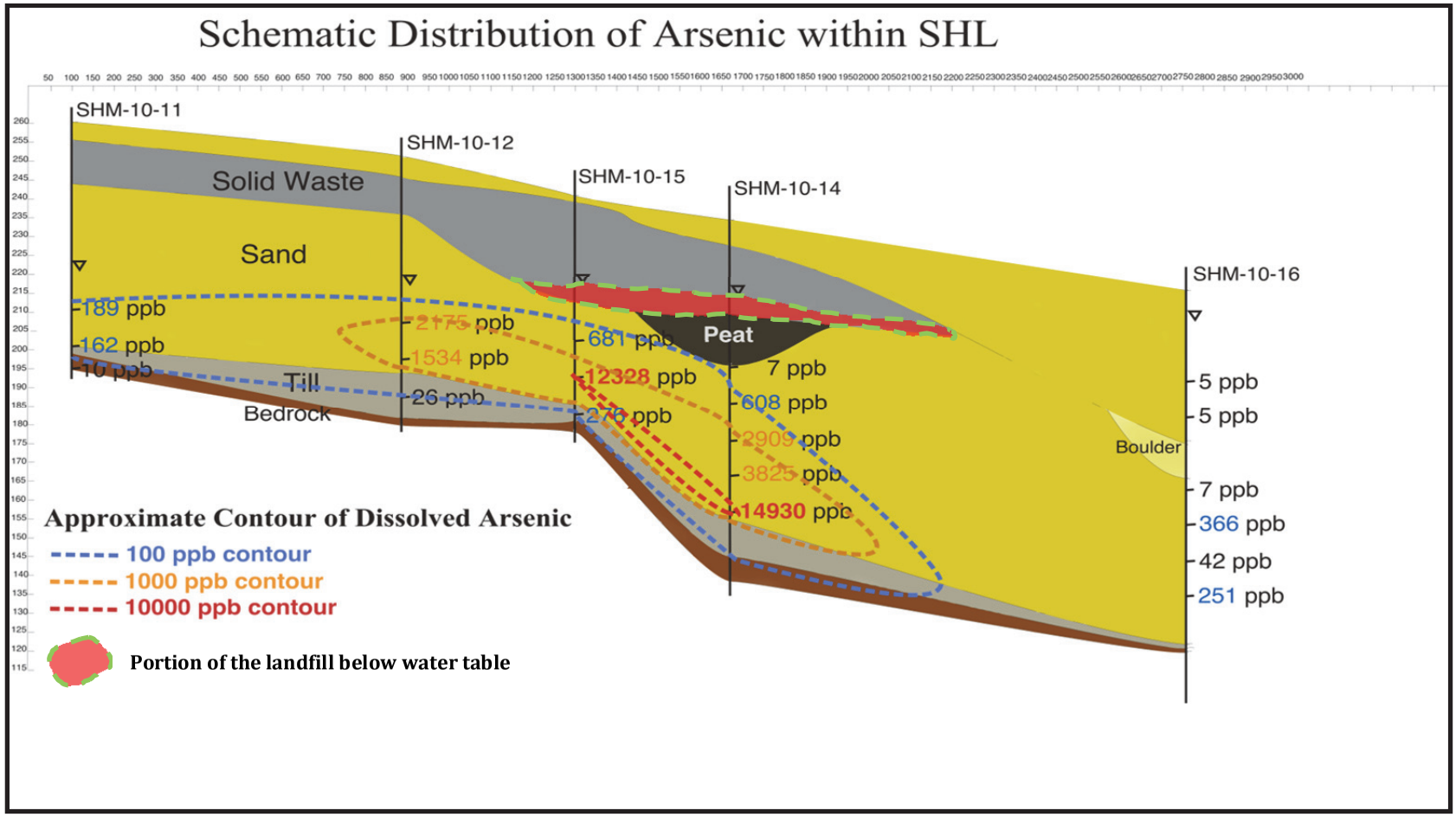

Figure 6 – Schematic distribution of Arsenic within SHL (Xie, 2013).

2.3 Arsenic within SHL waste

SHL waste contains more than 20,000 tons of household waste and construction debris. After subsurface investigations, researchers have not found evidence of hazardous waste deposits after November 19, 1980 (HLA, 2000). The disposal of asbestos and building foundations can potentially contain materials that can produce As under reducing conditions. The direct sampling of materials within the landfill waste has not been done because wells were never drilled into the landfill waste itself.

2.4 Arsenic in Peat Layers

2.4.1 Origin of Arsenic in Peat

The presence of As in peat can be due to natural accumulation of As through physical and chemical erosion of rocks surrounding wetlands, marsh, or bogs. However, with increasing population and industrialization, human activity has become one of the primary factors affecting the global biogeochemical cycling of many trace elements including As. Wetlands tend to be a sink for trace elements (including As) (Langner, Mikutta, & Kretzschmar, 2011), showing higher accumulations around industrial zones. A study by Shotyk et al. (1996) shows that a peat core from a Swiss bog reveals substantial enrichment of As, Sb, and Pb that extends back to Roman times, indicating that in certain locations, anthropogenic fluxes of trace metals have exceeded natural fluxes for over 2000 years.

2.4.2 Peat layer at SHL

The concentration of arsenic in groundwater can be influenced by the presence of peat (Rothwell, Taylor, Chenery, Cundy, Evans, & Allott, 2010). When in contact with groundwater under anaerobic conditions, the dissolved organic matter in peat can produce a reducing condition due to microbial activity (Bergman, Lundberg, & Nilsson,

1999; McArthur, Ravenscroft, Safiulla, & Thirlwall, 2001) which can mobilize arsenic (Stuben, Berner, Chandrasekharam, & Karmakar, 2003; Zheng, et al., 2004; Rothwell, Taylor, Ander, Evans, Daniels, & Allott, 2009). Unfortunately for the sake of this project, isotopic analysis of hydrogen and oxygen has not been done on groundwater that has come in contact with peat layers. Previous analysis of the landfill has shown the presence of peat submerged below the water table underneath the landfill.

2.5 Arsenic from Glacial Deposits

2.5.1 Origin of Arsenic in Unconsolidated Glacial Lake Sequences

The underlying unconsolidated glacial lake sequences of New England were formed during the retreat of glaciation. This layer of glacial deposit contains the highest concentration of insoluble arsenic in the region. The origin of arsenic within the unconsolidated strata varies based on the bedrock source of the sediments. Studies suggest some unconsolidated strata in central Massachusetts may be attributed to glaciation and weathering of rocks from the Merrimack-Belt, a region of bedrock consisting of upper Ordovician to Lower Devonian age units located west of Clinton-Newbury Fault (Hon et al., 2001a, 2001b, 2001c, 2002a, 2002b).

2.5.2 Glacial Lake Sediments (glacial deposits) at SHL

The layer of glacial deposits is located 25 meters below SHL, 30 meters below the groundwater table. The insoluble arsenic within the lake sediments can potentially be mobilized by redox reactions when coming in contact with the leachate plumes of the landfill. Glacial deposits have been known to carry inorganic arsenic species within groundwater (ex: southern Saskatchewan (Yan, Kerrich, & Hendry, 2000)).

2.6 Bedrock Arsenic

2.6.1 Origin of Arsenic in Bedrock

In the New England area, bedrock wells dug into fractured silicate bedrock aquifers tend to have higher As concentrations than surficial wells. Most of the As found in bedrock wells is known to be from natural sources. These aquifers can potentially transport As contaminated waters from a different location. The aquifers can also carry anoxic waters that chemically react with the composition of the bedrock, in which case, the composition of the bedrock contributes to the arsenic concentrations. Reason behind higher concentrations of As bearing rocks in certain bedrocks have been extensively studied however no theory confidently lean toward a conclusion to the clear mechanistic process of accumulating As bearing rocks in only certain geologic units (Peters and Blum, 2003).

2.6.2 Shepley's Hill Bedrock

The fractured bedrock beneath the landfill consists of Chelmsford Granite (Devonian) and Ayer Granodiorite (Devonian) (Kopera, 2008) (*Figure 4*). These types of rocks commonly carry arsenopyrite (FeAsS) and cobaltite (CoAsS), which are credited with sourcing high concentrations of arsenic to groundwaters (Peters & Blum, The source and transport of arsenic in a bedrock aquifer, New Hampshire, USA, 2003; Barnard, 2006; Lipfert, Reeve, Sidle, & Marvinney, 2006; Peters, Blum, Karagas, Chamberlain, & Sjostrom, 2006; Yang, et al., 2009). It can also be found in common minerals such as quartz, feldspar, other aluminosilicates, and iron ore minerals (Onishi & Sandell, 1955). High arsenic in bedrock is also correlated with high pH, low iron, and either high Eh or some measurable amount of dissolved oxygen (Ayotte, Montgomery,

Flanagan, & Robinson, 2003; Peters & Blum, The source and transport of arsenic in a bedrock aquifer, New Hampshire, USA, 2003).

3. Objective

The principal objective of this research is to apply the systematics analysis of hydrogen and oxygen stable isotope fractionation to various zones within and around SHL in order to better understand the groundwater geochemical activities occurring around the landfill region. The goal is to locate and identify any dependency of isotopic signatures on As concentrations in order to identify groundwater geochemical processes that are involved in the mobilization, transport, and attenuation of arsenic.

4. Application of Stable Isotope to Groundwater Systems

4.1 Isotope Ratios of Hydrogen and Oxygen

Isotopes of hydrogen and oxygen are given based on the abundance ratio of the minor, heavier isotope of the element to the major, lighter isotope (i.e. $^{2}H/^{1}H$). This ratio is normally compared to a standard. The International Atomic Energy Agency (IAEA) supplies a range of natural abundance standards. The universal standard for stable isotopes of hydrogen, oxygen, and nitrogen is the Vienna Standard Mean Ocean Water (VSMOW). The isotope ratios of samples are measured relative to universal standards and are reported in delta notation (δ):

$$\delta = 1000 \frac{R_{sample} - R_{standard}}{R_{standard}}$$

The R_{sample} is the isotope ratio of the element of interest. The $R_{standard}$ values are based on water samples that are common and easily obtainable. The values are ratios and thus are unit-less. Most analyzed substances, being depleted in the heavy-isotope relative to the standard, will yield negative delta values. Guidelines for standard selection and a review of strategies to institute universal isotopic referencing procedures have been reported by Werner and Brand (2001).

4.2 Atmospheric processes and the meteoric water line

The three stable isotopes of oxygen (^{16}O, ^{17}O and ^{18}O) and the two stable isotopes of hydrogen (^{1}H and ^{2}H) are intimately associated in water molecules (Craig, 1961a). In most physical processes, heavy isotopes are dominantly present in liquid/solid phases while light isotopes are preferentially in the gaseous phase. Consequently, ocean water is isotopically heavier relative to atmospheric water. The

partitioning of isotopes during a phase change causes progressive evolution of water isotope composition as it travels across the surface of the earth (*Figure 7*).

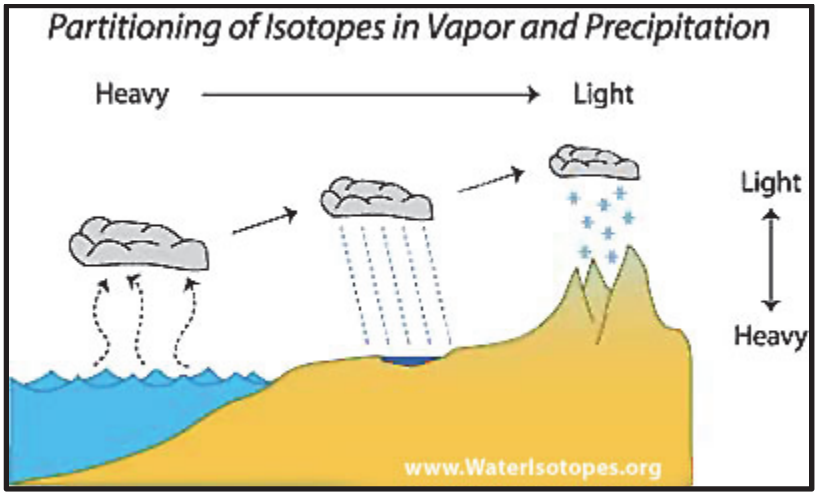

Figure 7 – The progression of isotopes over time. As the isotope changes phase, the isotopic composition of the water changes to be heavier or lighter based on the phase change.

Initial evaporation of ocean water produces water molecules that are isotopically lighter in composition (containing higher counts of ^{16}O, ^{17}O, and ^{1}H) relative to the ocean water. As the water cools in the atmosphere, the condensation of the molecules causes further change to the isotopic composition in the vapor (containing higher counts of ^{18}O and ^{2}H relative to the water molecules surrounding it). Based on how the condensed water (clouds) precipitate, typical rainwater contains a distinct isotopic signature compared to snow, ice, etc. There are multiple variables that affect isotopic ratios in water. Temperature is the primary driving force responsible for change in isotopic composition. When plotted on a graph of $\delta^{18}O$ vs. δD (deuterium) values over a range of temperatures, the average trend tends to differ. The isotopic composition of rainwater in North America during the winter is on average isotopically lighter compared to rainwater during the summer. *Figure 8* shows the average isotopic composition of rainwater during the winter. Due to lower temperature, only the lightest isotopes are

evaporated and precipitated as rainwater. During the summer (*Figure 9*), higher temperature causes an increase in activity and a higher number of heavier isotopes are evaporated and precipitated as rainwater.

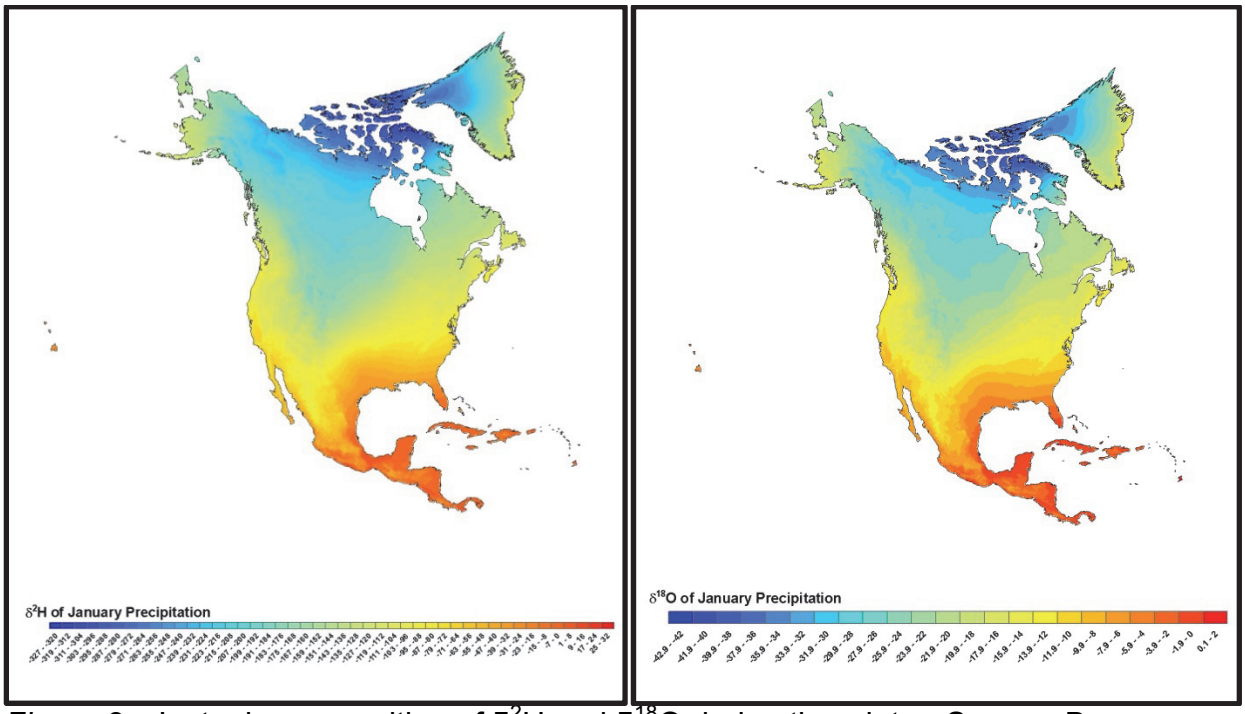

Figure 8 – Isotopic composition of $\delta^{2}H$ and $\delta^{18}O$ during the winter. Source: Bowen, (2013).

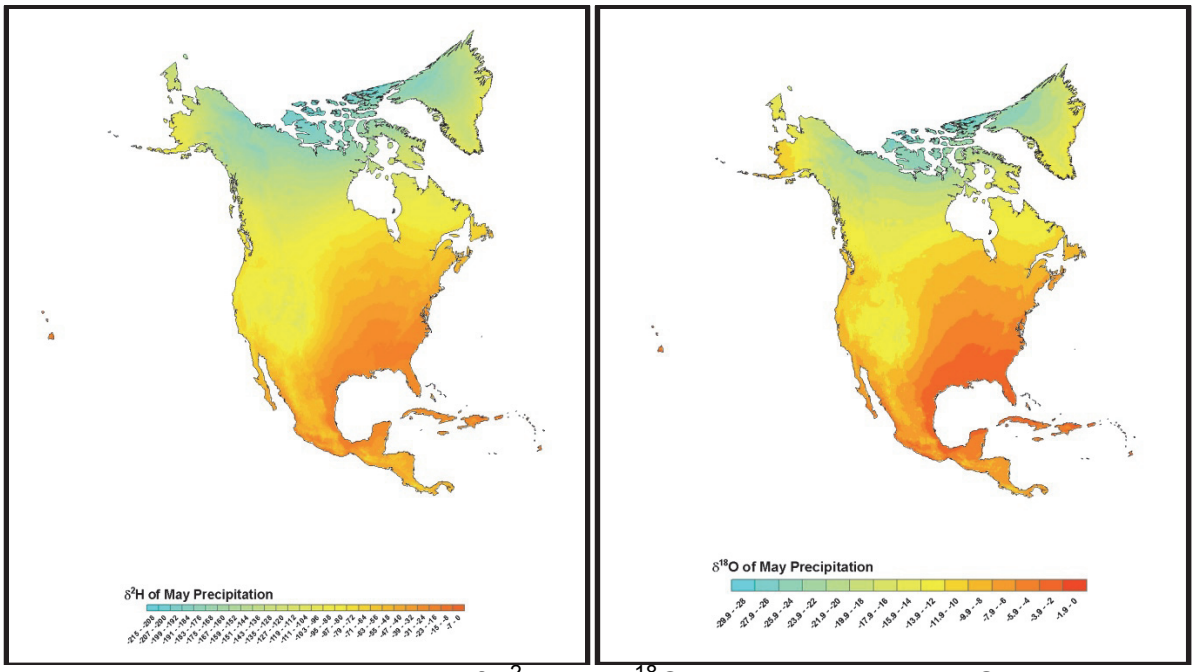

Figure 9 – Isotopic composition of δ^2H and $\delta^{18}O$ during the summer. Source: Bowen, (2013).

When ratios of heavier/lighter isotopes are plotted on $\delta^{18}O$ vs. δ^2H graph, the average trend over change in meteorological regime is called the meteoric water line (MWL). *Figure 10* shows the local meteoric water line based on interpolated data collected by Bowen (2013) at the University of Utah's Spatio-Temporal Isotope Analytics Lab (SPATIAL). Overall, physical changes in isotopic composition are categorized based on change(s) in latitude, altitude, spatial location (i.e. continents), amount of water, and seasons.

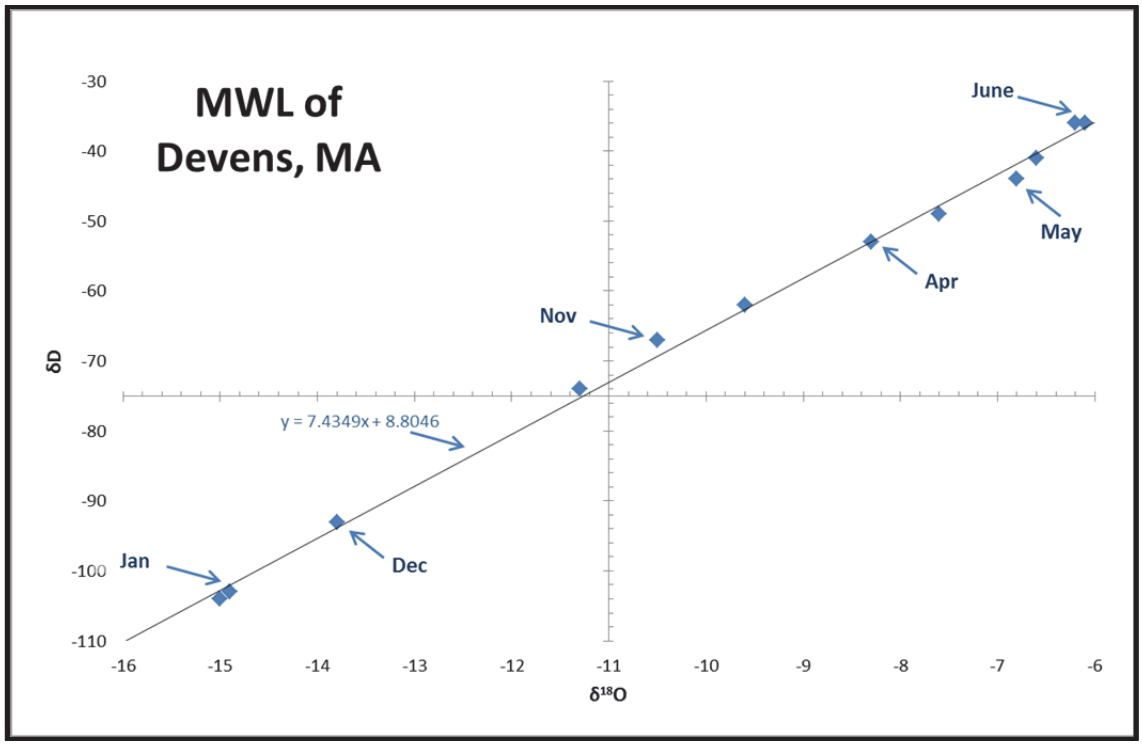

Figure 10 – SPATIAL's interpolated meteoric water line for Devens, MA.

4.3 Isotopic variations in groundwater

When precipitation contributes to groundwater, the groundwater isotopic signature will reflect that of the precipitation. If areas of groundwater undergo physicochemical processes, the isotopic signature of the groundwater can potentially fractionate away from the meteoric line. Isotopic fractionation in different directions reflects various processes, whose patterns were studied in the past (shown in *Figure 11*). Known processes include evaporation, high and low temperature water-rock interactions, hydration of silicates, CO_2-exchange reactions, and H_2S-exchange reactions (IAEA, 1994; Hackley, Liu, & Coleman, 1996). In 1996, the effect of methanogenesis on isotopic composition of $\delta^{18}O$ and δD was observed to fractionate δD above the meteoric line and is also shown in *Figure 11* (Hackley, Liu, & Coleman, 1996).

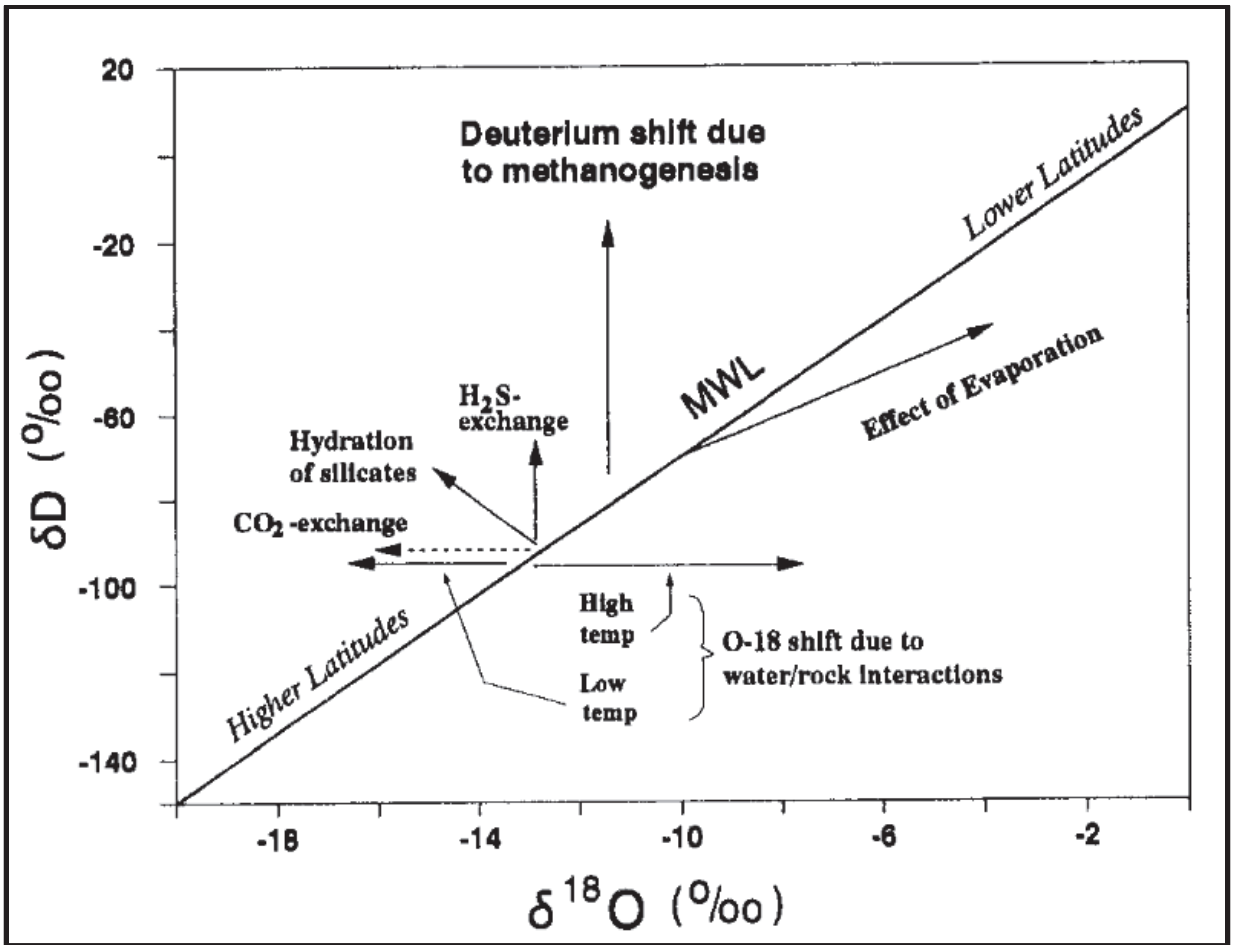

Figure 11 – Plot of a common meteoric water line showing the effects of certain physicochemical processes on isotopic composition of water. (IAEA T.R.S. No. 228, 1983; modified by Hackley et al., 1996).

4.4 Association of δ18O and δD in landfill leachates

When undergoing methanogenesis, leachates from a landfill produce higher concentrations of deuterium relative to undisturbed groundwater (*Figure 11*) (Hackley, Liu, & Coleman, 1996). *Figure 12* shows Hackley's data from a municipal landfill in Illinois that is undergoing methanogenesis. The $\delta^{18}O$ and δD values from the leachates contain higher δD than the average precipitation and uncontaminated groundwater. In methanogenic zones, there is no precipitation pathway for arsenic. Therefore, in the presence of methanogenesis, arsenic accumulates to high levels in groundwater (Kirk, et al., 2004). If isotopic signatures from the arsenic-contaminated samples indicate that

there is a significantly higher concentration of deuterium relative to isotopic signatures of samples from other areas, it can indicate high activity of methanogenesis in the landfill. This can possibly be sufficient evidence to label the landfill as a mobilizer for insoluble arsenic within the glacial lake sediments. If the source of arsenic is the waste deposits within the landfill, direct sampling from the landfill will indicate whether arsenic is present.

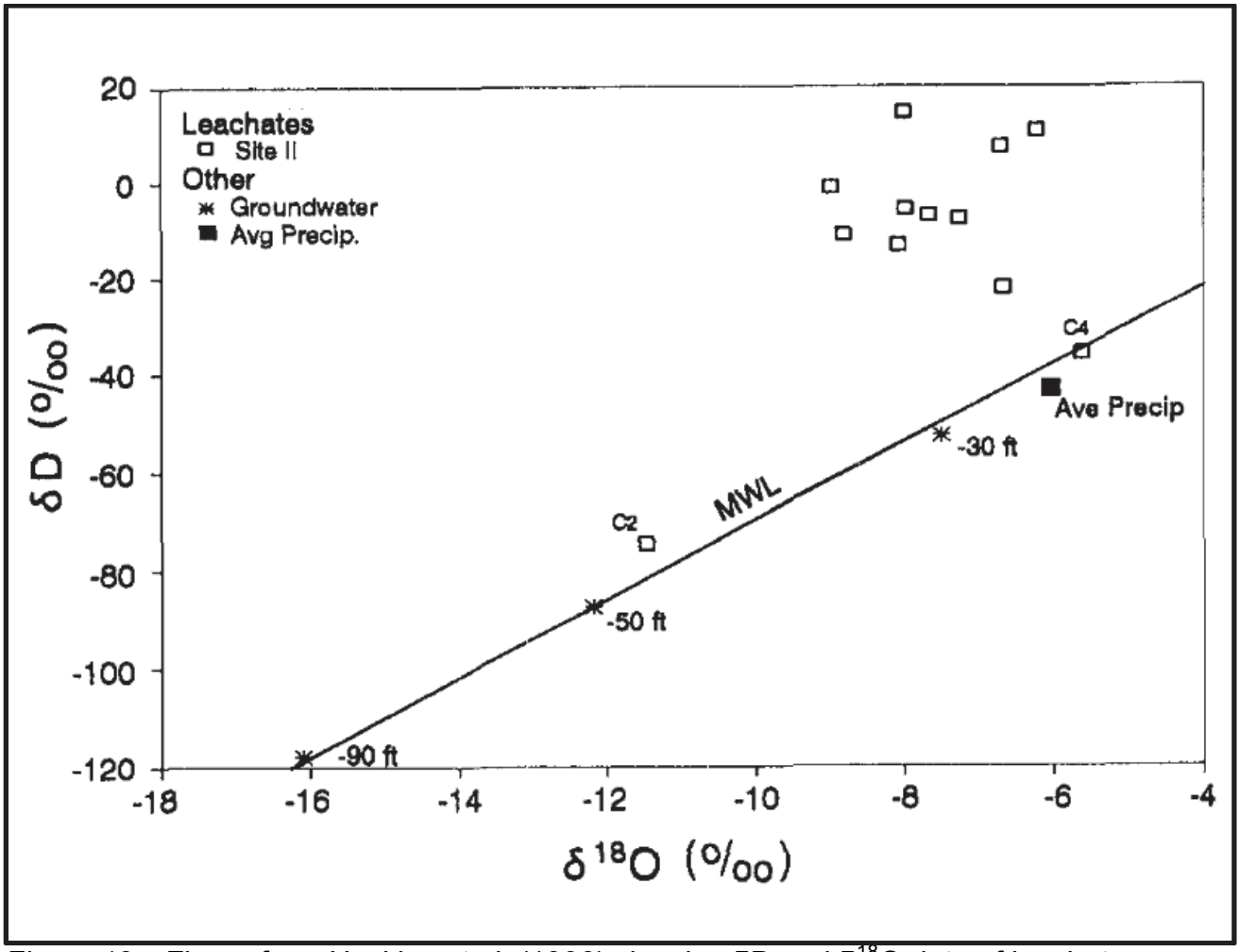

Figure 12 – Figure from Hackley et al. (1996) showing δD and $\delta^{18}O$ data of leachates from a municipal landfill in Illinois.

4.5 $\delta^{18}O$ and δD variations in groundwaters within glacial deposits

Very few studies have been done that correlate distinctive isotopic signatures associated with groundwater through unconsolidated glacial lake sequences. A study by Hendry and Wassenaar (1999) shows that deuterium in glacial deposit aquifers show very little change due to water-rock interaction. If arsenic is becoming soluble from the glacial lake sequences due to the landfill plumes, all the arsenic-contaminated groundwater samples should have higher concentrations of deuterium relative to isotopic signatures of samples from other areas around the landfill. Analyzing the groundwater composition around the glacial lake sediments will further clarify whether the arsenic contaminated samples are originating from the lake sediments. Groundwater composition can be used to eliminate the landfill or bedrock as a dominant source, and could possibly lead to concluding that the glacial deposit is the dominant source of the arsenic.

4.6 $\delta^{18}O$ and δD variations in groundwaters within bedrock

The bedrock beneath SHL is hypothesized to carry deep and aged groundwater. Due to the slow movement of groundwater through the bedrock, rock-water interaction over long periods of time produce distinctive isotopic signatures that tend to fractionate isotopic ratios away from the local meteoric water line. Vuataz and Goff (1986) show that groundwater along the Redondo Creek fault zone in Jemez Mountains, New Mexico produces isotopic signatures with higher abundance of ^{18}O relative to the meteoric line (*Figure 13*).

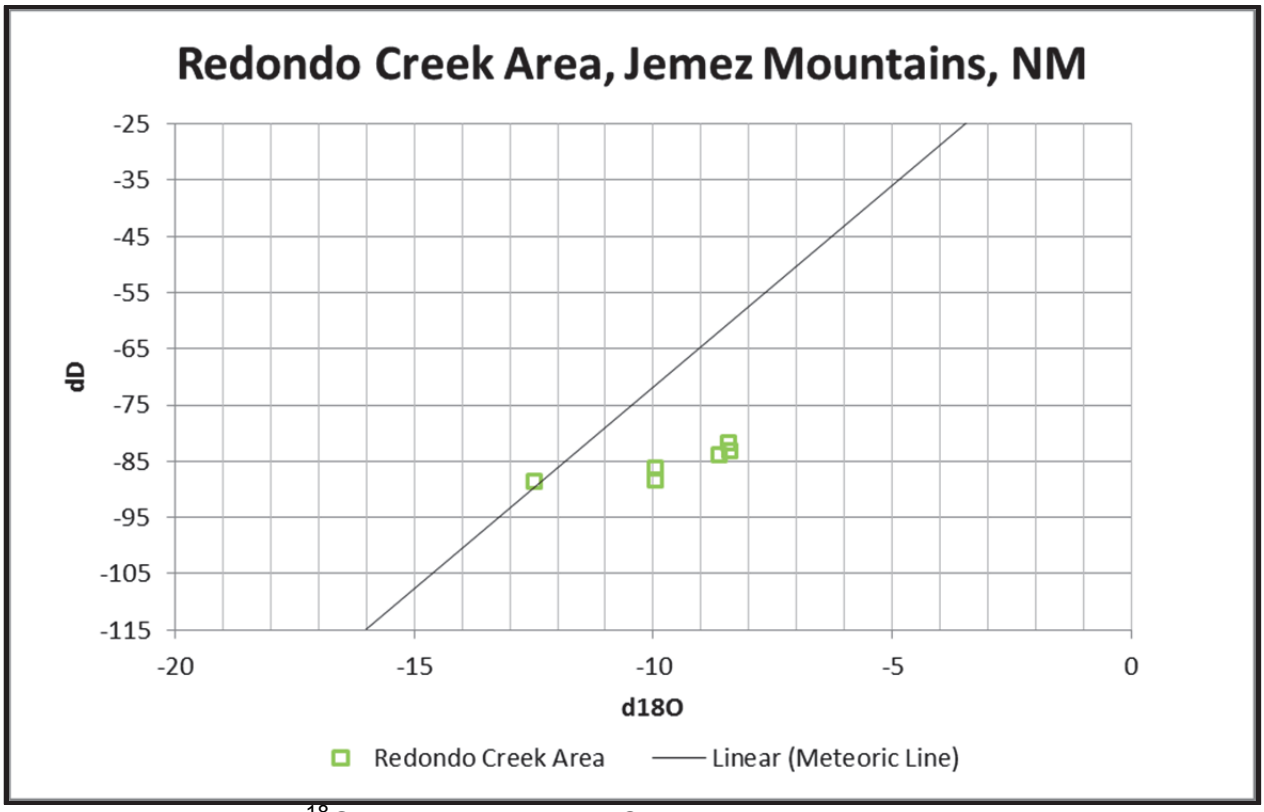

Figure 13 – δD and $\delta^{18}O$ trend in Redondo Creek Area (Vuataz, 1986). Isotopic data from fracture zone groundwater within the Jemez Mountains, NM. Notice that the $\delta^{18}O$ values are isotopically heavier than the isotopic signatures of the meteoric line.

4.7 $\delta^{18}O$ and δD variations in groundwaters within peat layers

Isotopic analyses of oxygen and hydrogen have not yet been performed on groundwater influenced by peat. Owing to the lack of data, fractionations in the δD and $\delta^{18}O$ signature due to peat-groundwater interaction will be difficult to detect. An acceptable assumption is that the peat layer is undergoing geochemical reactions due to microbial activity similar to the landfill leachates. This should yield isotopic variations that are similar to those found in landfill leachate plumes (mentioned above in *Landfill Leachates*).

5. Methodology

5.1 Location of samples

Collected water samples vary both laterally and with depth around the landfill. Water samples were collected from 5 different areas: 1) screened wells within the landfill, 2) boreholes that reach down into bedrock located west of the landfill, 3) from Nonacoicus Brook located to the north, 4) from swamps south of the landfill, 5) from Plow Shop Pond located to the east, and 6) around the water treatment plant north of the landfill (*Figure 14*).

Figure 14 – Location map of sample areas: 1) landfill. 2) bedrock wells. 3) Nonacoicus Brook. 4) swampland. 5) Plow Shop Pond 6) North of landfill.

Screened wells were placed within the landfills by the Army Corps of Engineers (ACOE) to survey quality of water within and near the landfill. Previous water samples from these wells show elevated levels of dissolved arsenic. Sampling these wells provided arsenic contaminated water that was analyzed for their isotopic signatures and compared to uncontaminated water. In total 115 samples were analyzed for various properties that were taken within and (at various depths) around SHL. *Figure 15* labels all sample names around SHL region.

Sample location around SHL (from *Table 1*)

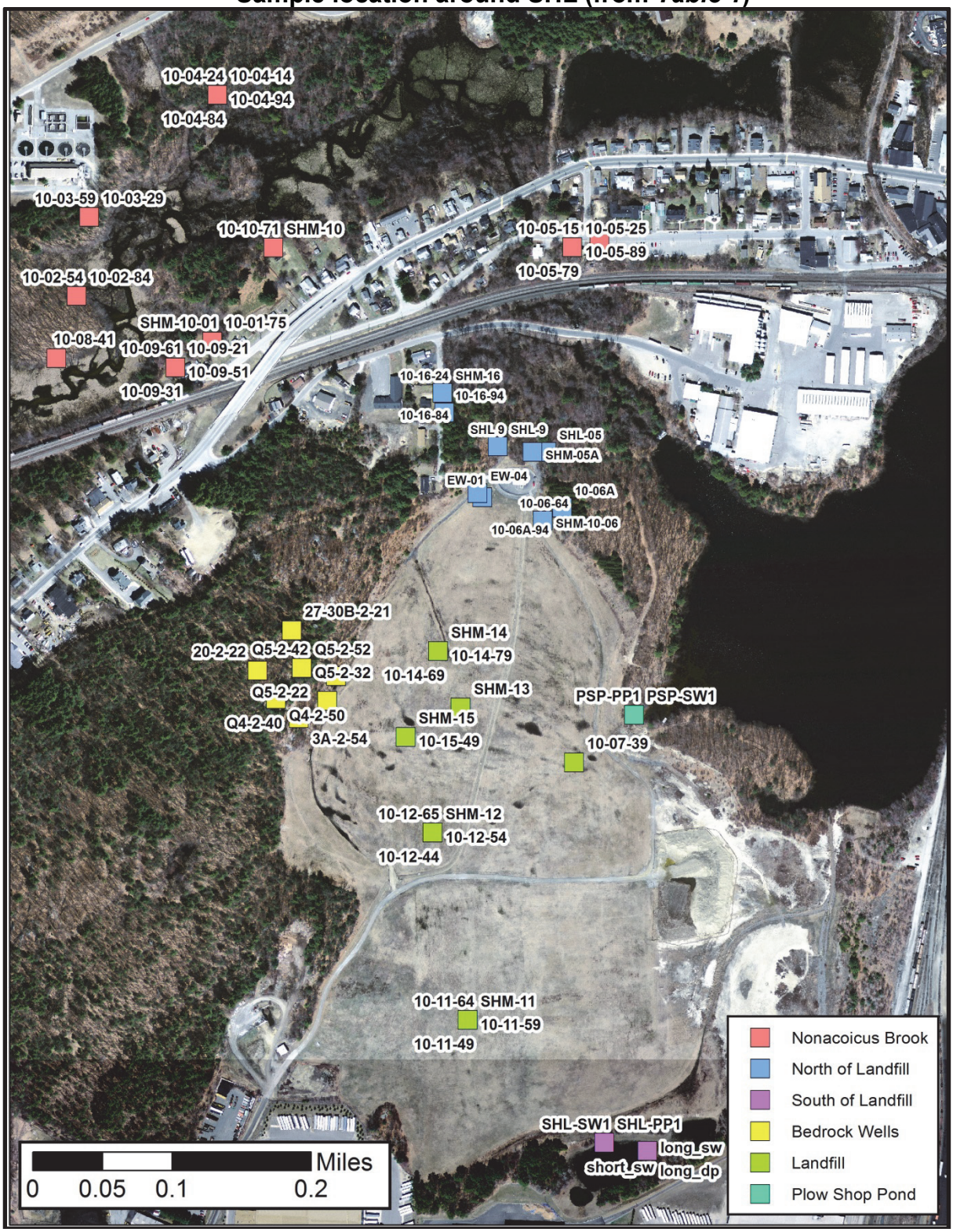

Figure 15 – Names and locations of all samples taken around SHL region.

West of the landfill are boreholes placed by the EPA that reach into the region's fractured bedrock. Bedrock wells can potentially show increased concentration of arsenic at different depths depending on the source of water coming through the fractures. Nonacoicus Brook, located north of the landfill, is down gradient from SHL. Sampling from this location will show whether the landfill plume has traveled over 500 meters down gradient. Plow Shop Pond contains high concentrations of insoluble arsenic that were formed by attaching with iron oxidizing due to the atmosphere.

If the conceptual model underlying this thesis is correct, then the swamp south of the landfill should contain very little to no landfill plume water due to its location up gradient from the landfill. Samples of the water from the swamp should illustrate original conditions of the region before the landfill was active.

5.2 Groundwater/surface water sampling methods

Groundwater/surface water samples were collected using push point sampling, Hydrasleeve, peristaltic pump, or a submersible pump. The type of instrument used varied contingent to well accessibility and the type of well.

5.2.1 Push point sampling

Push point sampling was used to obtain shallow GW (groundwater) samples where GW is near the surface. The marsh south of the landfill and Nonacoicus Brook (north) were the main locations of push point sampling for shallow GW. Push point sampling is the fastest most portable way of sampling shallow surface water without disturbing the water table. The disadvantage is that the instrument can only sample at a maximum depth of six feet from the surface.

5.2.2 Hydrasleeve

Hydrasleeve is a technique for sampling monitoring wells. This technique was used to collect well water from the open hole bedrock wells and a few landfill wells. The advantage of utilizing Hydrasleeve for groundwater collection is that the samples are collected from boreholes at different depths without disturbing the water above or below the sampling location. Since well water is not displaced in the sampling process, the old well water cannot be replaced with new well water from the surrounding geology.

5.2.3 Peristaltic/Submersible pumps

Peristaltic and/or submersible pumps were used to sample screened wells. The distance from the surface to the hydraulic head within each well dictate the appropriate pump for sample collecting. Peristaltic pumps are unable to collect water from a well where depth-to-water is greater than 25 feet due to the maximum capacity of the peristaltic engine. In these situations, the submersible pump was utilized instead. When using the submersible or peristaltic pumps, the wells were pumped for at least 20 minutes before withdrawing water for sampling.

There are certain advantages when using pumps to withdraw well water. The instruments allow sample withdrawal directly from well screens. It also allows old well water to be pumped out before taking a sample. The disadvantage of using these instruments is that the well water is disturbed during the process of sample withdrawal.

5.3 Verifying Reliability of SPATIAL Meteoric Water Line

5.3.1 SPATIAL Meteoric Water Line

In order to determine isotopic fractionations in relation to the meteoric water line, isotopic signatures of annual precipitation were analyzed for the meteoric water line. The slope of the meteoric line near the SHL region was calculated based on

interpolated data from SPATIAL (*Figure 10*) (Bowen, 2013). SPATIAL methodology of collecting water samples is based on 40+ years dataset maintained by the International Atomic Energy Agency (IAEA) and World Meteorological Organization (WMO) containing stable hydrogen and oxygen isotope measurements from rainwater and snowfall collected at several hundred sites worldwide (Bowen, 2013). Even after the compilation of tens of thousands of measurements worldwide, limited spatial and temporal coverage of the measurements limit their usefulness. SPATIAL overcame this obstacle by using simple contouring of data. Over time, they used more sophisticated spatial interpolation methods to produce higher resolution maps and regional MWL.

5.3.2 Local analysis of MWL

In order to test the accuracy of the meteoric line calculated by SPATIAL, local rainwater was collected and tested. The procedure that was followed for collecting rainwater samples is based on the guidelines given by the International Atomic Energy Agency (IAEA, 1994). A 10 oz bottle with a funnel attached to the opening was used to collect rainwater during rain events on or near the study site. The samples collected are analyzed for isotopic composition. The isotopic signature for a rain event will be considered the average representation of the isotopic signature of rainwater for the respective month.

To reduce the environmental factors that will influence the isotopic signature of the collected rainwater, the 10 oz bottle is opaque to prevent light penetration and thickly insulated to prevent change in temperature of the collected rainwater. A 2-3 centimeter layer of mineral oil is placed inside the bottle to prevent wind shear on the surface of the collected water, thus preventing evaporation. Mineral oil creates a well-insulated “liquid lid” above the collected rainwater for preservation. The oil is less dense

than water, causing the film to float above the water, acting as a shield from environmental factors. The hydrophobic properties of mineral oil prevent the oil from interacting with collected water. Most importantly, mineral oil is composed of heavier compounds which prevent the oil from evaporating, thus preventing the rainwater collected beneath the oil from changing its isotopic signature.

The effectiveness of using oil as a liquid lid when collecting rain samples was tested by doing a bench top experiment using mineral oil to preserve water under severe wind conditions. The experiment consisted of testing several beakers containing the same amount of water. Half of the beakers were left open where the water was fully exposed to wind shear. The rest of the beakers were introduced to a 2 cm layer of mineral oil. All the beakers were left untouched for seven days under a ventilation unit. Results show that the open beakers lost on average 85% of its water, while beakers that contained mineral oil lost on average .04% of its water/oil content.

5.4 Sample handling/storage

During sample collection, the samples were collected and immediately capped for preservation. They were stored in ice coolers submerged in ice during the travel back to Boston College. The samples were stored in 10 oz High Density Polyethylene (HDPE) wide-mouth bottle in a refrigerator set to 4°C in the laboratory. Analyzing for both hydrogen and oxygen isotope ratios is usually made on the same bottle of water. If stored correctly, samples have a long shelf life (4-6 years) and can be archived for future analysis. When sending the samples to labs for isotopic analysis, a well-representative portion of the sample was sent in 2 ml HDPE capsules wrapped in parafilm.

5.5 Stable isotopic analysis of δD and $\delta^{18}O$

Analyses of hydrogen and oxygen isotope were done at multiple locations for cross-comparison, accuracy, and analytical accessibility. The majority of the isotopic analysis occurred at the University of Wyoming Stable Isotopes Facility using the Cavity Ring-Down Spectrometer (CRDS). The instrument uses the absorption of light from a single-frequency laser diode to measure isotope ratios of $H_2{}^{16}O$, $H_2{}^{18}O$, and $HD^{16}O$. The laboratory normalizes their sample analysis values according to IAEA guidelines (Coplen, 1994) and reports values relative to Vienna Standard Mean Ocean Water (VSMOW).

Some samples were also sent to other institutions for data comparison. Other institutions include Boston University Stable Isotope Laboratory and a commercial institution, ISOTech, both utilizing an Isotope Ratio Mass Spectrometer (IRMS).

5.5.1 Cavity Ring-Down Spectrometer (CRDS)

Primarily, the cavity ring-down spectrometer (CRDS) from University of Wyoming Stable Isotopes Facility was used to measure isotopic ratios of $\delta^{18}O$ and δD. The instrument works by inserting the sample as a gas into a container (cavity) (*Figure 16*). Light from a diode laser then enters the cavity containing analyte gas. When the optical frequency of the light matches the resonance frequency of the gas atoms, energy begins building up in the cavity. When the energy build-up reaches a certain level, the laser shuts off. The energy decays (“rings down”) with a characteristic decay time. This energy is measured as a function of time on a photodiode. The decay is measured at different wavelengths. The wavelength where the gas is strongly absorbing, ring-down time is short, and vice versa. The concentrations of specific isotopes are proportional to the difference in the ring-down time.

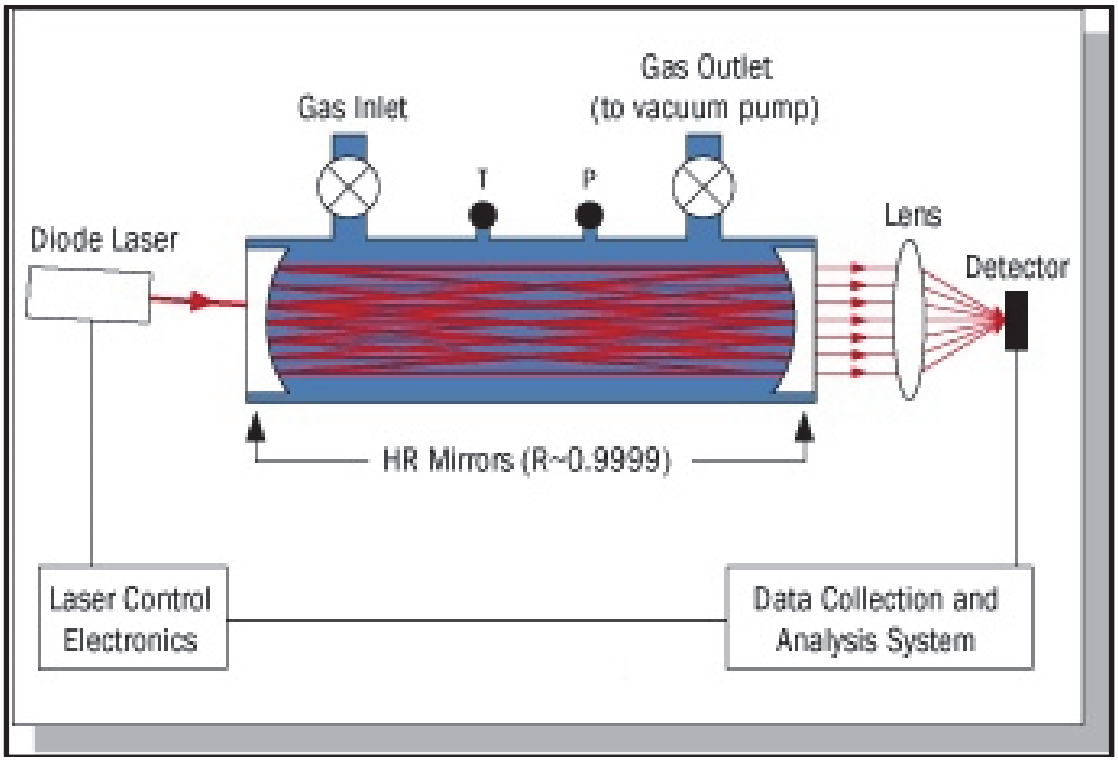

Figure 16 – Diagram of the mechanics of cavity ring down spectrometers (Credit: http://www.uwyo.edu/sif/stable-isotopes).

5.5.2 Isotope Ratio Mass Spectrometer (IRMS)

A general isotopic ratio mass spectrometer (IRMS) from Boston University Stable Isotopes Laboratory and ISOTech works by using a tungsten-coated iridium filament that ionizes the sample as a stream of gas. The gas enters a chamber containing electrostatic plates that strip the gas molecules of the electrons. The elements enter through the ion pump that sends the elements to the magnetic sector where the magnet separates the molecules into a spectrum of masses. The elements are displaced by the magnetic field based on their mass. An ion detector identifies the ratios of heavier elements to lighter elements based on where they are detected (*Figure 17*).

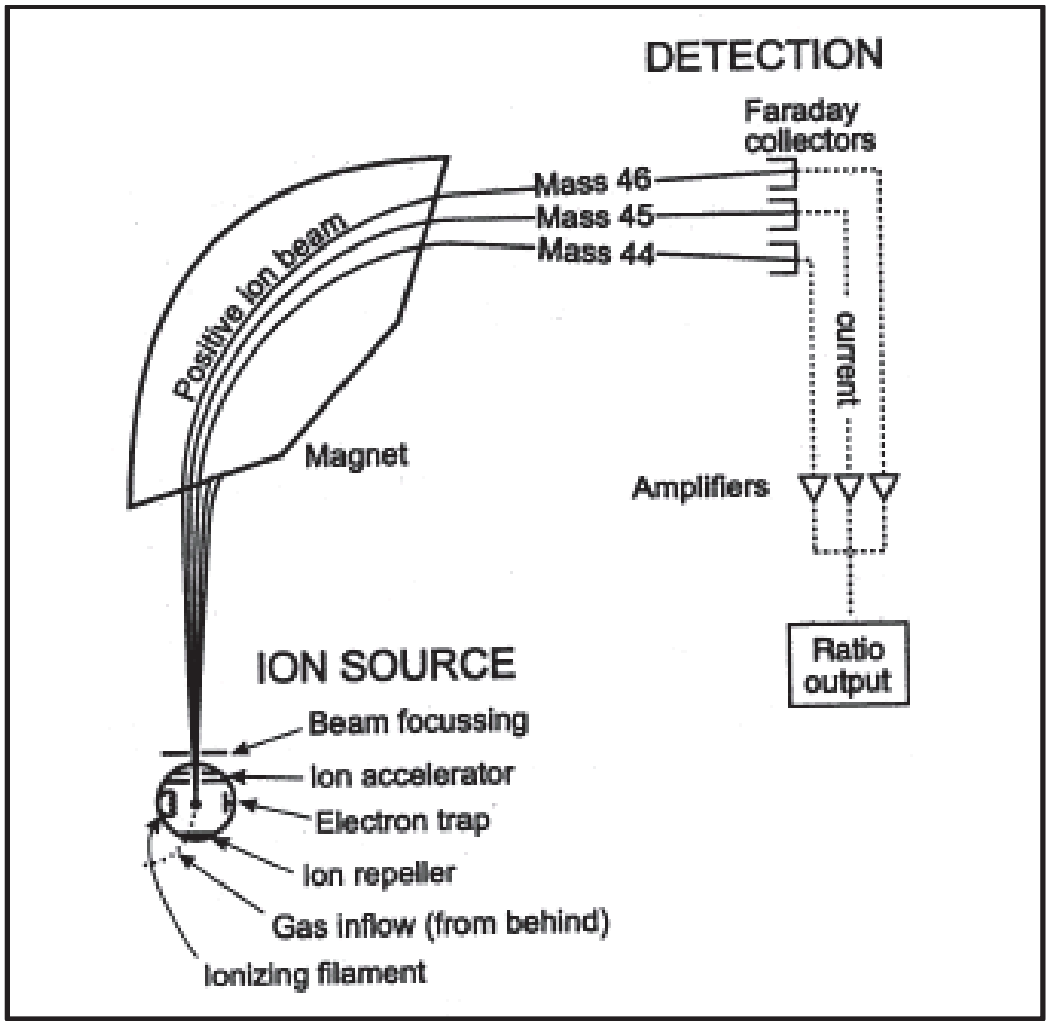

Figure 17 – Diagram of the mechanics of an isotope ratio mass spectrometer (Credit: http://academics.keene.edu/enst/CEB/facilities/IRMS.html).

5.6 Hydrogeochemical Analysis

5.6.1 Inductively Coupled Plasma Optical Emission Spectrometry (ICP-OES)

The groundwater samples from SHL were analyzed for manganese, molybdenum, sodium, nickel, phosphorus, lead, strontium, antimony, tin, titanium, vanadium, and zinc using the inductively coupled plasma optical emission spectrometry (ICP-OES) at Wellesley College Chemistry Department.

The ICP-OES works with the sample in a liquid form. The samples are injected into a radiofrequency (RF)-induced Argon plasma chamber using a nebulizer. The sample, which becomes a mist, is quickly dried, vaporized, and energized through

collisional excitation at high temperatures. The atomic emission emanating from the plasma is viewed at radial or axial configuration using a lens or mirror. The detector creates an image using wavelength selection device. Since certain elements produce certain signatures on a spectrum, the detector identify which elements are present and which are not present (*Figure 18*).

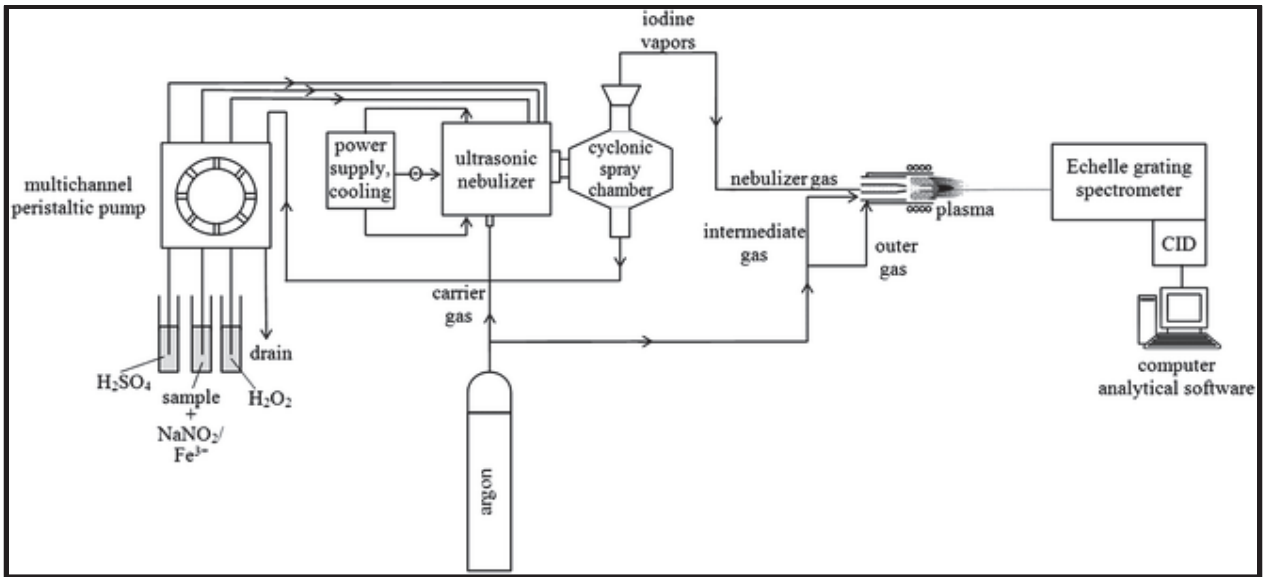

Figure 18 – Diagram of the mechanics of an inductively coupled plasma optical emission spectrometer (Credit: Matusiewicz and Slachcinski, 2010).

5.6.2 Ion Chromatography (IC)

Groundwater samples from SHL were analyzed for sodium, ammonium, potassium, calcium, fluoride, chloride, nitrite, sulfate, and phosphate concentrations. Entire Ion Chromatography (IC) analysis was done at the Boston College Department of Earth and Environmental Sciences.

The IC works by pumping liquid samples through the injector along with sodium hydroxide (NaOH) which helps weaken the ionic bond between the atoms. A pump forces the sample through the anion and cation columns based on the concept that different ions migrate through the IC columns at different rates. The samples go through

the suppressor that enhances detection of the sample ions while suppressing the conductivity of the eluent. The detector measures the electrical conductance of the sample ions as they emerge from the suppressor. The computer analyzes the data by comparing the sample peaks to those produced in standard solution. It then identifies the ion based on retention time, quantifying the concentration by integrating the peak areas (*Figure 19*).

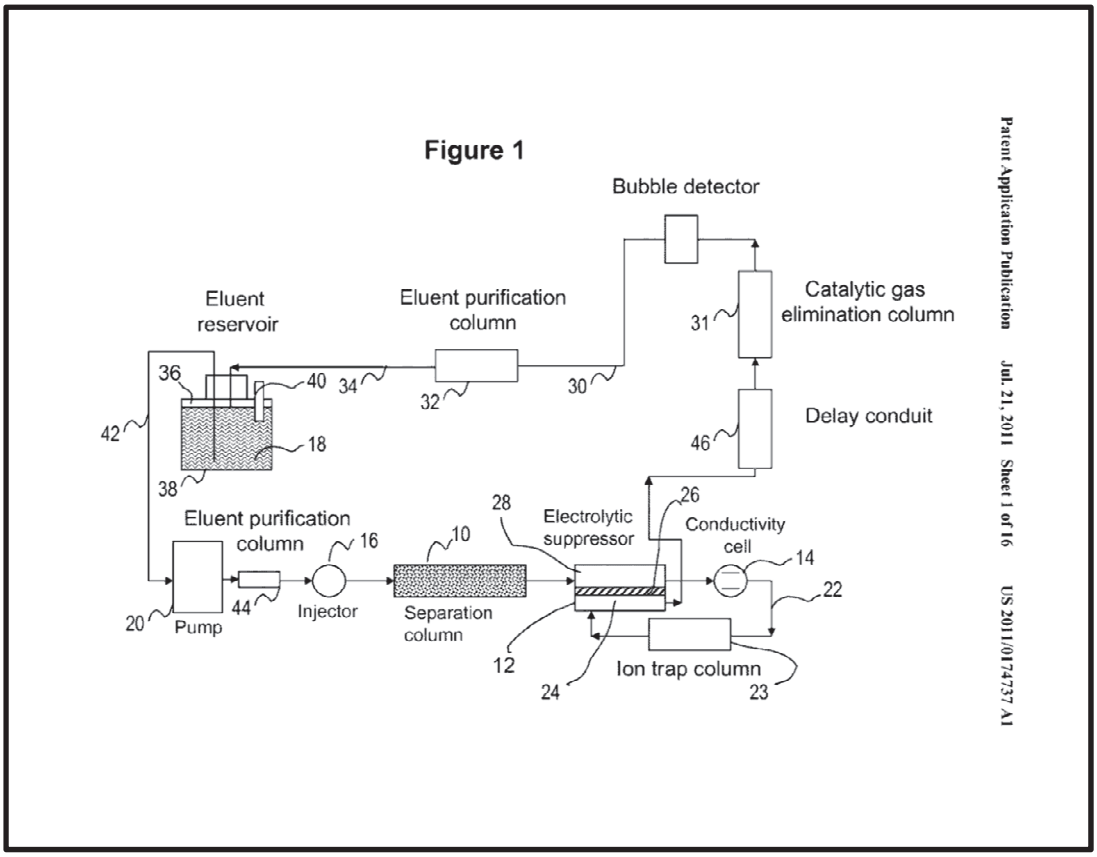

Figure 19 – Diagram of the mechanics of an ion chromatographer (Credit: Chromeleon Tutorial Booklet).

The Dionex ICS-2100 was used for anion analysis during the study. The samples were injected through a 3mm System Injection Loop (SIL) adjusted to a flow of 5 – 25 µL, with laboratory pressure conditions of less than 2,000 psi. Sodium hydroxide

(NaOH) eluent was used for this column at a flow rate of 0.5 mL/min. The column was periodically flushed with 50 mL of eluent through the 2-mm ATC-3 column.

The Dionex ICS-1000 was used for analysis of cations during the study. The samples were injected through a 3mm SIL (5 – 25 µL flow) with less than 2,000 psi laboratory pressure. NaOH eluent was used at a flow rate of 0.5mL/min. The column was periodically flushed with 50 mL of eluent.

5.7 Anoxic Water experiment

In an attempt to mimic the natural environmental reduction process, a bench top experiment on SHL water was concocted within a Winogradsky column. The surface water sample was taken from the swamp, south of SHL. The swamp is known to contain no arsenic contamination. Because the swamp represents the original condition of the area (before As contamination), the samples taken from the swamp should show isotopic fractionation of oxic water transitioning into anoxic water without the influence of As-mobilizing reactions. The samples were turned into a Winogradsky column which included swamp water along with mud and vegetation within the swamp. The columns were left with a tightly closed lid for 8 months to allow reduction. Afterwards, the waters within the columns were tested for its isotopic composition.

6. Results

Sample analysis for this thesis included hydrogen and oxygen stable isotope and groundwater composition analysis on samples collected at SHL. Additionally, precipitation data was collected from major storm events around the region to compare with the SPATIAL meteoric water line. The raw data from these analyses are listed in *Table 2* through *Table 7*, organized by location. *Table 1* shows the summary of which instrumental analysis was applied to each sample. The samples are sorted by their location around SHL (based on Area 1-6 from *Figure 14*).

Table 1: Summary of all instrumental analyses that were applied to the samples taken around SHL. The samples are sorted based on Area 1-6 from *Figure 14*.

Area	Sample ID	Latitude	Longitude	Isotope Data $\delta^{18}O$ and δD (*Table 5*)	ICP Data (*Table 6*)	IC Data (*Table 6*)
1	10-07-39	42.554050	-71.596008	✓	✖	✖
1	10-11-49	42.551367	-71.597503	✓	✓	✖
1	10-11-59	42.551367	-71.597503	✓	✓	✖
1	10-11-64	42.551367	-71.597503	✓	✓	✖
1	10-12-44	42.553317	-71.598000	✓	✓	✖
1	10-12-54	42.553317	-71.598000	✓	✓	✖
1	10-12-65	42.553317	-71.598000	✓	✓	✖
1	10-13-39	42.554619	-71.597606	✓	✖	✖
1	10-13-68	42.554619	-71.597606	✓	✖	✖
1	10-13-69	42.554619	-71.597606	✓	✖	✖
1	10-14-39	42.555206	-71.597925	✓	✓	✓
1	10-14-49	42.555206	-71.597925	✓	✓	✓
1	10-14-59	42.555206	-71.597925	✓	✓	✓
1	10-14-69	42.555206	-71.597925	✓	✓	✓
1	10-14-79	42.555206	-71.597925	✓	✓	✓
1	10-15-49	42.554314	-71.598383	✓	✖	✖
1	SHM-10-11	42.551367	-71.597503	✓	✓	✖
1	SHM-10-12	42.553317	-71.598000	✓	✖	✖
1	SHM-11	42.551367	-71.597503	✓	✓	✓
1	SHM-12	42.553317	-71.598000	✓	✖	✓
1	SHM-13	42.554619	-71.597606	✓	✖	✓
1	SHM-14	42.555206	-71.597925	✓	✖	✓

1	**SHM-15**	42.554314	-71.598383	✓	✖	✓
2	**20-2-22**	42.555003	-71.600473	✓	✓	✓
2	**27-30B-2-21**	42.555422	-71.599989	✓	✓	✓
2	**3A-2-34**	42.554506	-71.599886	✓	✓	✓
2	**3A-2-44**	42.554506	-71.599886	✓	✓	✓
2	**3A-2-54**	42.554506	-71.599886	✓	✓	✓
2	**CAP-1B-25**	42.554946	-71.599366	✓	✓	✓
2	**CAP-1B-35**	42.554946	-71.599366	✓	✓	✓
2	**CAP-1B-45**	42.554946	-71.599366	✓	✓	✓
2	**CAP-1B-55**	42.554946	-71.599366	✓	✓	✓
2	**CH-1D-20**	42.554687	-71.599491	✓	✓	✓
2	**CH-1D-30**	42.554687	-71.599491	✓	✓	✓
2	**CH-1D-40**	42.554687	-71.599491	✓	✓	✓
2	**CH-1D-50**	42.554687	-71.599491	✓	✓	✓
2	**CH-1D-60**	42.554687	-71.599491	✓	✓	✓
2	**CH-1D-70**	42.554687	-71.599491	✓	✓	✓
2	**CH-1D-80**	42.554687	-71.599491	✓	✓	✓
2	**CH-1D-90**	42.554687	-71.599491	✓	✓	✓
2	**Q4-2-30**	42.554706	-71.600213	✓	✓	✓
2	**Q4-2-40**	42.554706	-71.600213	✓	✓	✓
2	**Q4-2-50**	42.554706	-71.600213	✓	✓	✓
2	**Q5-2-22**	42.555029	-71.599849	✓	✓	✓
2	**Q5-2-32**	42.555029	-71.599849	✓	✓	✓
2	**Q5-2-42**	42.555029	-71.599849	✓	✓	✓
2	**Q5-2-52**	42.555029	-71.599849	✓	✓	✓
3	**10-01-75**	42.558428	-71.601117	✓	✖	✖
3	**10-02-54**	42.558900	-71.603028	✓	✖	✖
3	**10-02-84**	42.558900	-71.603028	✓	✖	✖
3	**10-03-29**	42.559722	-71.602850	✓	✖	✖
3	**10-03-59**	42.559722	-71.602850	✓	✖	✖
3	**10-04-14**	42.560997	-71.601047	✖	✓	✖
3	**10-04-24**	42.560997	-71.601047	✓	✓	✓
3	**10-04-34**	42.560997	-71.601047	✓	✓	✓
3	**10-04-44**	42.560997	-71.601047	✓	✓	✓
3	**10-04-54**	42.560997	-71.601047	✓	✓	✓
3	**10-04-64**	42.560997	-71.601047	✓	✓	✓
3	**10-04-74**	42.560997	-71.601047	✓	✓	✓
3	**10-04-84**	42.560997	-71.601047	✓	✓	✓
3	**10-04-94**	42.560997	-71.601047	✓	✓	✓
3	**10-05-15**	42.559414	-71.596042	✓	✓	✓
3	**10-05-25**	42.559414	-71.596042	✓	✓	✓

3	**10-05-35**	42.559414	-71.596042	✓	✓	✓
3	**10-05-45**	42.559414	-71.596042	✓	✓	✓
3	**10-05-69**	42.559414	-71.596042	✓	✓	✓
3	**10-05-79**	42.559414	-71.596042	✓	✓	✖
3	**10-05-89**	42.559414	-71.596042	✓	✓	✓
3	**10-05A-109**	42.559453	-71.595658	✓	✖	✖
3	**10-08-41**	42.558253	-71.603314	✓	✖	✖
3	**10-09-21**	42.558158	-71.601633	✓	✖	✖
3	**10-09-31**	42.558158	-71.601633	✓	✖	✖
3	**10-09-51**	42.558158	-71.601633	✓	✖	✖
3	**10-09-61**	42.558158	-71.601633	✓	✖	✖
3	**10-10-71**	42.559406	-71.600256	✓	✖	✖
3	**SHM-10**	42.559406	-71.600256	✓	✓	✓
3	**SHM-10-01**	42.558428	-71.601117	✓	✓	✓
3	**SHM-10-04**	42.560997	-71.601047	✓	✓	✖
3	**SHM-93-22C**	42.572980	-71.620798	✓	✖	✓
4	**long_dp**	42.550007	-71.594970	✓	✓	✖
4	**long_sw**	42.550007	-71.594970	✓	✓	✖
4	**SHL-PP1**	42.550089	-71.595577	✓	✓	✓
4	**SHL-SW1**	42.550089	-71.595577	✓	✓	✓
4	**short_sw**	42.550089	-71.595577	✓	✖	✖
4	**AOC57-PP-1**	42.545633	-71.582043	✓	✓	✓
4	**AOC57-SW**	42.545633	-71.582043	✓	✓	✓
5	**PSP-PP1**	42.554549	-71.595160	✓	✓	✓
5	**PSP-SW1**	42.554549	-71.595160	✓	✓	✓
6	**10-06-64**	42.556569	-71.596453	✓	✖	✖
6	**10-06A**	42.556703	-71.596178	✓	✓	✓
6	**10-06A-34**	42.556703	-71.596178	✓	✓	✓
6	**10-06A-44**	42.556703	-71.596178	✓	✓	✓
6	**10-06A-54**	42.556703	-71.596178	✓	✓	✓
6	**10-06A-64**	42.556703	-71.596178	✓	✓	✓
6	**10-06A-74**	42.556703	-71.596178	✓	✓	✓
6	**10-06A-84**	42.556703	-71.596178	✓	✓	✓
6	**10-06A-94**	42.556703	-71.596178	✓	✓	✓
6	**10-06A-104**	42.556703	-71.596178	✓	✓	✓
6	**10-06A-110**	42.556703	-71.596178	✓	✓	✓
6	**10-16-24**	42.557897	-71.597869	✓	✓	✓
6	**10-16-34**	42.557897	-71.597869	✓	✓	✓
6	**10-16-54**	42.557897	-71.597869	✓	✓	✓
6	**10-16-74**	42.557897	-71.597869	✓	✓	✓
6	**10-16-84**	42.557897	-71.597869	✓	✓	✓

6	**10-16-94**	42.557897	-71.597869	✓	✓	✓
6	**EW-01**	42.556811	-71.597306	✓	✓	✖
6	**EW-04**	42.556853	-71.597372	✓	✓	✖
6	**SHM-05-41C**	42.557694	-71.597842	✓	✓	✖
6	**SHM-05A**	42.557282	-71.596600	✓	✓	✓
6	**SHM-10-06**	42.556569	-71.596453	✓	✓	✓
6	**SHM-10-06A**	42.556703	-71.596178	✓	✓	✓
6	**SHM-10-16**	42.557897	-71.597869	✓	✖	✖
6	**SHM-16**	42.557897	-71.597869	✓	✖	✓
6	**SHL-5**	42.557282	-71.596401	✓	✓	✓
6	**SHL-9**	42.557339	-71.597085	✓	✓	✓

Table 2: Extrapolated data from SPATIAL showing the average isotopic signatures of rain water that create the local meteoric water line at SHL. The SPATIAL data was extracted from Bowen (2013) on January, 2013.

SPATIAL's monthly average isotopic signature of rainwater at SHL		
Month	**$\delta^{18}O$ (‰, V-SMOW)**	**δD (‰, V-SMOW)**
Jan	-15	-104
Feb	-14.9	-103
Mar	-11.3	-74
Apr	-8.3	-53
May	-6.8	-44
Jun	-6.6	-41
Jul	-6.2	-36
Aug	-6.1	-36
Sept	-7.6	-49
Oct	-9.6	-62
Nov	-10.5	-67
Dec	-13.8	-93

Table 3: Extrapolated data from SPATIAL showing the average isotopic signatures of rain water at Boston College for comparison (Ref: Bowen, 2013).

SPATIAL's monthly average isotopic signature of rainwater at Boston College		
Month	**$\delta^{18}O$ (‰, V-SMOW)**	**δD (‰, V-SMOW)**
Jan	-14.8	-102
Feb	-14.6	-101
Mar	-11.1	-72
Apr	-8.1	-52
May	-6.7	-43
Jun	-6.4	-40
Jul	-6.1	-35
Aug	-5.9	-35
Sept	-7.5	-48
Oct	-9.4	-60
Nov	-10.3	-65
Dec	-13.5	-91

Table 4: Measured MWL around Boston College region.

Measured MWL		
Samples	**$\delta^{18}O$ (‰, V-SMOW)**	**δD (‰, V-SMOW)**
precip-7-18-12	-8.6	-54
precip-5-19-13	-8.6	-54
precip-3-12-13	-4.8	-25
precip-10-29-12	0.2	12

Table 5 – Isotopic composition of groundwater samples at SHL. Grouping refers to the location of where the samples were taken relative to *Figure 14*.

Isotopic Composition of groundwater at SHL								
Nonacoicus Brook	**$\delta^{18}O$**	**δD**	**North of Landfill**	**$\delta^{18}O$**	**δD**	**South of Landfill**	**$\delta^{18}O$**	**δD**
Area 3			**Area 6**			**Area 4**		
10-09-31	-8.74	-53.79	10-16-34	-6.90	-49.00	long_dp	-4.00	-36.00
10-04-34	-8.58	-58.10	10-16-54	-6.30	-49.00	long_sw	-2.20	-33.00
10-05-35	-5.20	-44.00	10-06-64	-9.12	-60.40	short_sw	-0.70	-15.00
10-08-41	-8.69	-58.50	10-16-74	-6.90	-55.00	AOC57-PP-1	-8.82	-52.75
10-04-44	-8.10	-57.00	10-16-84	-8.79	-58.60	AOC57-SW	-4.99	-37.96
10-05-45	-7.20	-49.00	10-16-94	-7.55	-54.00	SHL-SW1	-1.40	-18.55
10-09-51	-7.77	-59.35	10-16-24	-8.30	-54.00	SHL-PP1	-4.55	-35.91
10-02-54	-8.30	-56.20	10-06A	-8.00	-53.00			
10-04-54	-8.10	-55.00	10-06A-104	-8.90	-59.00			
10-03-59	-7.85	-61.42	10-06A-110	-6.50	-54.00			
10-09-61	-8.49	-53.01	10-06A-34	-8.52	-55.30			
10-04-64	-8.60	-55.00	10-06A-44	-7.20	-56.00			
10-05-69	-7.80	-53.00	10-06A-54	-5.00	-50.00			
10-10-71	-8.56	-59.56	10-06A-64	-6.80	-49.00			
10-04-74	-3.80	-45.00	10-06A-74	-4.80	-45.00			
10-01-75	-8.74	-57.20	10-06A-84	-7.90	-54.00			
10-05-79	-7.20	-48.00	10-06A-94	-7.60	-57.00			
10-02-84	-8.36	-59.89	EW-01	-8.94	-59.05			
10-04-84	-7.00	-55.00	EW-04	-8.66	-57.00			
10-05-89	-5.08	-45.30	SHL 9	-8.98	-56.16			
10-04-94	-9.10	-58.00	SHM-16	-8.90	-58.00			
10-05-15	-7.70	-54.00	SHL-05	-8.20	-58.00			
10-09-21	-7.45	-53.44	SHL-9	-8.80	-59.00			
10-04-24	-9.56	-62.00	SHM-05-41C	-8.10	-58.00			
10-05-25	-7.10	-49.00	SHM-10-16	-8.00	-58.00			
10-03-29	-7.82	-55.45	SHM-05A	-9.20	-58.00			
10-05A-109	-7.55	-55.55	SHM-10-06	-9.80	-60.00			
SHM-10	-7.10	-51.00	SHM-10-06A	-8.80	-54.00			
SHM-10-04	-5.80	-52.00						
SHM-10-01	-8.40	-54.00						

Table 5 (cont.) – Isotopic composition of groundwater samples at SHL. Grouping refers to the location of where the samples were taken relative to *Figure 14*.

Bedrock Wells	$\delta^{18}O$	δD	Landfill	$\delta^{18}O$	δD	P. Shop Pond	$\delta^{18}O$	δD
Area 2			**Area 1**			**Area 5**		
Q4-2-30	-9.15	-53.12	10-07-39	-8.01	-56.71	PSP-PP1	-8.61	-51.21
Q4-2-40	-8.75	-52.18	10-13-39	-8.20	-57.00	PSP-SW1	-4.89	-35.56
Q4-2-50	-8.68	-53.74	10-14-39	-8.61	-58.93			
CH-1D-20	-8.36	-55.10	10-12-44	-8.49	-56.98			
CH-1D-30	-8.77	-58.20	10-11-49	-8.04	-55.88			
CH-1D-40	-8.36	-56.25	10-14-49	-8.50	-59.00			
CH-1D-50	-8.22	-56.72	10-15-49	-8.98	-55.28			
CH-1D-60	-7.78	-55.78	10-12-54	-8.40	-57.00			
CH-1D-70	-9.03	-56.95	10-11-59	-8.25	-58.50			
CH-1D-80	-5.45	-48.35	10-14-59	-8.68	-58.50			
CH-1D-90	-8.29	-55.46	10-11-64	-9.10	-60.00			
3A-2-34	-8.26	-52.20	10-12-65	-8.60	-59.00			
3A-2-44	-7.78	-50.51	10-13-68	-8.40	-55.00			
3A-2-54	-8.04	-50.22	10-13-69	-8.75	-57.80			
CAP-1B-25	-8.54	-55.41	10-14-69	-8.60	-57.00			
CAP-1B-35	-6.60	-47.33	10-14-79	-8.55	-58.64			
CAP-1B-45	-7.94	-52.00	SHM-11	-6.70	-51.00			
CAP-1B-55	-7.18	-49.88	SHM-12	-7.20	-53.00			
27-30B-2-21	-8.12	-50.27	SHM-13	-9.50	-60.00			
20-2-22	-6.54	-44.66	SHM-14	-8.60	-57.00			
Q5-2-22	-9.03	-53.37	SHM-15	-8.50	-57.00			
Q5-2-32	-9.00	-54.10	SHM-10-11	-6.20	-51.00			
Q5-2-42	-8.64	-52.49	SHM-10-12	-5.70	-52.00			
Q5-2-52	-8.79	-52.89						
Q4-2-30	-9.15	-53.12						
Q4-2-40	-8.75	-52.18						
Q4-2-50	-8.68	-53.74						
Q5-2-22	-9.03	-53.37						
Q5-2-32	-9.00	-54.10						
Q5-2-42	-8.64	-52.49						
Q5-2-52	-8.79	-52.89						

Table 6 – Hydrogeochemical analysis for most water samples collected around SHL. Units: ppb. BDL: Below detection level. N/A: Not analyzed.

Hydrogeochemical Composition																		
	Units: ppb	Instrument-->	ICP						IC									
Area	Sample ID	Well Depth	As	Ba	Fe	Mn	Sr	Zn	Br	Ca	Cl	F	K	Mg	NO3-	Na	PO_4^{3-}	SO_4^{2-}
1	10-11-49	49	7.9	18.6	1281	987.5	61.5	63.4	--	13950	--	--	--	--	--	14060	--	--
1	10-11-59	59	BDL	16.3	421.2	4807	237.9	65.6	--	39170	--	--	--	--	--	20280	--	--
1	10-11-64	64	44.2	112.5	7303	2090	295.4	91.9	--	95340	--	--	--	--	--	39550	--	--
1	10-12-44	44	67.1	15.5	1630	3848	104.7	67.4	--	25430	--	--	--	--	--	4449	--	--
1	10-12-54	54	58.3	16.4	1861	3207	110.4	215.1	--	35180	--	--	--	--	--	9464	--	--
1	10-12-65	65	BDL	22.5	2136	3757	187.9	57.6	--	49280	--	--	--	--	--	26630	--	--
1	10-14-39	39	BDL	44.3	1078	423.2	355.8	158	975.7	35860	12790	33.8	4033	8055	213.1	16770	BDL	1994
1	10-14-49	49	55.8	90.7	10640	1956	280.8	114.5	1299	47720	5473	118.9	8170	3982	644.4	7065	BDL	2654
1	10-14-59	59	68.3	12.7	5458	4862	377.5	90.5	1037	45640	10920	150.4	7661	4917	269.6	12620	BDL	4197
1	10-14-69	69	118.3	13	3009	2189	141.4	161.4	1084	34880	4106	136.6	7372	3092	348.7	4685	BDL	3468
1	10-14-79	79	406.8	0	943.7	3859	121	117.1	650.3	25130	6654	107.6	4469	3107	182.6	5114	BDL	5814
1	SHM-11	--	438.0	14.2	19.9	1583	78.3	17.7	36580	22460	22180	68.9	4861	5146	--	17480	161.4	--
1	SHM-12	--	BDL	BDL	BDL	4092	96.7	BDL	2770	24740	7900	275.8	4378	2690	--	8487	138.7	--
1	SHM-13	--	569	31.5	14.1	609.7	564	BDL	572.6	80570	21460	180.2	10480	18660	--	22830	71.6	--
1	SHM-14	--	5.6	BDL	BDL	2270	166.1	BDL	2049	43480	7753	85.1	6515	5931	--	11060	120.3	--
1	SHM-15	--	5770	BDL	15.3	5671	286.6	BDL	14140	48800	12670	114.5	5121	10490	--	14360	150.7	--
2	20-2-22	22	42.6	BDL	BDL	18.8	111	--	18200	41750	1987	347	1952	2393	458	4415	1524	4965
2	27-30B-2-21	21	2.8	BDL	5.7	BDL	336.7	BDL	62020	78800	2370	332	4754	7030	770	6553	1066	7158
2	3A-2-34	34	68.3	BDL	2019	391.6	56.4	--	12920	10870	2034	255	423	843	36	3353	252	1733
2	3A-2-44	44	50.9	BDL	BDL	BDL	23.5	--	13100	10700	2129	261	432	826	33	3426	307	1806
2	3A-2-54	54	53.7	BDL	BDL	3.4	22.8	--	13000	10670	2141	270	415	828	BDL	3414	345	1768
2	CAP-1B-25	25	41.4	BDL	BDL	91.9	24.8	--	17140	78	2769	162	341	795	23	4248	382	1169
2	CAP-1B-35	35	42	BDL	BDL	137.7	35.8	--	17180	107	2121	144	308	1244	46	3152	305	2076
2	CAP-1B-45	45	41	BDL	BDL	132.1	38.2	--	17570	101	2351	152	322	1402	53	3403	324	2389
2	CAP-1B-55	55	42.5	BDL	BDL	117.4	28.9	--	17700	86	2699	153	373	1213	43	3703	385	2083
2	CH-1D-20	20	408.6	39.1	BDL	34.6	159.8	--	14290	38260	3712	1102	3453	6140	137	19420	723	5770
2	CH-1D-30	30	444.7	23.5	BDL	26.9	156.9	--	13890	38240	2817	1105	3033	6121	168	18560	689	5769
2	CH-1D-40	40	468.9	23.8	BDL	BDL	164.9	BDL	13910	38270	2699	1112	2995	6125	537	18450	620	5806
2	CH-1D-50	50	495.1	24.2	BDL	BDL	169.2	BDL	14100	38450	2699	1116	2945	6135	545	18430	650	5807
2	CH-1D-60	60	483	16.7	BDL	17.7	165.8	--	10010	39000	2783	1134	2770	6186	542	18080	547	5871
2	CH-1D-70	70	493.2	12.6	BDL	83.8	168.2	--	14150	39370	2640	1149	2581	6192	580	17660	553	5864
2	CH-1D-80	80	487.7	14.4	BDL	95.8	164.1	--	14730	39530	2827	1172	2539	6233	131	17690	506	5865
2	CH-1D-90	90	420.4	15.4	BDL	157.2	150.7	--	15270	40350	2563	1217	1929	6413	11	17330	95	4961
2	Q4-2-30	30	56.4	BDL	BDL	14.6	38.7	--	13190	14400	2095	171	501	1015	40	3539	312	1961
2	Q4-2-40	40	53.9	BDL	BDL	12.4	41.9	--	13350	16260	1819	172	385	1107	155	3331	266	2171
2	Q4-2-50	50	65.5	BDL	BDL	18	43.8	--	14150	18850	2081	158	548	1310	48	3583	302	2433
2	Q5-2-22	22	38.7	BDL	BDL	82.7	18.6	--	13150	58	2410	372	336	676	23	3502	122	905
2	Q5-2-32	32	43.2	BDL	BDL	34.5	19.2	--	15800	10830	2259	212	380	1257	33	3499	332	1709
2	Q5-2-52	42	50.2	BDL	BDL	17	33	--	15980	12460	2157	161	364	1419	37	3372	297	1907

2	**QS-2-42**	52	47.6	BDL	BDL	19.8	32.8	--	16400	12840	2546	170	398	1485	BDL	3662	335	2257
3	**10-04-14**	14	BDL	BDL	49.1	204.1	16.1	185.2	--	4031	--	--	--	--	--	3857	--	--
3	**10-04-24**	24	BDL	BDL	41.7	57.1	17.5	86.9	21.7	2440	1982	51.8	516.6	172.4	240.7	2886	909.6	207.3
3	**10-04-34**	34	BDL	BDL	13.6	46.8	15.7	82.8	58.2	3637	2652	87.8	824.5	467	1128	4633	15.3	408.7
3	**10-04-44**	44	BDL	21.4	58	BDL	122.9	84.6	26.4	21160	23780	53.2	1483	2135	19110	16430	16.1	28710
3	**10-04-54**	54	BDL	18.7	34.4	381.7	646.2	108.6	21.9	64770	79160	96.4	4174	16200	30470	38110	6.7	80190
3	**10-04-64**	64	BDL	32.3	86.7	657.7	531.2	103.3	BDL	78070	127900	1	3543	14290	22160	73160	7.7	98890
3	**10-04-74**	74	BDL	11.4	29	348.1	91.3	139.2	86	16470	216300	307.8	3971	2201	2228	177800	BDL	34510
3	**10-04-84**	84	BDL	BDL	55.5	115.1	29.5	136.8	56.4	5226	153700	156.2	2822	648.8	244.8	168000	BDL	36550
3	**10-04-94**	94	11	67.5	255.7	512.5	792.9	47.2	225.7	145400	739200	530.8	10630	20940	143.2	332700	17.5	31470
3	**10-05-15**	15	BDL	12.5	38.7	481.3	54.1	49	11.9	8330	16710	88.8	1495	1028	2841	12360	13.4	9752
3	**10-05-25**	25	BDL	24.7	19.5	10460	240.2	76.3	36.6	16350	49130	62.8	1757	2545	416.9	24980	14.4	4384
3	**10-05-35**	35	15.4	21.6	748.8	4393	84.5	106.1	28.1	12820	37310	209.3	1526	2389	12990	21620	20.6	2959
3	**10-05-45**	45	BDL	11.7	223.9	1800	157.8	49.1	34.8	17090	56130	125.6	1891	2344	29.6	28660	12.8	2162
3	**10-05-69**	69	BDL	11.9	85.2	451	114.2	118.3	25.1	19840	32240	64.3	2261	2290	5634	22130	13.7	13530
3	**10-05-79**	79	BDL	BDL	12.5	363.2	73.5	52.1	--	17260	--	--	--	--	--	20240	--	--
3	**10-05-89**	89	BDL	BDL	20.1	BDL	79.6	96.9	23.9	19410	20300	146.3	2211	1869	4079	17940	BDL	10400
3	**SHM-10**	--	8.8	10.6	13.1	54.5	334.5	BDL	591.6	77200	21090	110.6	2798	14320	--	22550	78.2	--
3	**SHM-93-22C**	--	14.3	59.2	286.5	15.9	272.5	13.7	563.4	43820	10680	143.7	4501	4042	143.7	9928	BDL	8442
3	**SHM-96-5C**	--	62.9	43.9	2856	13060	1134	--	--	68240	--	--	16320	11010	--	184200	--	--
3	**SHM-96-5B**	--	1395	36.5	18260	9681	788.3	--	--	78870	--	--	7910	12600	--	192900	--	--
4	**AOC57-pp-1**	3	115.5	135.8	6307	40.3	57.4	--	10840	4159	8016	143	821	844	BDL	9594	2168	1086
4	**AOC57-SW**	0	BDL	158.5	80.8	578	113.5	241.8	26770	158	23620	150	6705	1455	50	23080	350	2962
4	**SHL-PP1**	1.5	50	62.5	78640	6106	375.2	--	2988	55490	173400	165	4110	4464	199	122200	135	8401
4	**SHL-SW1**	0	BDL	20.1	1097	65.5	25.2	27.5	10710	137	75910	159	5808	1032	23	57280	388	1969
5	**PSP-PP1**	2.5	BDL	21.9	11.4	BDL	94.3	BDL	2766	22740	28840	95	3189	2869	163	31130	314	5440
5	**PSP-SW1**	0	40	BDL	1383	991.6	87.3	--	6755	565	53700	104	2139	4536	78	33830	306	2610
6	**10-06A**	0	BDL	30.7	890.4	1476	134.5	126.6	520.6	16310	3869	135.5	5761	2078	211.5	7587	BDL	4028
6	**10-06A-34**	34	BDL	BDL	103.7	10.4	28.2	50.7	30.3	3054	1651	56.5	516.9	367.1	--	2585	BDL	5192
6	**10-06A-44**	44	BDL	BDL	65.5	1770	52.6	75	184.1	8015	1120	53.7	2584	565.6	218.8	1501	18.1	9623
6	**10-06A-54**	54	BDL	21.4	124.9	5923	155	81.3	632.3	23630	1619	74.1	2185	1732	488.3	2286	99.7	17010
6	**10-06A-64**	64	BDL	21.9	491.8	2069	120.9	105.5	499.7	16880	4623	190	4239	2081	266.4	4405	17.1	5207
6	**10-06A-74**	74	BDL	23.6	556.5	1737	202.9	81	606	24380	6428	154.4	7768	2878	4597	11230	BDL	4156
6	**10-06A-84**	84	BDL	31.8	1208	2264	258.3	289.9	766.4	22950	5609	128.9	9140	3930	566.1	12840	29.4	4914
6	**10-06A-94**	94	BDL	34.4	1066	9009	659.7	167.6	533.8	55170	26440	67.9	11180	10470	1747	35610	BDL	5904
6	**10-06A-104**	104	BDL	17.2	277.4	864.4	487.3	60.3	243.2	31050	30390	47.6	8993	14470	358.3	37840	BDL	4905
6	**10-06A-110**	110	BDL	10.7	340.1	302.8	328.1	104.3	227.9	24050	29440	43.7	8516	14800	986.1	38970	BDL	5083
6	**10-16-24**	24	BDL	BDL	10.3	378.4	91.8	BDL	337.7	21540	4053	65	2798	1833	2706	2871	BDL	11020
6	**10-16-34**	34	BDL	BDL	23.9	11.3	66.5	166.6	79.2	31620	22400	244.6	5367	2538	1023	13380	59.6	14080
6	**10-16-54**	54	BDL	BDL	32.1	52.7	121.6	51.6	76.5	33650	69340	80.2	5283	3578	2150	35300	238.9	12840
6	**10-16-74**	74	BDL	14	837.8	559.3	223.4	109.7	45.8	39720	56770	214.7	16430	7528	6276	37390	BDL	10470
6	**10-16-84**	84	106	57	5726	290.3	467.3	161	157.8	34160	43790	110.2	6287	19510	261.5	44190	10	1265
6	**10-16-94**	94	BDL	11.2	21	374.2	140.2	118.5	19.5	36810	68520	116.8	6046	4436	528.5	35860	99.9	10660
6	**EW-01**	--	2192	64.8	7760	2078	430.2	--	--	52660	--	--	11100	9333	--	169100	--	--
6	**EW-04**	--	2514	BDL	BDL	405.4	55.7	--	--	8122	--	--	1584	1315	--	2313	--	--

6	**SHL-5**	--	3937	22.8	54190	2368	243.1	--	27	8095	2777	13.5	1214	1016	131.1	1977	BDL	2580
6	**SHL-8D**	--	51.1	BDL	BDL	BDL	80.1	--	--	13570	--	--	796.3	1799	--	151900	--	--
6	**SHL-9**	--	83.2	BDL	9370	350.4	131.1	--	406.9	24950	7220	50.1	2514	2250	3168	6946	BDL	6280
6	**SHM-05-41A**	--	77.8	64.5	600.8	128.2	276.5	--	--	42290	--	--	3985	3787	--	184900	--	--
6	**SHM-05-41B**	--	842.9	14.8	13310	295.5	83.1	--	--	7492	--	--	6607	1105	--	159800	--	--
6	**SHM-05-41C**	--	834.0	BDL	38	2709	393.3	--	--	88870	--	--	3320	12050	--	33790	--	--
6	**SHM-05-42A**	--	49.7	BDL	BDL	BDL	22.5	--	--	9216	--	--	391.6	453.3	--	140100	--	--
6	**SHM-05-42B**	--	232.5	58.9	48270	2381	339.2	--	--	46200	--	--	9404	7848	--	168300	--	--
6	**SHM-05A**	--	6.6	BDL	BDL	BDL	83.2	BDL	10440	16670	22590	84.9	1717	3563	--	17180	6441	--
6	**SHM-10-01**	--	BDL	BDL	11.4	6530	110.4	19.4	7857	24840	7690	68.2	1842	2847	--	7891	278.6	--
6	**SHM-10-04**	--	BDL	29.7	27.7	2503	484.2	149.3	--	63390	--	--	--	--	--	34680	--	--
6	**SHM-10-06**	--	BDL	BDL	BDL	750.2	341.7	BDL	1828	36010	16580	128.8	11670	11740	--	24620	215.6	--
6	**SHM-10-06A**	--	BDL	12.5	10.8	1698	117.1	BDL	3987	1214	5383	103.2	3693	4671	--	8155	412.4	--
6	**SHM-10-11**	--	BDL	20.2	656.1	1989	83.6	109.5	--	20850	--	--	--	--	--	16140	--	--
6	**SHM-10-12**	--	23.3	22.5	1006	4552	128.4	119.9	--	25300	--	--	--	--	--	8606	--	--
6	**SHM-10-16**	--	21.1	53	3015	729	606.7	198.6	--	63120	--	--	--	--	--	36370	--	--
6	**SHM-16**	--	36.8	12.5	BDL	486.5	634.4	BDL	4519	74810	26450	115.3	10360	21990	--	32600	83.3	--

Table 7 – Data on water isotope signatures undergoing reduction within a Winogradsky Column done as a bench top experiment. The samples were collected from the swamp south of SHL.

Sample ID		Winogradsky Column	Latitude	Longitude	Collection Date	Analysis Date	$\delta^{18}O$	δD
Oxic	SHL-SW1	1	42.550520	-71.595600	12-Sep-12	N/A	-1.4	-18.6
	SHL-PP1	2	42.550490	-71.595000	12-Sep-12	N/A	-4.6	-35.9
Anoxic	SW1_sw	1	42.550520	-71.595600	N/A	23-May-13	-0.7	-15.0
	PP1_sw	2	42.550490	-71.595000	N/A	23-May-13	-2.2	-33.0
	PP1_dp	2	42.550490	-71.595000	N/A	23-May-13	-4.0	-36.0

6.1 Local Meteoric line

To find accurate isotopic fractionations of groundwater, a precise MWL needs to be used for comparison. The slope of the meteoric line near SHL region was calculated based on interpolated data from SPATIAL (*Table 2*, *Figure 10*). Based on the SPATIAL data at SHL, the equation of the MWL is:

$$y = 7.4349(\delta^{18}O) + 8.80$$

To verify the accuracy of this meteoric water line (referring back to *Methodology section 5.3*), local rainwater samples were collected over a one year period. Since the site restricted collecting rainwater data, rainwater data was collected at Boston College (BC) (for comparison, SPATIAL data for Boston College is displayed in *Table 3*).*Table 4* shows the five samples collected at BC during different rain events (*Table 4*). The MWL was calculated by plotting the values against a δD vs. $\delta^{18}O$ graph. The equation of the measured MWL for Boston College yielded:

$$y = 7.383(\delta^{18}O) + 6.19$$

SPATIAL MWL at SHL and BC compared to the measured MWL is shown in *Figure 20*. The slope difference between SHL and measured MWL is ~0.05 with a y-intercept difference of ~2.5. The slope difference between the measured MWL model

and SPATIAL MWL model at BC is ~0.02 with a y-intercept difference of ~2.4. Considering that the measured MWL was based on four data samples while SPATIAL interpolation is based on average values of thousands of samples collected over multiple years, the measured MWL matches the SPATIAL MWL very closely. Thus, MWL interpolated from SPATIAL is considered to be an accurate representation of the MWL at Devens, MA, and the SPATIAL MWL is used for the remainder of this analysis.

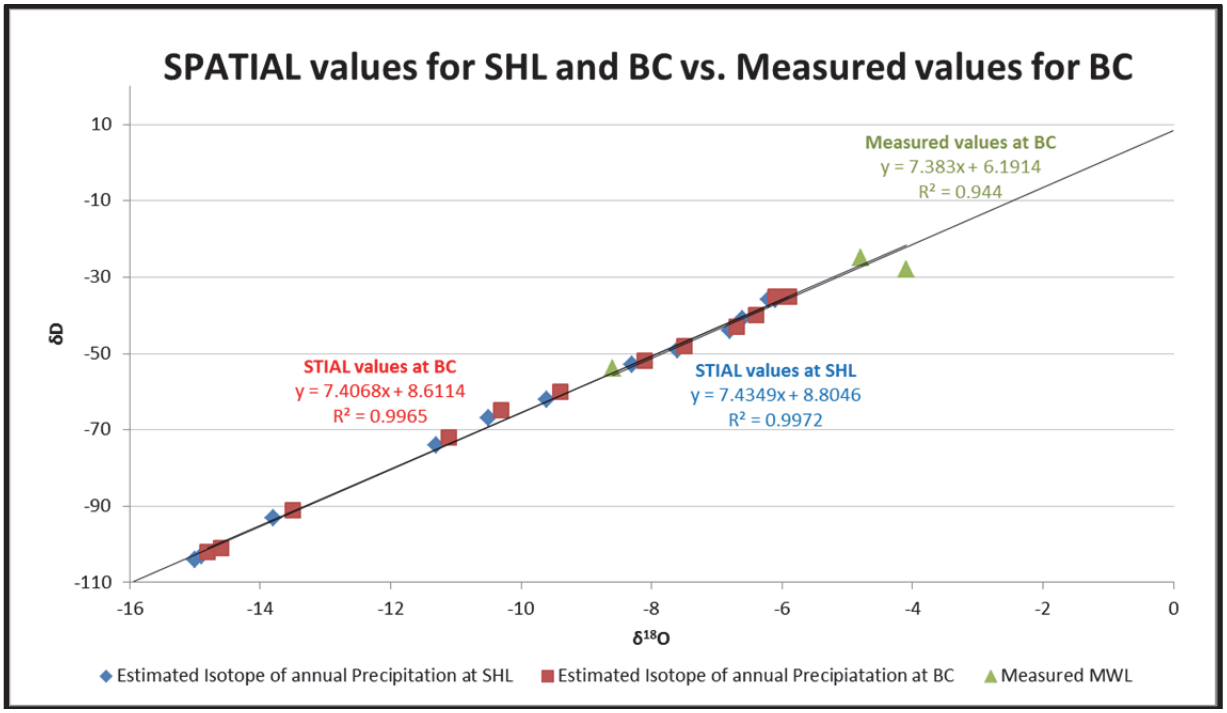

Figure 20 – Comparison of measured MWL to MWL extrapolated by SPATIAL at SHL and BC (including slope values). Red (BC) and blue (SHL) points are SPATIAL interpolated data. Green points are the measured MWL data collected at BC.

6.2 Stable Isotope Results

6.2.1 All Isotope Samples against the MWL

Isotopic composition values are displayed as $\delta^{18}O$ and δD. *Table 5* summarizes all isotopic composition values of samples collected for this study at and around SHL. The isotopic composition of each sample may vary over spatial scales. *Figure 21* shows the isotopic composition of all collected water samples categorized by location. Most

samples had a $\delta^{18}O$ value between -9 and -7.5 and δD values between -60 and -50. Samples at every location contained samples that fractionated from the main group toward counts of heavier oxygen and hydrogen isotopes. *Figure 22* redisplayed the data from *Figure 21* showing the isotopic trends categorized by the sites. The color of the line corresponds to the location of sample. The slope and R^2 value for each trend is displayed next to the trendline. The meteoric water line values (black) correspond to the month the isotopic signature of precipitation produced the respective values. If the sample water did not undergo chemical changes after entering groundwater, the location where the trendline intercepts with the MWL shows a relative time (month of the year) when precipitation water became groundwater. As can be seen in *Figure 22*, Nonacoicus Brook, landfill, and the area north of the landfill all show a similar trendline with a slope between 2.5 (landfill) and 3.0 (Nonacoicus Brook) and an interception with the meteoric line around δD of -60. The swamp south of the landfill (purple) shows a dissimilar trendline with a slope of 4.2 , and a meteoric line interception at δD of -48. Bedrock well samples show a different trend with the lowest slope of 2.2 and an MWL interception point in between south of landfill trendline and other site trendlines (δD of -53).

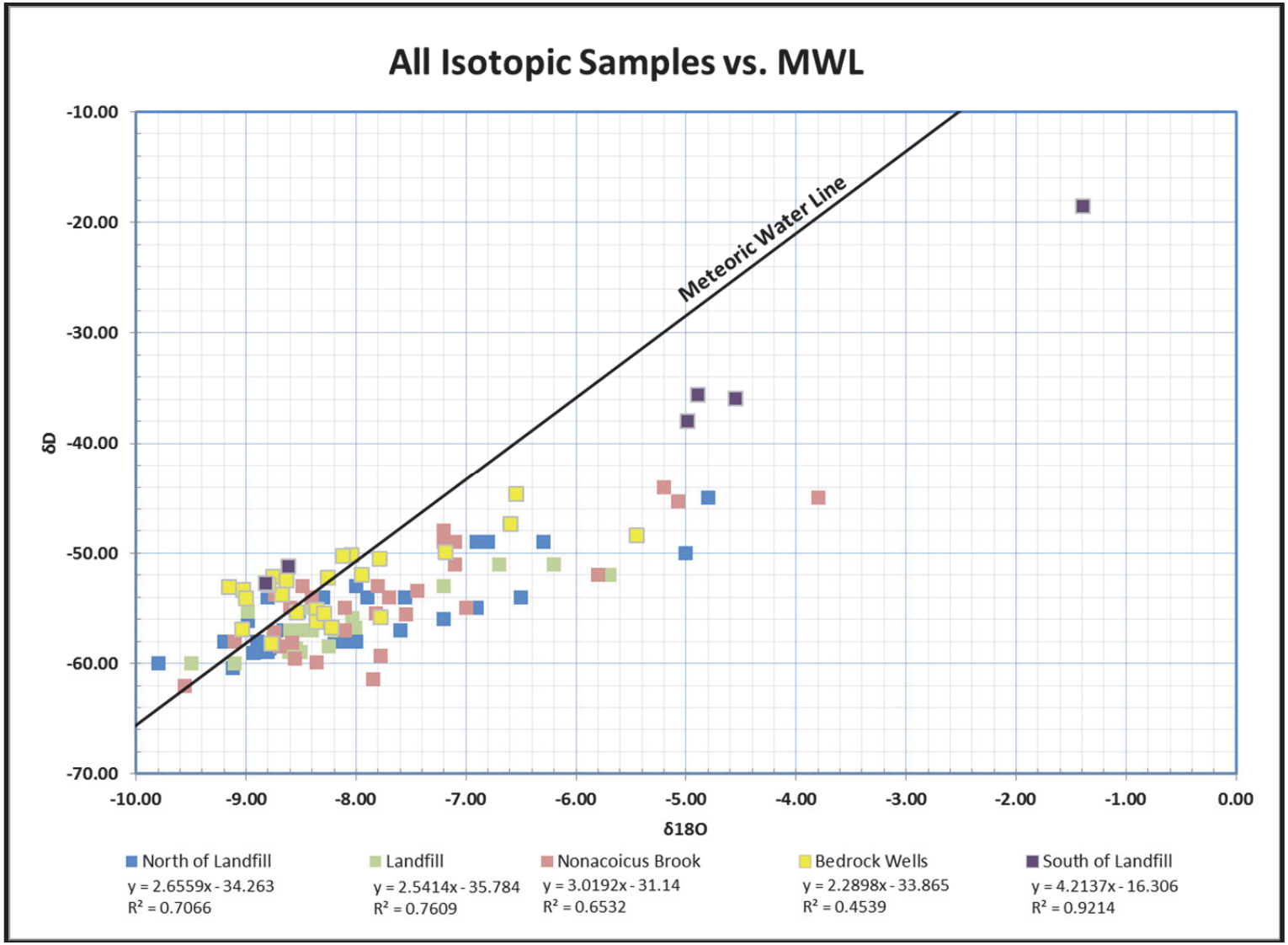

Figure 21 – Isotopic samples from area 1 through 5 plotted with the SPATIAL interpolated meteoric water line.

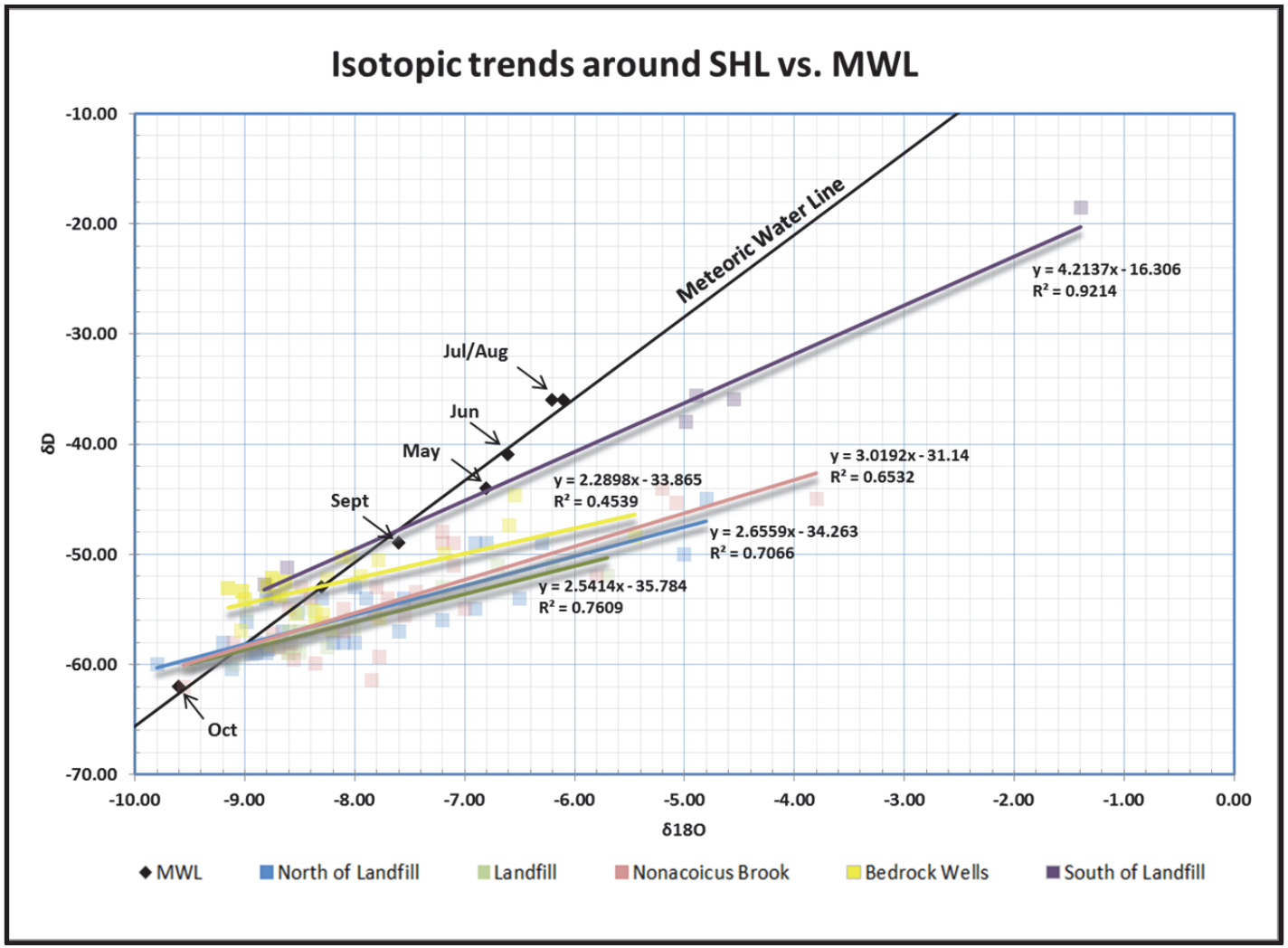

Figure 22 – The isotopic trends at the landfill (Area 1), north of landfill (Area 6), Nonacoicus Brook (Area 3), bedrock wells (Area 2), and south of landfill (Area 4). The color of the line corresponds with the site of sample. The slope and R^2 value for each trend is displayed next to the trendline. The meteoric water line values (black) correspond to the month the isotopic signature of precipitation produced the respective values.

Table 8 – Statistical summary of all isotopic samples.

	Landfill		Bedrock Wells		Nonacoicus Brook		South of Landfill		North of Landfill	
	Area 1		Area 2		Area 3		Area 4		Area 6	
	$\delta^{18}O$	δD	$\delta^{18}O$	δD	$\delta^{18}O$	δD	$\delta^{18}O$	δD	$\delta^{18}O$	δD
Mean	-8.20	-56.62	-8.30	-52.87	-7.66	-54.26	-4.46	-35.11	-7.91	-55.27
Median	-8.50	-57.00	-8.64	-53.12	-7.83	-55.00	-4.55	-35.91	-8.15	-56.08
Mode	-8.60	-57.00	-9.15	-53.12	-8.10	-55.00	N/A	N/A	-6.90	-54.00
Std. Dev	0.91	2.66	0.85	2.90	1.27	4.75	2.86	12.57	1.23	3.90
Equations	y = 2.54x - 5.784		y = 2.29x - 3.865		y = 3.019x - 1.14		y = 4.21x - 6.306		y = 2.66x - 4.263	
R^2	R^2 = 0.7609		R^2 = 0.4539		R^2 = 0.6532		R^2 = 0.9214		R^2 = 0.7066	
Count	30		28		9		31		23	

Even though there were limited number of samples from the southern swamp, the isotopic composition shows the highest fractionation with the heaviest isotopic values reach $\delta^{18}O$=-1.4 and δD=-18.55. Bedrock samples displayed the most conservative fractionation, where the heaviest isotopic sample were only $\delta^{18}O$=-5.45 and δD=-48.35. This correlates with their respective isotopic signature's R^2 values. The samples south of the landfill had the highest R^2 value of 0.9 while bedrock samples had the lowest (0.5). The slope of fractionation for each location is different, ranging from 2.29 to 4.21 δD for every $\delta^{18}O$.

6.3 IC/ICP Results

A select number of samples have been analyzed for their hydrogeochemical composition using the IC and the ICP. The results from both instruments were combined and are listed in *Table 6*. The metals include arsenic, barium, bromide, calcium, chloride, copper, fluoride, iron, potassium, magnesium, manganese, nitrate, sodium, phosphate, sulfate, strontium, and zinc. Individual elements were analyzed based on instrument accuracy. The ICP was used to analyze for arsenic, barium, copper, iron, manganese, strontium, and zinc. The IC was used to analyze for the anion/cations.

6.4 Comparing isotopic composition with As concentration

In order to find patterns between the isotopic composition of the groundwater samples to their arsenic concentration, arsenic concentration data must be integrated with isotopic composition data. *Figure 23* displays all arsenic concentration data in order of concentration. Samples with a concentration of 10 ppb or below are shown in green. Samples between 10 ppb and 100 ppb (which are above EPA standards for safe drinking water) are shown in yellow, and samples that have As concentration higher than 100 ppb are shown in red. *Figure 24* displays the arsenic concentration data categorized by location, using the same color code to display As concentration.

Figure 25 (a-d) shows the integration of arsenic color categorization with isotopic composition values. The values are plotted alongside the SPATIAL meteoric water line. Most areas contain samples that isotopically fractionate toward heavier δD and $\delta^{18}O$ values. The figure displays trendlines (slope and R^2 values) for each As concentration categorization. In general, there are more samples with lower As concentration in all regions. When looking at the bedrock samples (*Figure 25*a), there is an apparent fractionation of samples with high As concentration toward isotopically lighter hydrogen (lower δD values). However, since all high As concentration samples are from the same well (bedrock well CH-1D) there is no direct correlation between isotopic fractionation of only high As concentration samples. In the landfill region (*Figure 25*b), other than two samples that show very high and low $\delta^{18}O$ values, high As concentrated samples contain similar isotopic signature as the low As concentrated samples. The region north of landfill (*Figure 25*c) also shows no correlation other than producing very little fractionation toward heavier ^{18}O levels in high As concentrated samples relative to low As concentration samples. Nonacoicus Brook (*Figure 25*d) shows very little As

contamination in all samples and no correlation between As concentration and its corresponding isotopic signature.

Figure 26 is a compilation of all samples with As concentration and isotopic analysis. Without accounting for regional bias, the slope of samples with >100 ppb As concentration is isotopically lighter in deuterium compared to samples that have As concentration < 10 ppb. When looking at the isotopic composition of samples with As concentration lower than 10 ppb, the overall trend looks more scattered (R^2 = 0.56) relative to samples with As concentration higher than 100 ppb (R^2 = 0.65). The scattering of samples with low As concentration occurs much greater in the $\delta^{18}O$ value range compared to samples with high As concentration.

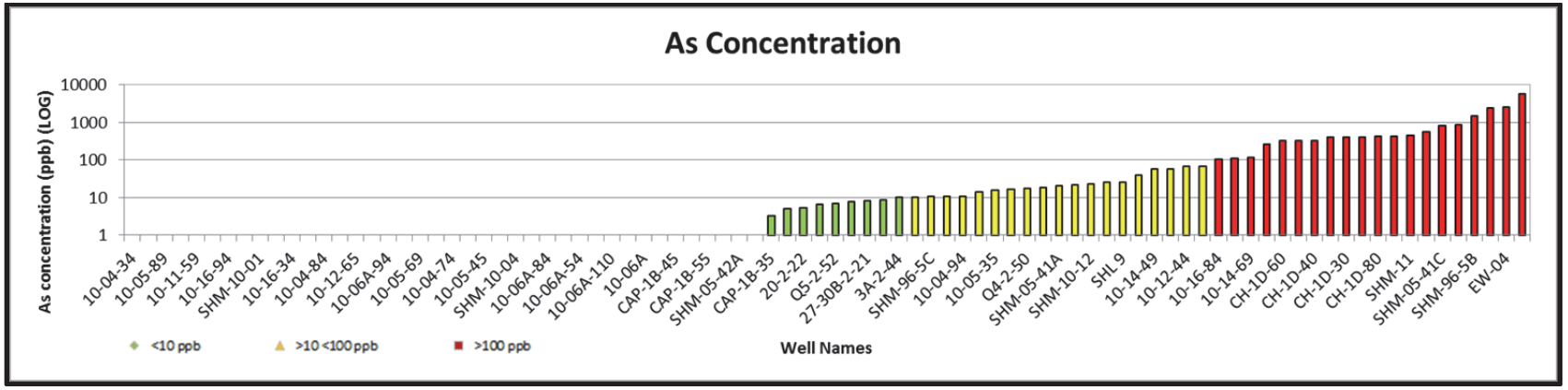

Figure 23 – Arsenic concentration data in order of concentration. The samples are color coded based on their As concentration values. Any sample with an As concentration less than 10 ppb or below instrument detection limit is categorized green. Any As concentration greater than 10 ppb but less than 100 ppb is categorized as yellow. Any concentration higher than 100 ppb is red. The names of the all wells are not included in this chart due to chart size however, it corresponds with the well names from *Table 5*.

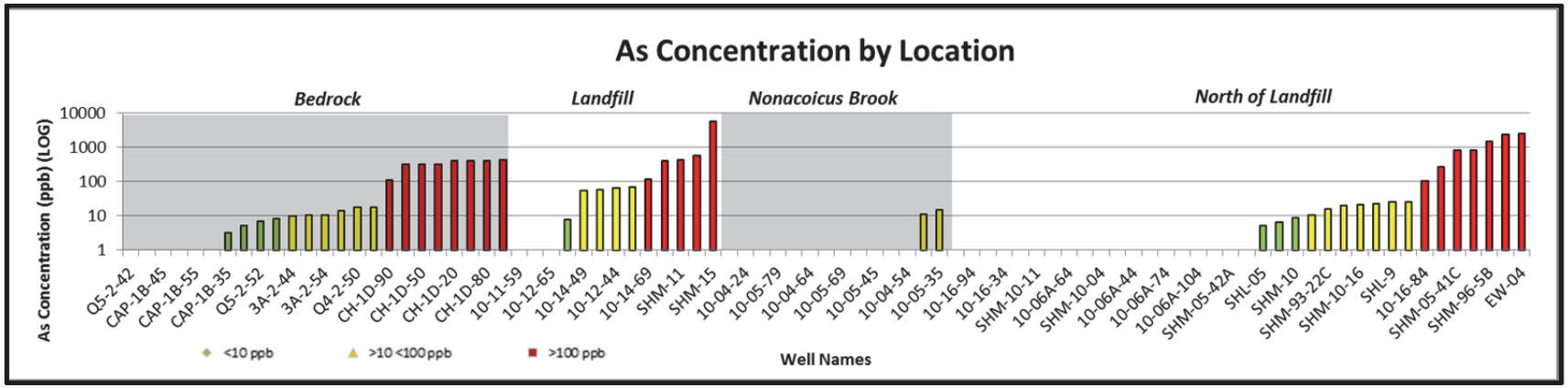

Figure 24 – Arsenic concentration data categorized by location. The samples are color coded based on their As concentration values stated in *Figure 23*. The names of the wells are not included in this chart due to chart size however, it corresponds with the well names from *Table 5*.

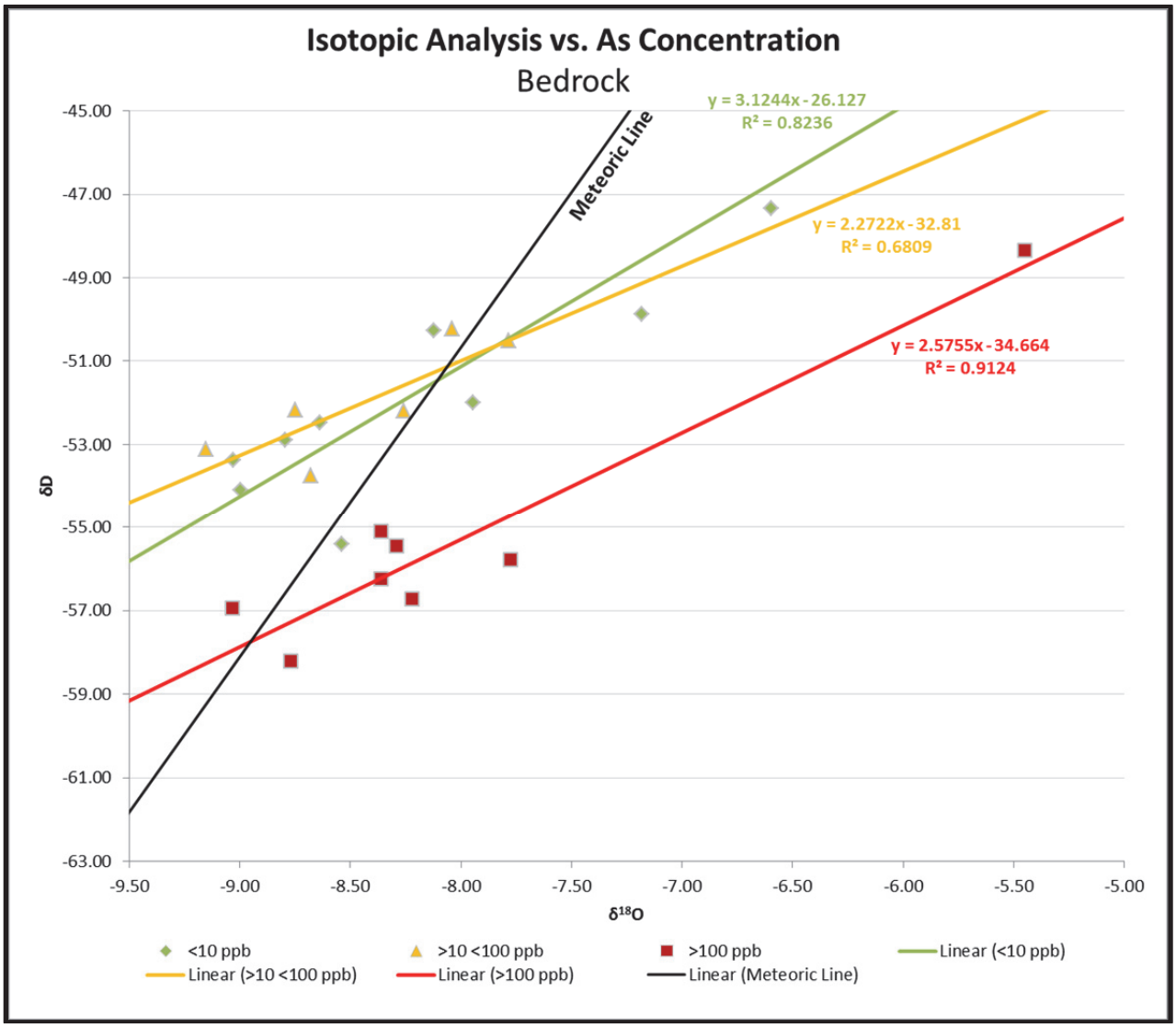

*Figure 25*a – Integration of arsenic color categorization with isotopic composition values for a) Bedrock, b) Landfill, c) North of landfill, d) Nonacoicus Brook. The high and low As concentration slopes indicate the average shift in isotope fractionation. Dashed lines represent average δD and δ18O values amongst high and low As concentrations.

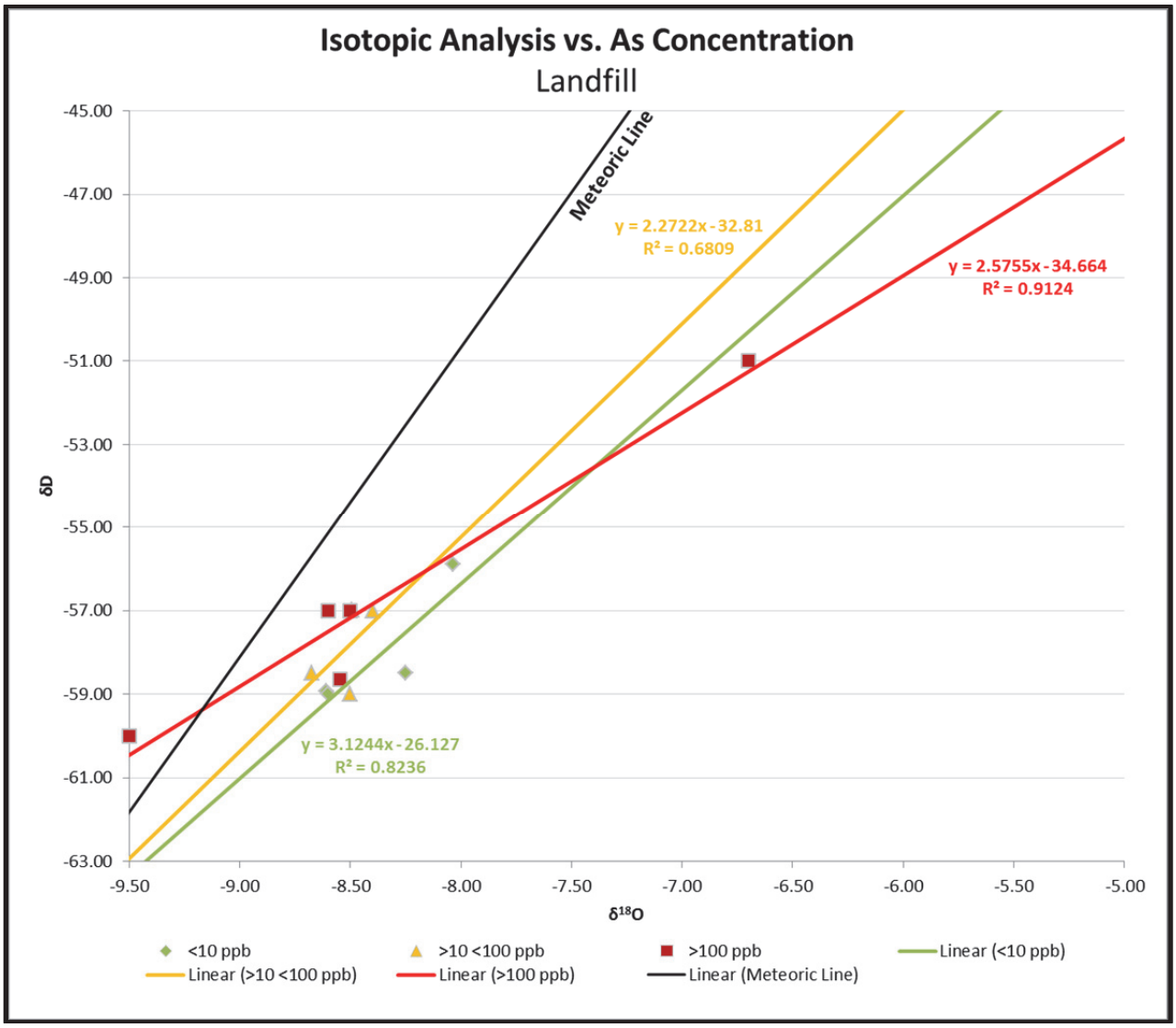
Isotopic Analysis vs. As Concentration
Landfill
Meteoric Line
y = 2.2722x - 32.81
R² = 0.6809
y = 2.5755x - 34.664
R² = 0.9124
y = 3.1244x - 26.127
R² = 0.8236
δD
δ18O
-45.00
-47.00
-49.00
-51.00
-53.00
-55.00
-57.00
-59.00
-61.00
-63.00
-9.50
-9.00
-8.50
-8.00
-7.50
-7.00
-6.50
-6.00
-5.50
-5.00
<10 ppb
>10 <100 ppb
>100 ppb
Linear (<10 ppb)
Linear (>10 <100 ppb)
Linear (>100 ppb)
Linear (Meteoric Line)

*Figure 25*b.

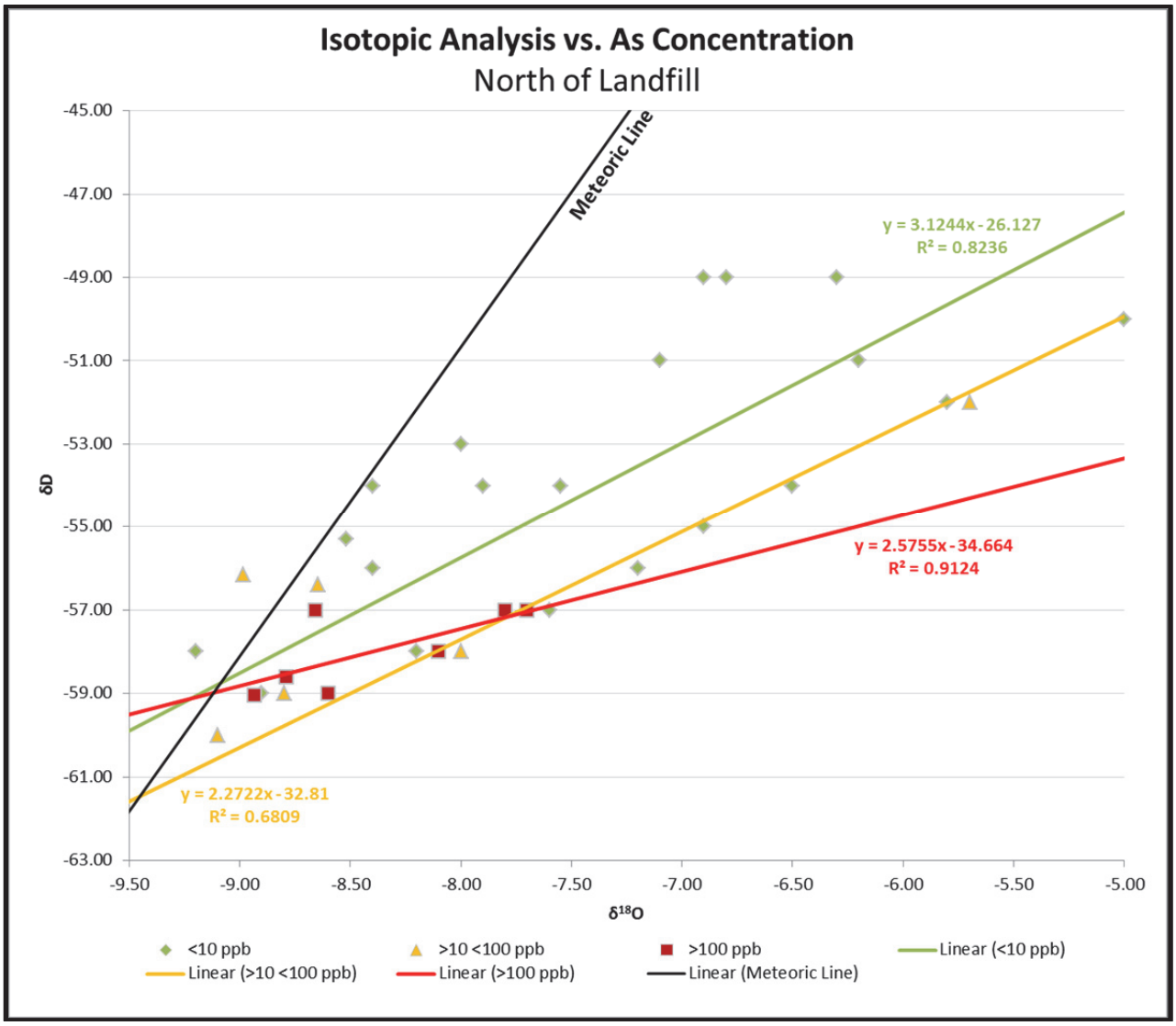
Isotopic Analysis vs. As Concentration
North of Landfill
Meteoric Line
y = 3.1244x - 26.127
R² = 0.8236
y = 2.5755x - 34.664
R² = 0.9124
y = 2.2722x - 32.81
R² = 0.6809
δD
δ18O
-45.00
-47.00
-49.00
-51.00
-53.00
-55.00
-57.00
-59.00
-61.00
-63.00
-9.50
-9.00
-8.50
-8.00
-7.50
-7.00
-6.50
-6.00
-5.50
-5.00
<10 ppb
>10 <100 ppb
>100 ppb
Linear (<10 ppb)
Linear (>10 <100 ppb)
Linear (>100 ppb)
Linear (Meteoric Line)

*Figure 25*c.

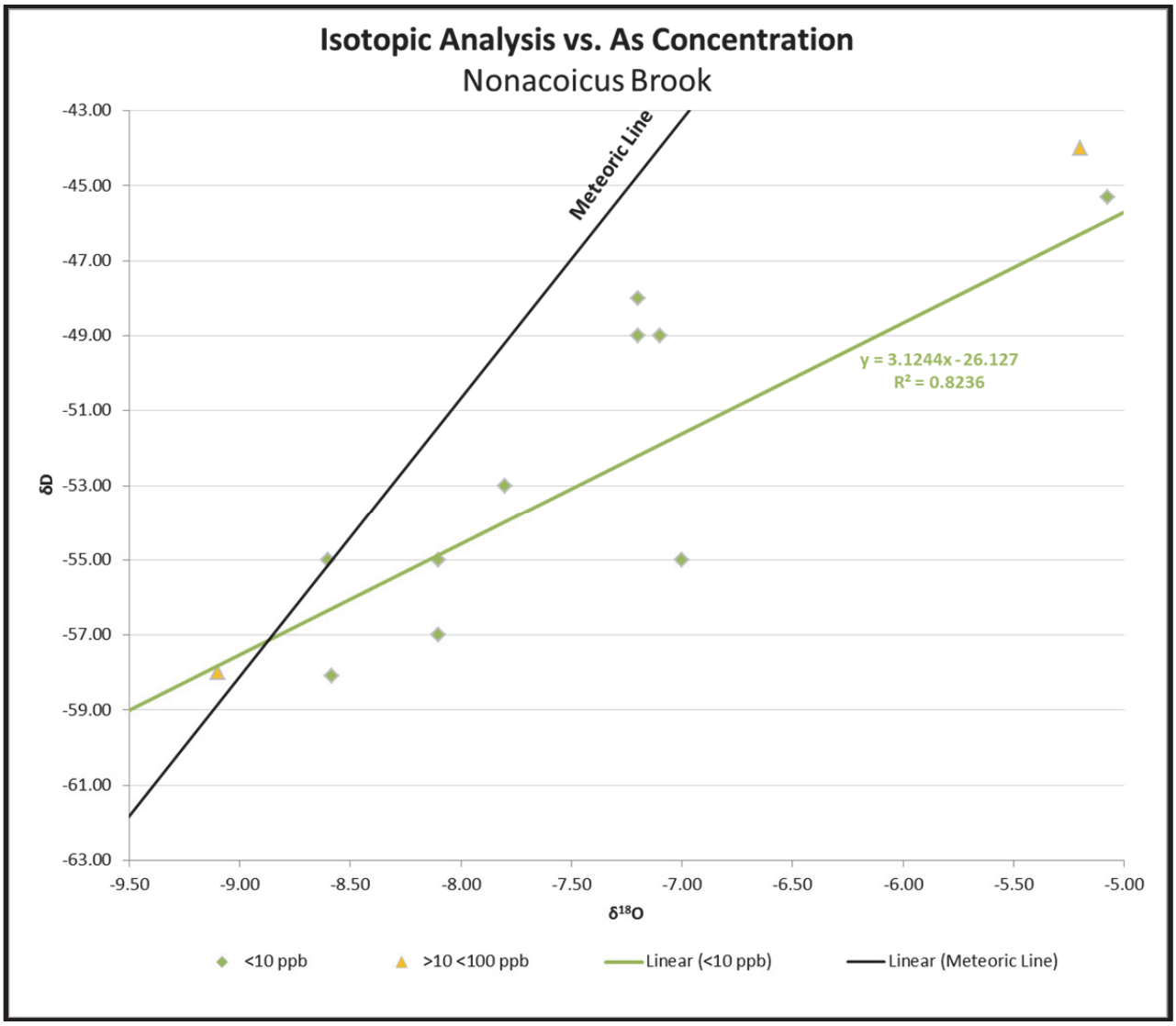
Isotopic Analysis vs. As Concentration
Nonacoicus Brook
Meteoric Line
y = 3.1244x - 26.127
R² = 0.8236
δD
δ18O
-43.00
-45.00
-47.00
-49.00
-51.00
-53.00
-55.00
-57.00
-59.00
-61.00
-63.00
-9.50
-9.00
-8.50
-8.00
-7.50
-7.00
-6.50
-6.00
-5.50
-5.00
<10 ppb
>10 <100 ppb
Linear (<10 ppb)
Linear (Meteoric Line)

*Figure 25*d.

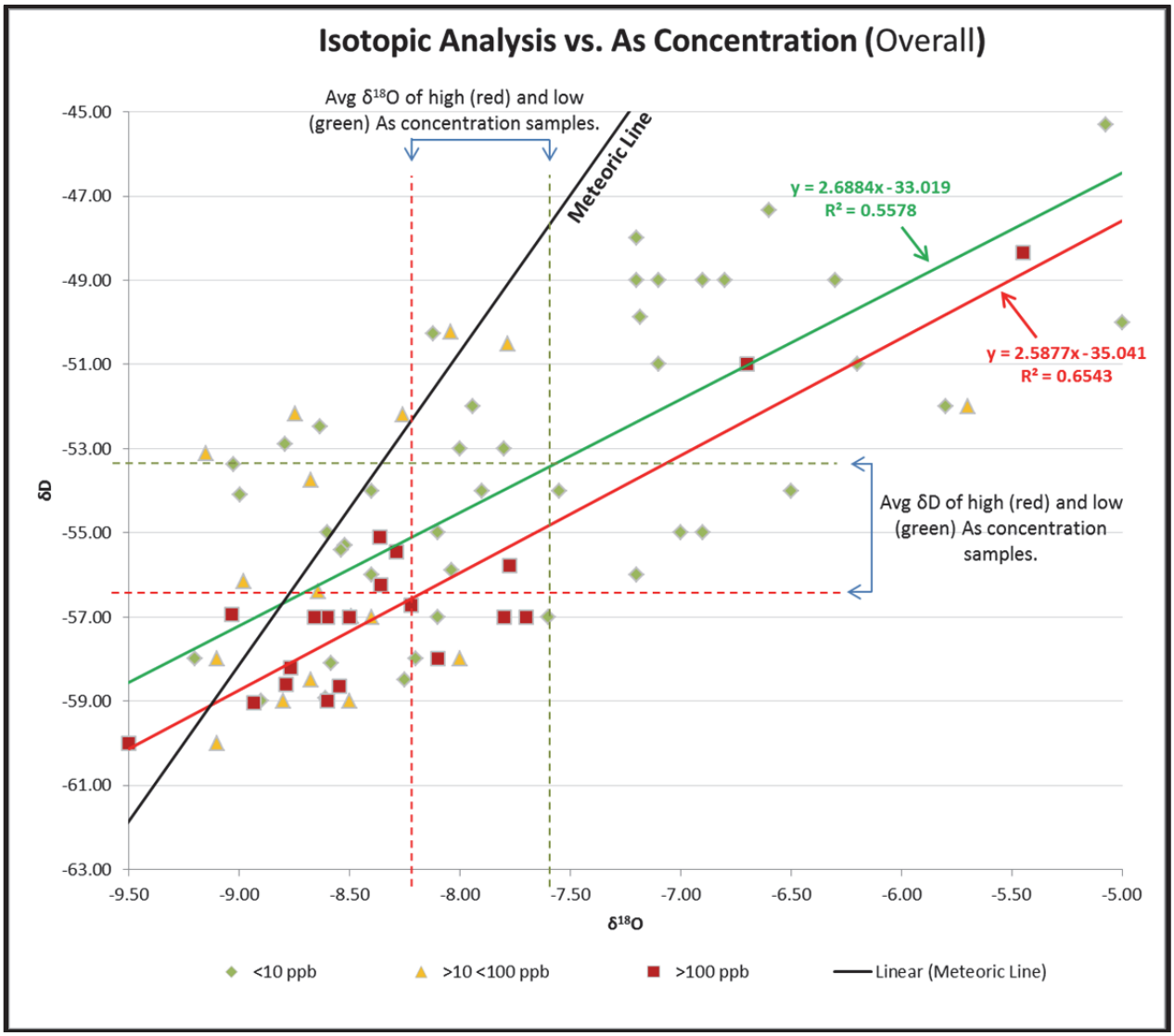

Figure 26 – Integration of arsenic color categorization with isotopic composition values. The high and low As concentration slopes indicate the average shift in isotope fractionation. Dashed lines represent average δD and $\delta^{18}O$ values amongst high and low As concentrations.

6.4.1 Vertical profiles: Isotopic composition vs. Hydrogeochemical Analysis

To see if locations of geochemical change truly influence isotopic composition of water samples, there has been enough sampling on certain wells to produce vertical profiles. *Figure 27*(a – l) shows a comparison of the isotopic composition of water samples from wells to their hydrogeochemical compositions over a range of depths. In this case, the δD and $\delta^{18}O$ values are plotted separately over depth. The direct

relationship between δD and $\delta^{18}O$ can still be seen clearly in every plot. The relationship between the isotopic composition and As concentration varies amongst well and depth.

*Figure 27*b shows a correlation between isotope signature (b1) and As concentration (b2) at 80ft. As the As concentration increases, both δD and $\delta^{18}O$ values seem to change toward heavier isotopes. This pattern can also be seen in *Figure 27*d and *Figure 27*g. The As concentration in (d) is very low and the pattern is not as distinguishable as in (g) and (b). This correlation toward heavier isotopes when there is an increase in As concentration in *Figure 27*b seems to deplete PO_4^{3-} and SO_4^{2-} and increase Mn (b3 & b4) directly below the high As concentration (at 90ft). *Figure 27*d does not seem to have any other changes corresponding with the increase in As and heavier isotopes. *Figure 27*g shows a huge change in metal concentration juxtaposing an increase in As concentration. There is a huge increase in Fe, NO^{3-}, Zn and F concentration at the same depth where there is a reduction in Cl, Ca, Na, and Mn.

In other wells, there are no significant correlation between the isotopic composition and the As concentration. *Figure 27*(a, f, i, j, k) shows an increase in As concentration at certain depths, however the increase is not evident in the isotopic analysis. There is an increase in heavier isotopes in *Figure 27*f at 74ft that shows a corresponding increase in Br, F, Cl, and Na and a decrease in Ca. However, there is no As present at that location. The increase in As at 94ft corresponds with an increase in nearly all mineral concentrations however does not correlate with the change in isotopic signature that occurs at 74ft. *Figure 27*k shows no correlation between the increase in As at 79 ft, isotopic signature, and other geochemical attributes.

SHM-10-16 (*Figure 27* (l)) shows an interesting pattern where the increase in As concentration at 85 ft produces isotopically lighter oxygen and hydrogen. This trend is inversely proportional to trends found in (b), (d), and (g) where there is a decrease in light isotopes. Other geochemical data shows fluctuations of concentrations throughout the vertical profile. However, higher concentration molecules such as Cl, Ca, and SO_4^{2-} decrease at 85ft, in conjunction with an increase in Mg.

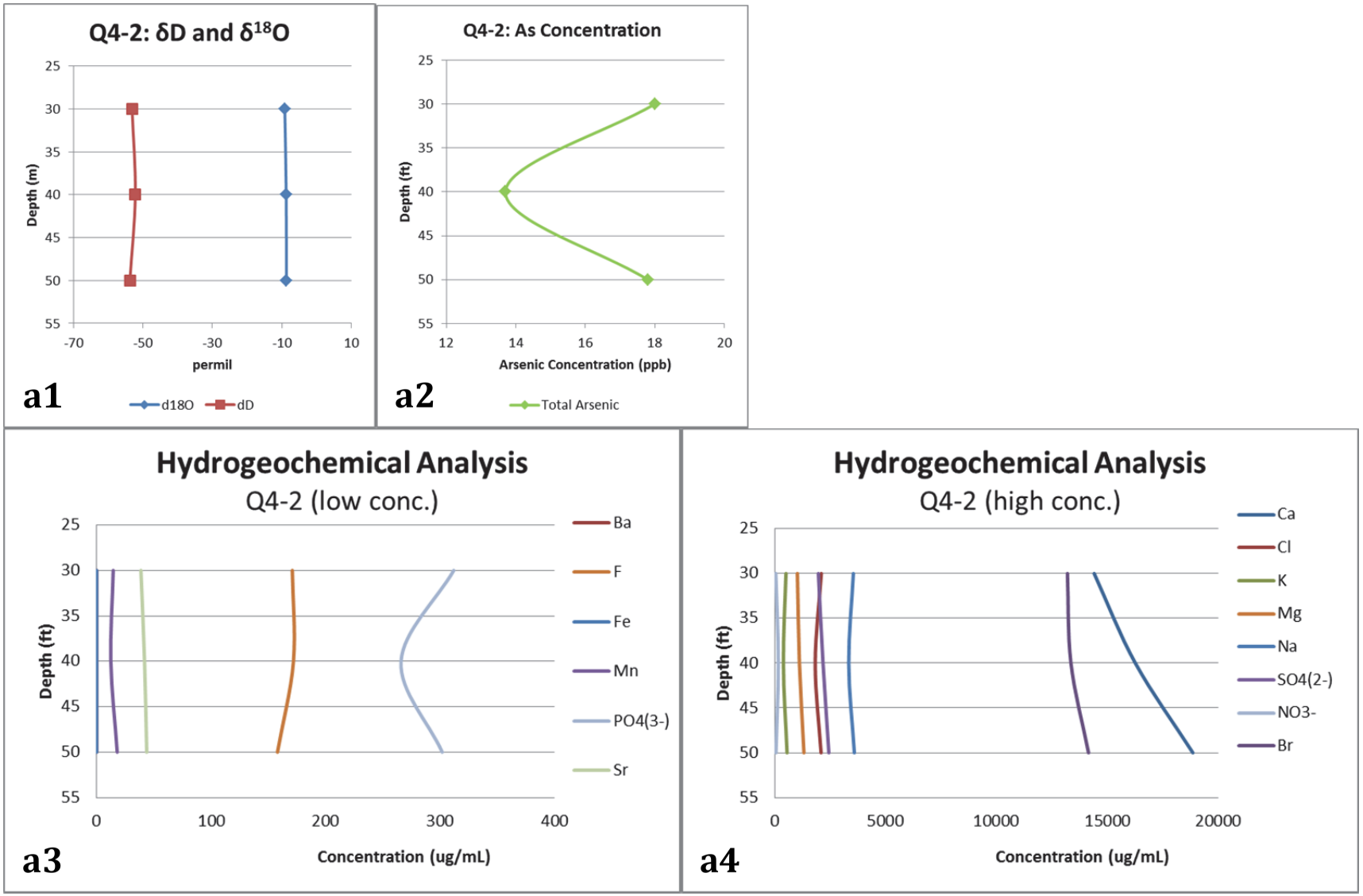

*Figure 27*a(1-4) – Vertical profile of wells comparing isotopic signatures to their corresponding hydrogeochemical signature (based on availability).

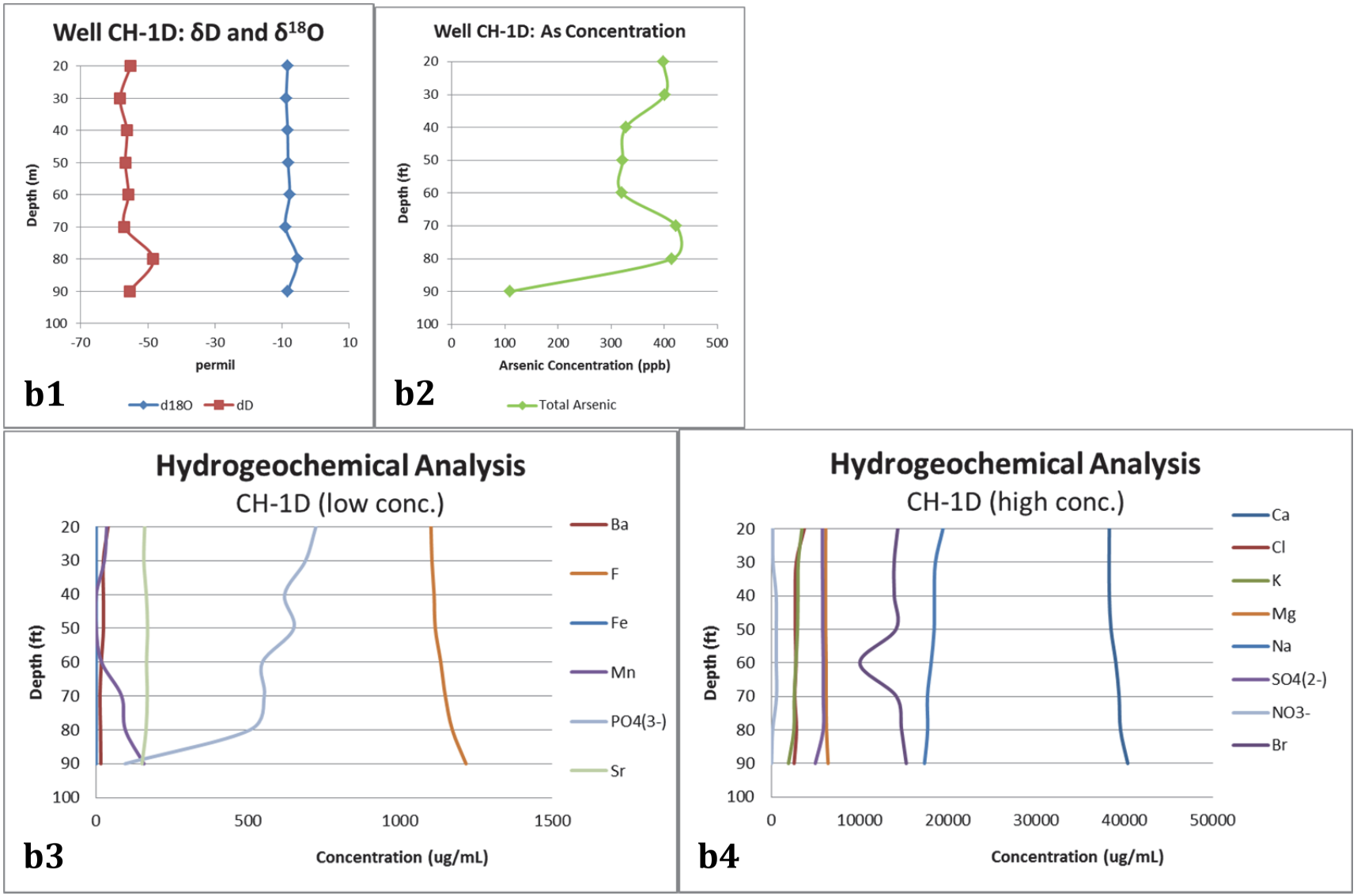

*Figure 27*b(1-4)

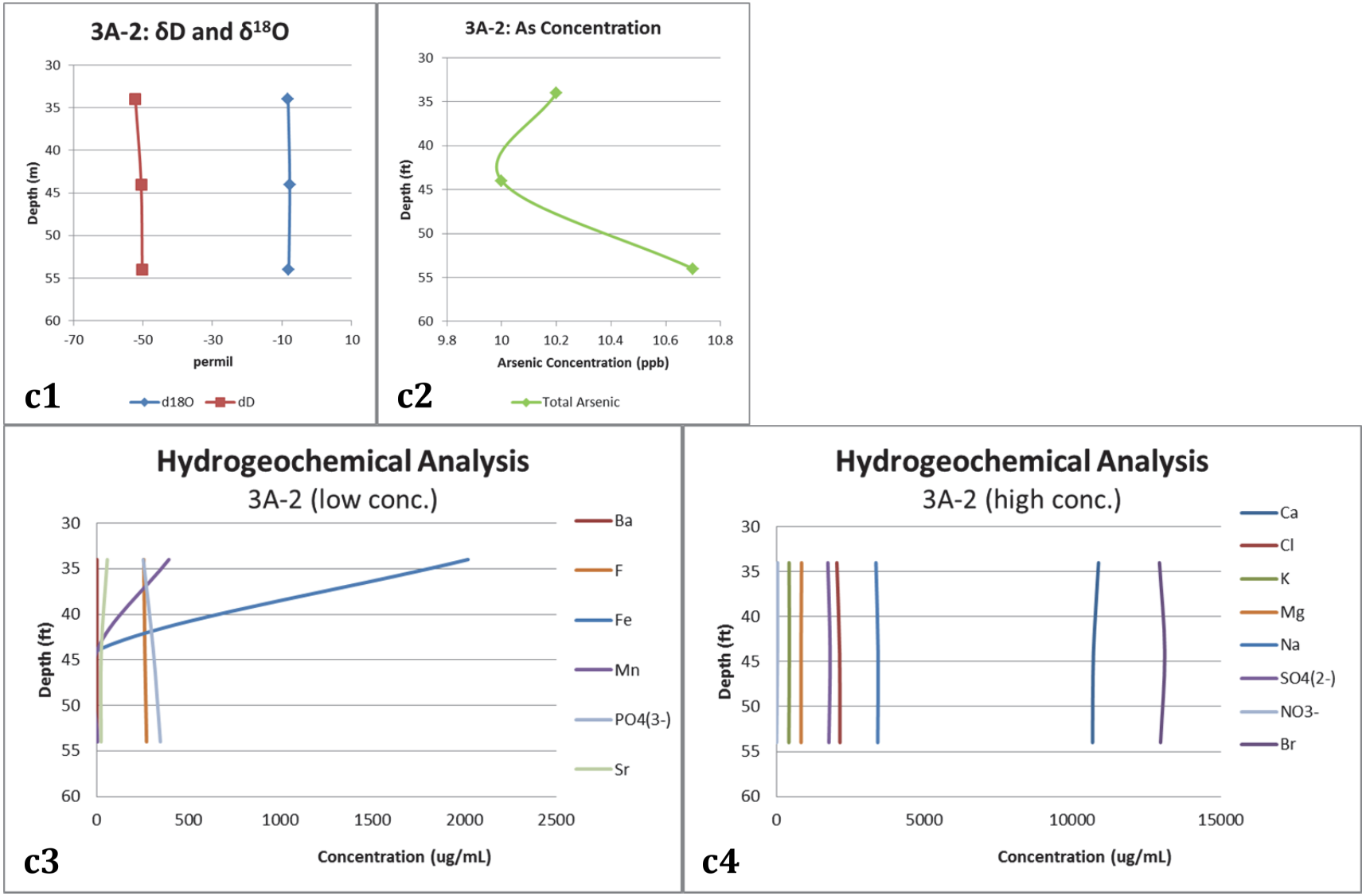

*Figure 27*c(1-4)

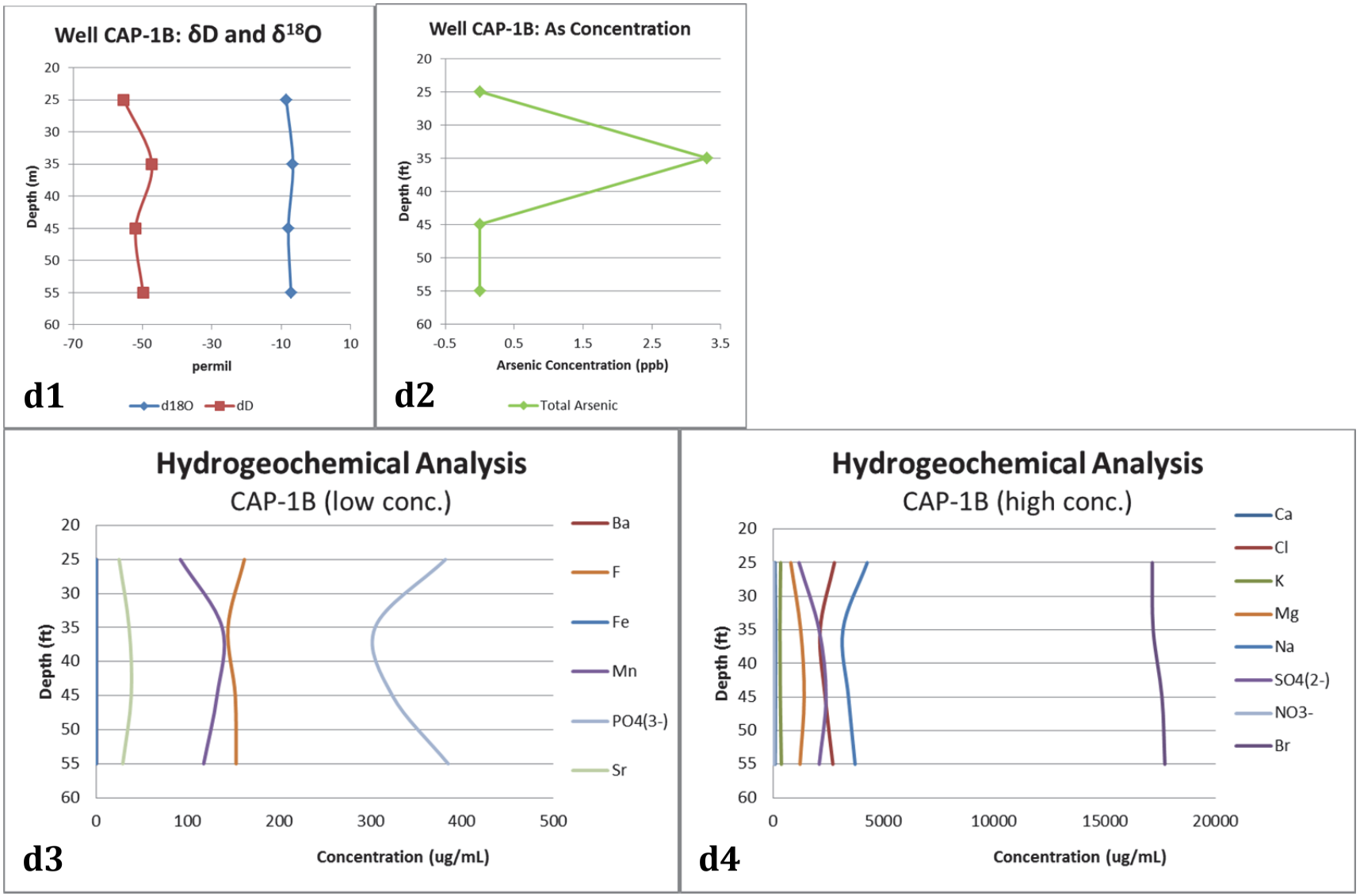

*Figure 27*d(1-4)

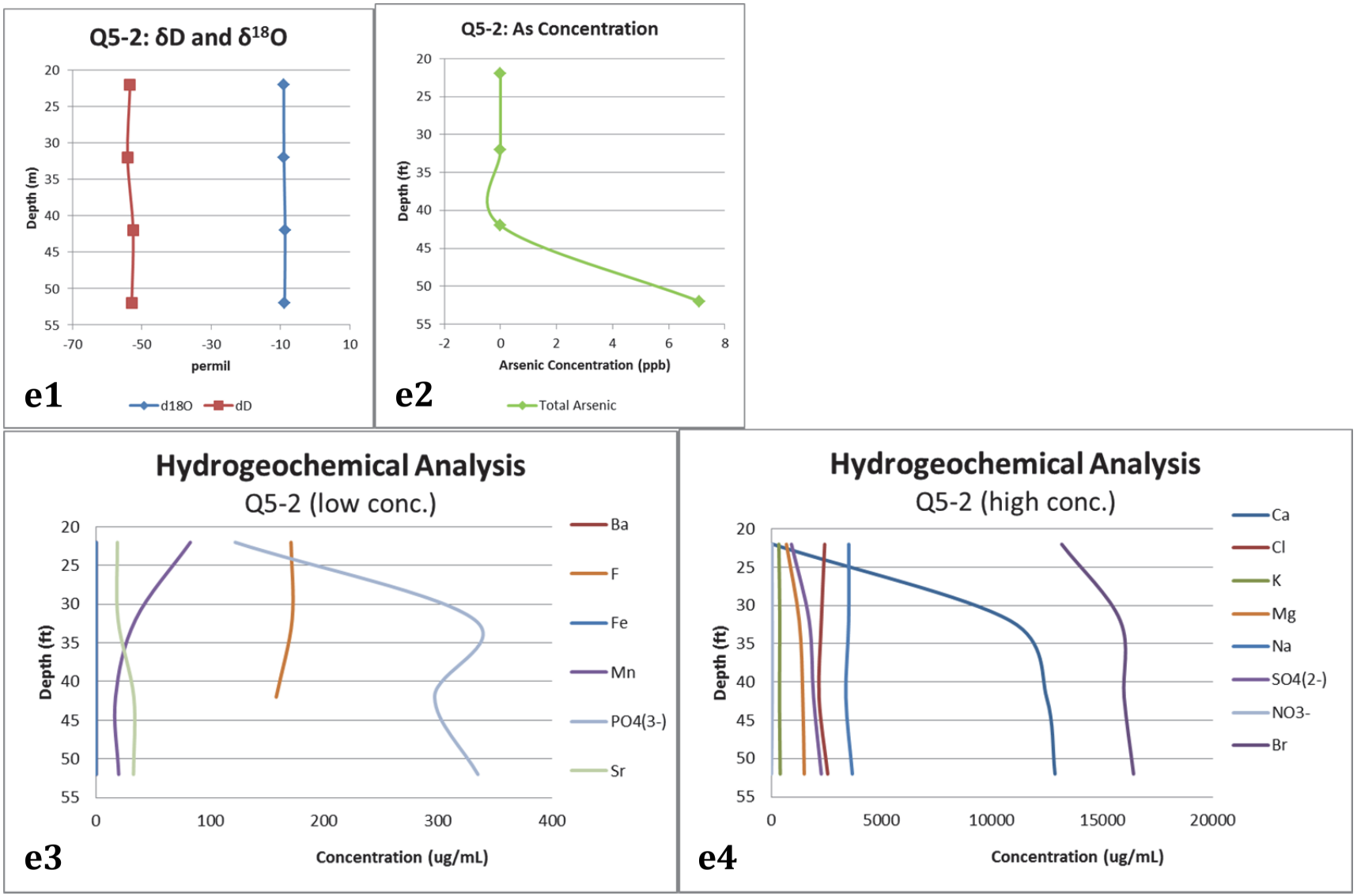

*Figure 27*e(1-4)

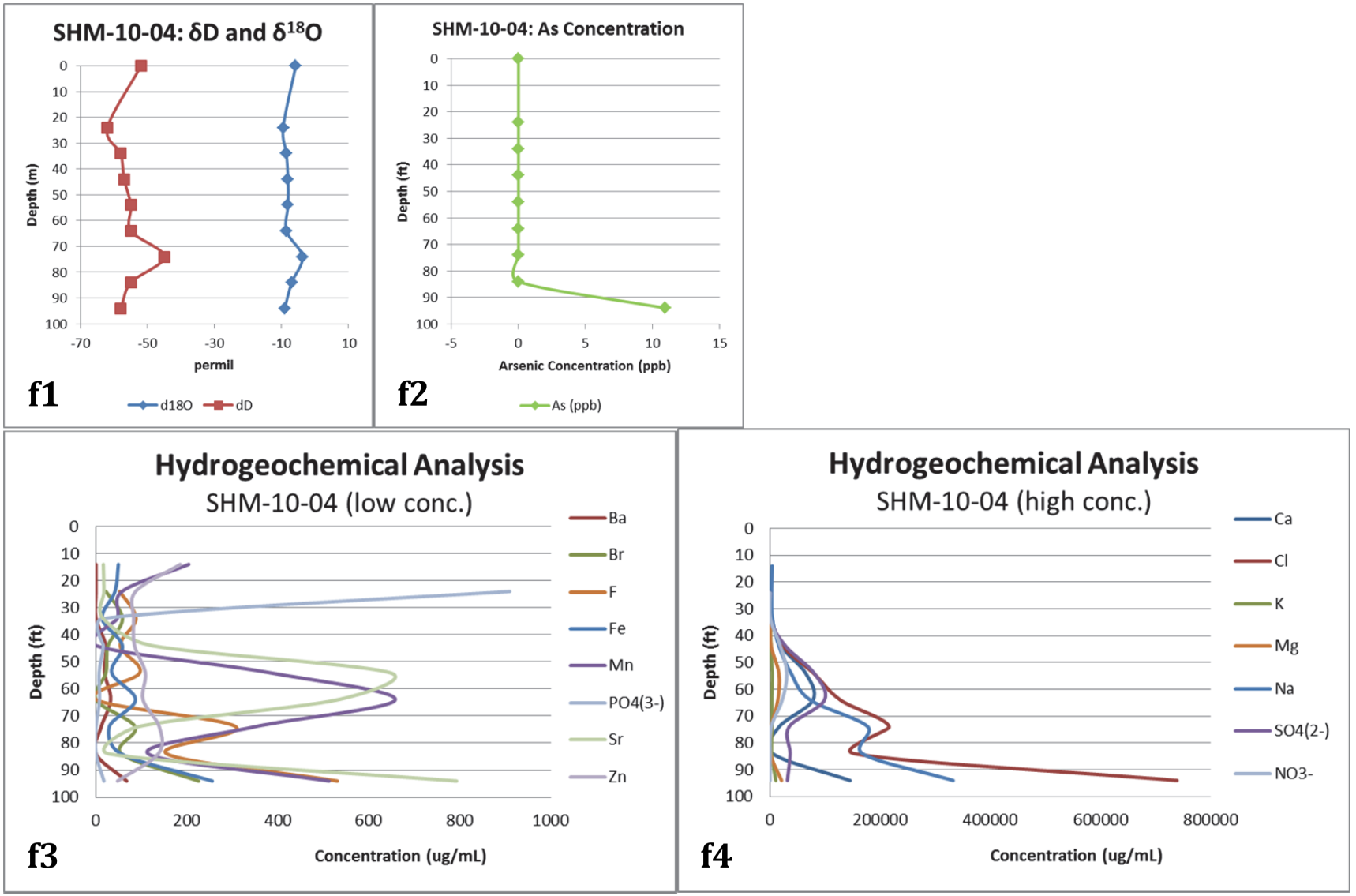

*Figure 27*f(1-4)

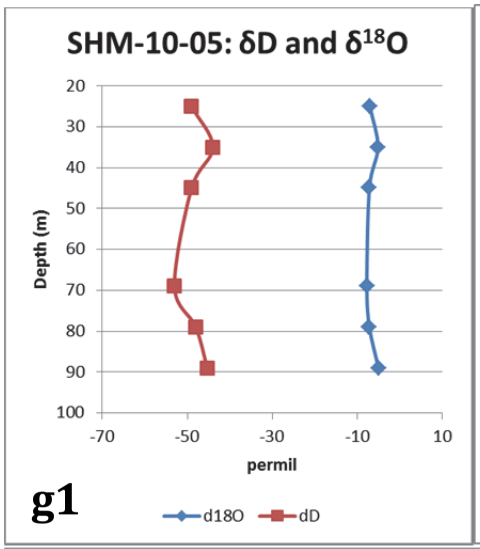

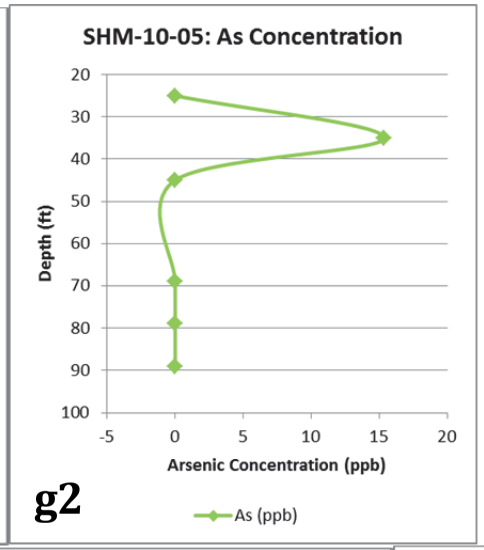

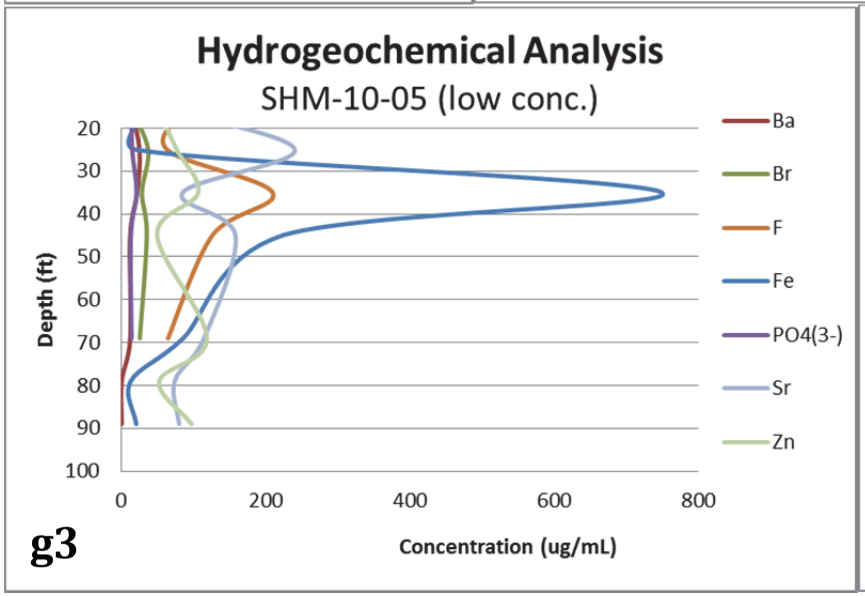

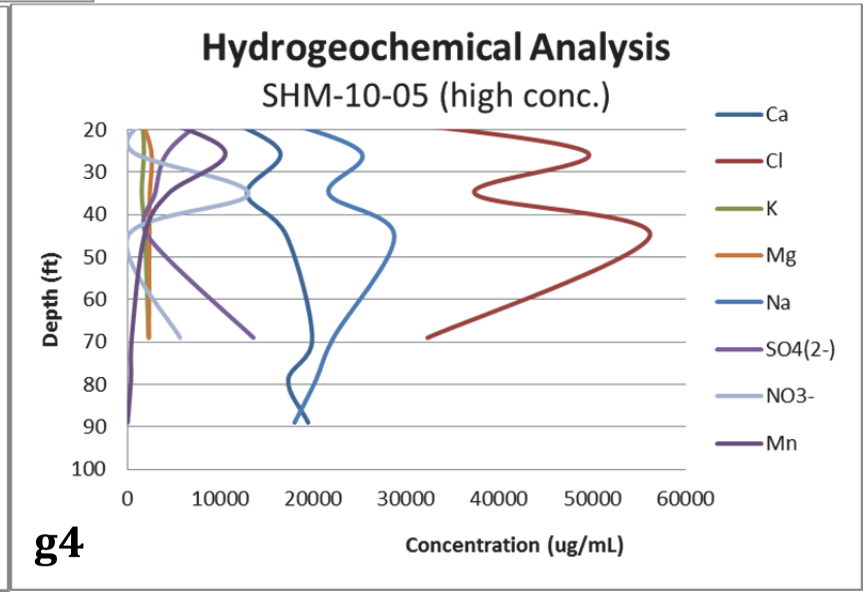

*Figure 27*g(1-4)

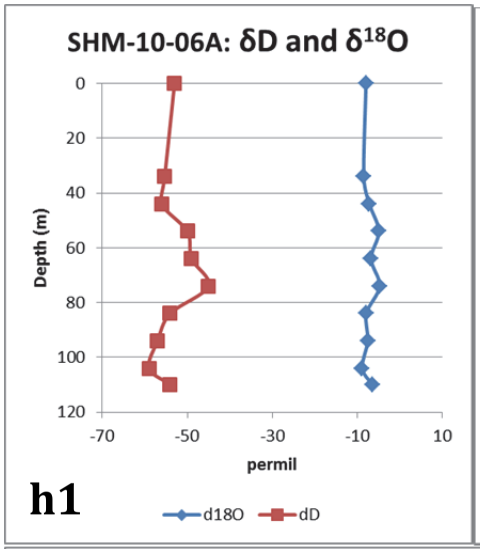

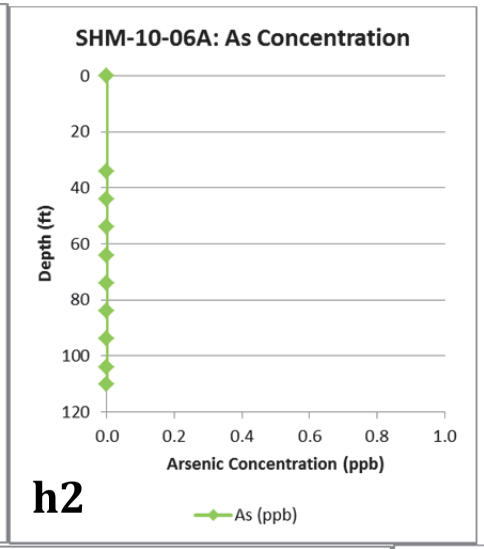

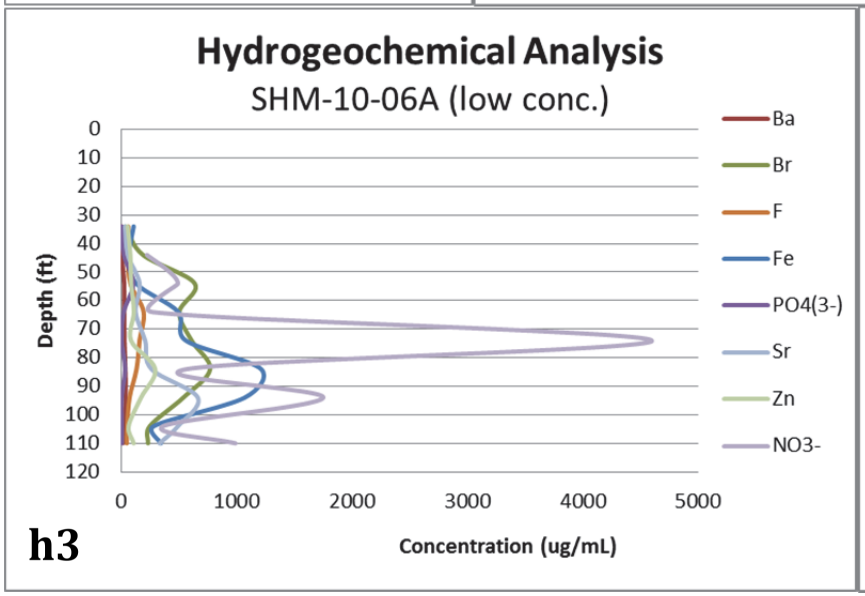

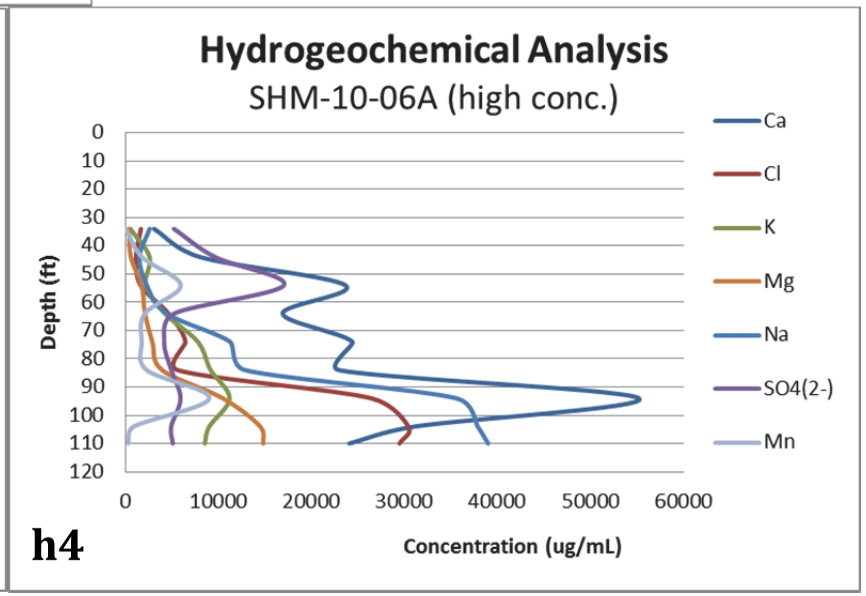

*Figure 27*h(1-4)

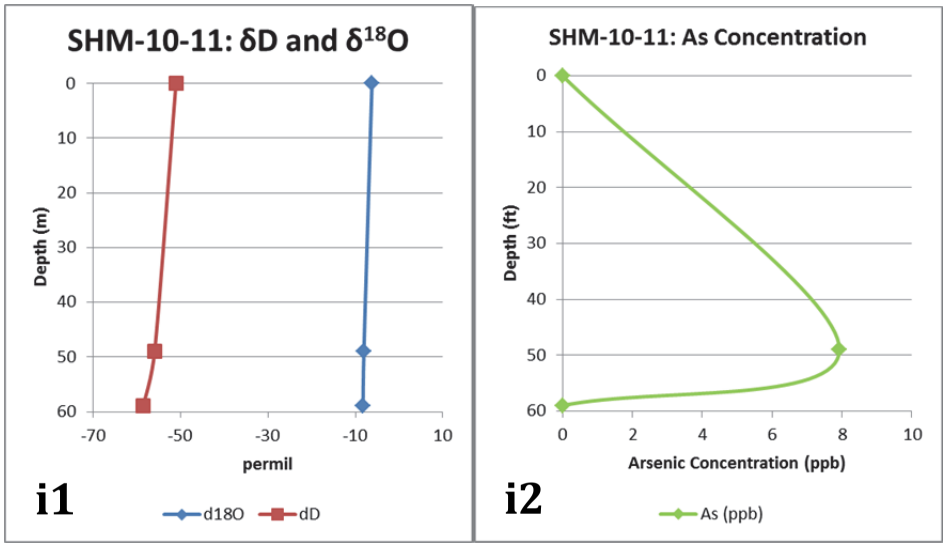

*Figure 27*i(1-2)

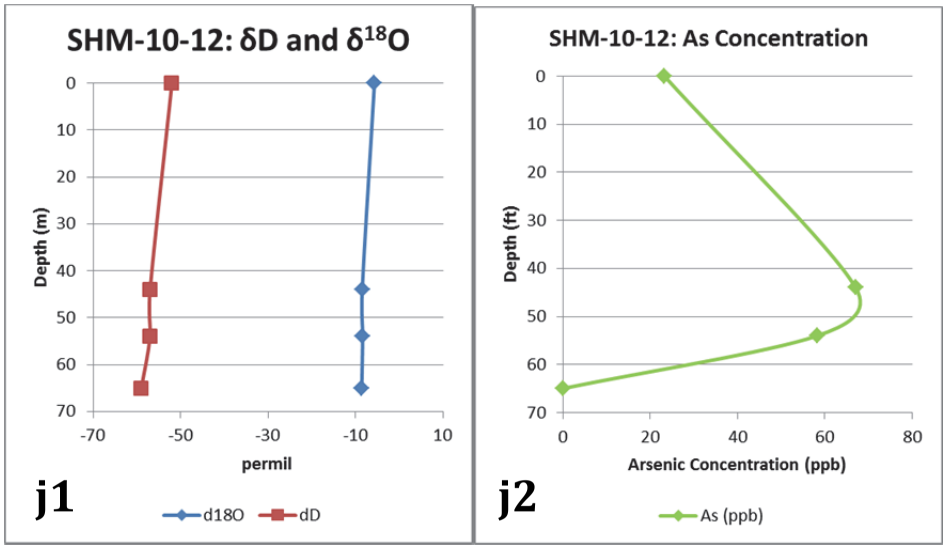

*Figure 27*j(1-2)

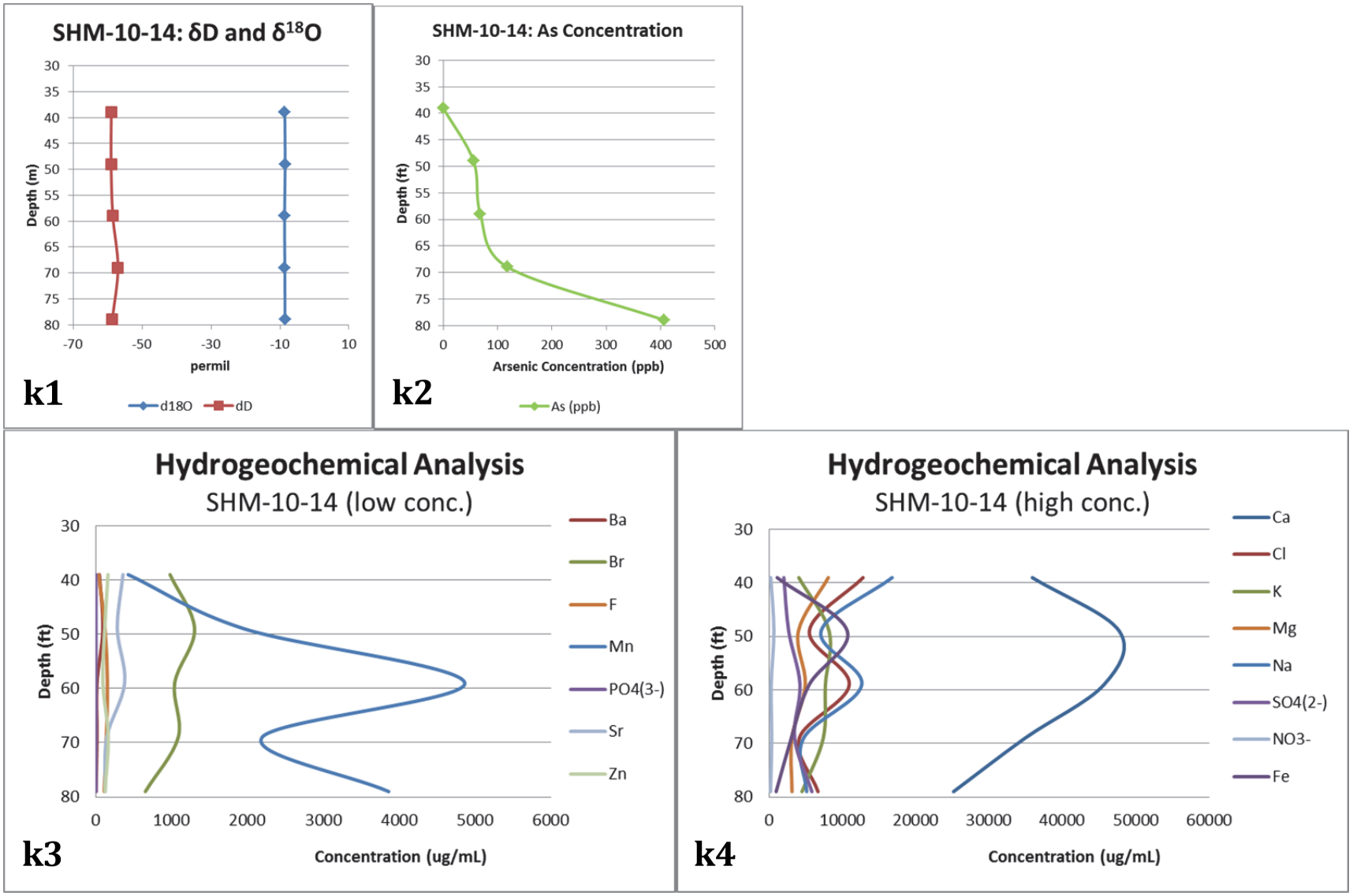

*Figure 27*k(1-4)

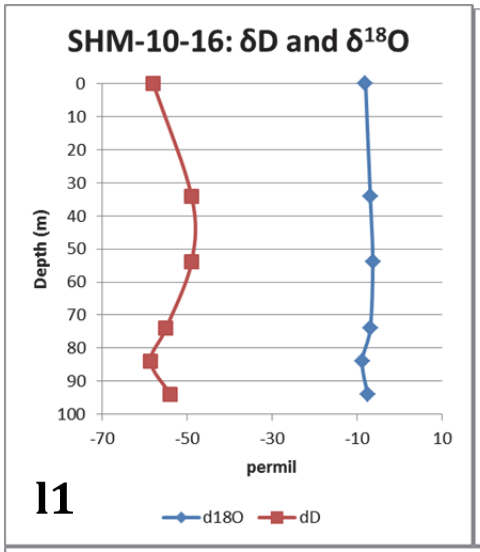

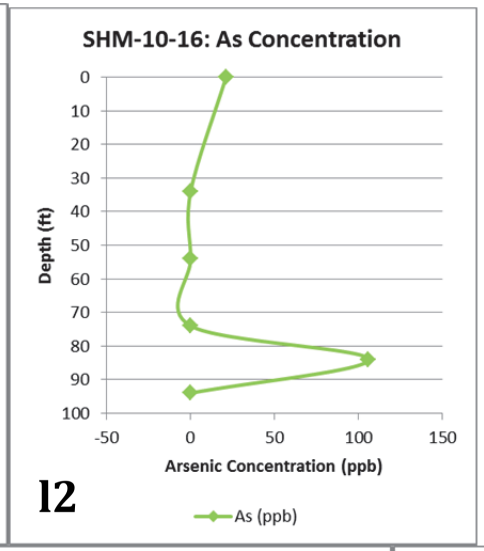

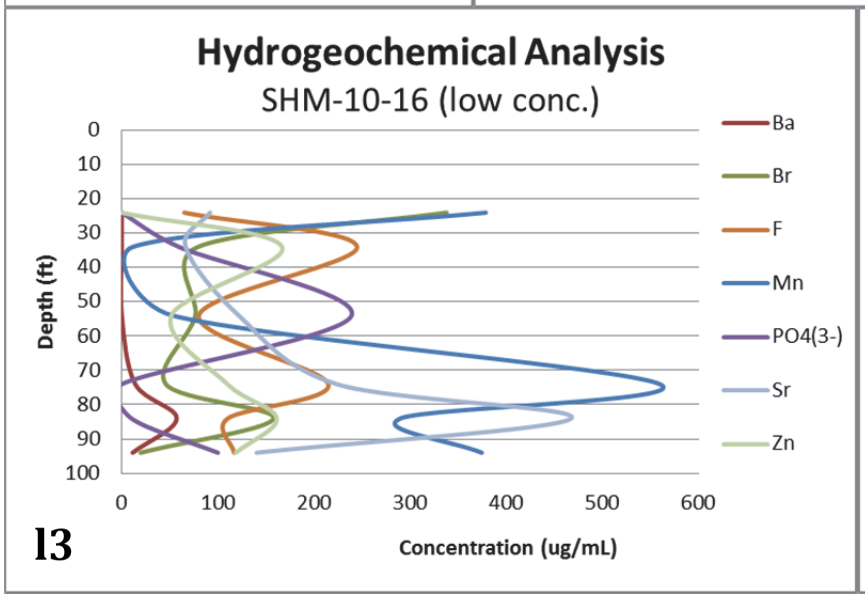

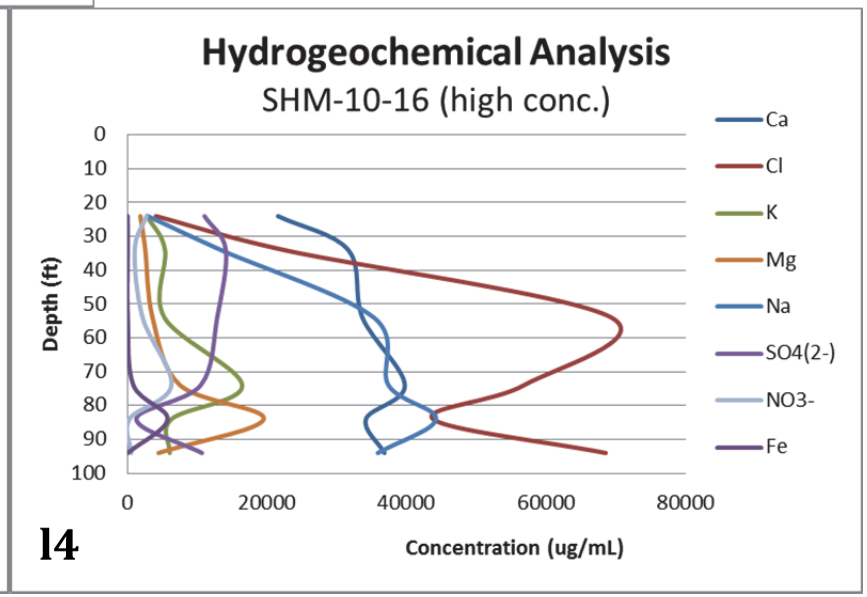

*Figure 27*l(1-4)

6.5 A bench top experiment on anoxic waters

Results from the bench top experiment are displayed in *Table 7*. When graphed, the data shows a slight fractionation in the isotopic signature of the swamp water (*Figure 29*). Overall, the initial oxic water shows to be isotopically lighter in oxygen and hydrogen relative to the average isotopic signatures of groundwater in the region. This is expected since the samples are surface waters that have direct contact with the atmosphere which causes evaporative isotopic depletion. The anoxic data points of Winogradsky column 2 labeled “shallow” and “deep” signify where the water was extracted from within the Winogradsky column. The sample extracted from the near surface (shallow) shows a distinctively different isotopic signature compared to the sample extracted from near the bottom of the column (deep). Generally, the anoxic isotopic signatures show further fractionation of the swamp water toward lighter isotopes.

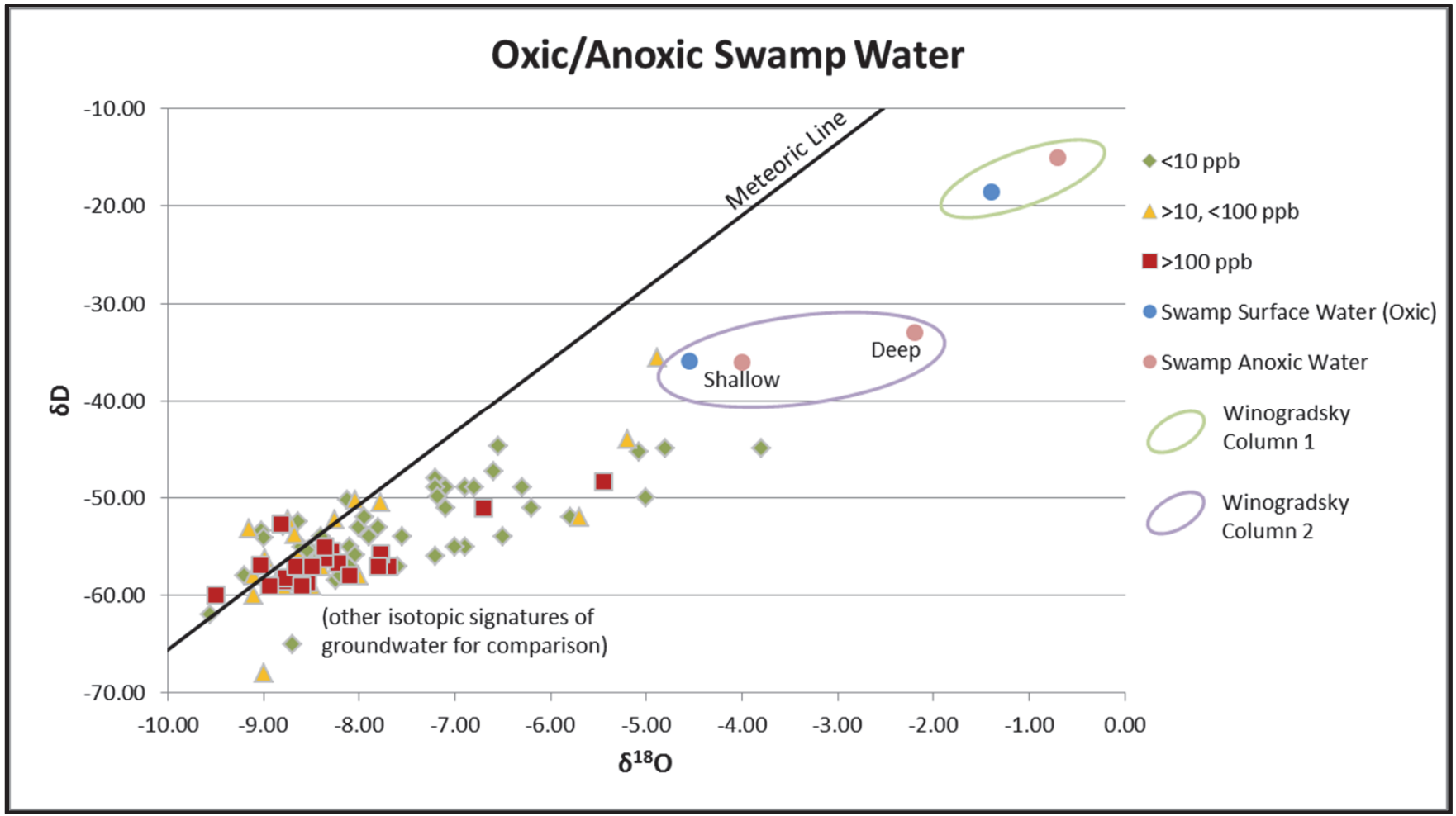

Figure 28 – The isotopic signatures of oxic and anoxic water from the swamp south of SHL. The circles represent data from the same Winogradsky column. The different colored circles represent oxic (blue) or anoxic (red) swamp water.

7. Discussion

7.1 Stable Isotope Analysis

The final compilation and trend of the stable isotope analysis (*Figure 22*) shows that certain regions experienced different physicochemical processes relative to other regions. North of landfill, Nonacoicus Brook, and the landfill itself experienced trends of isotope fractionation similar to each other when compared to the samples south of the landfill and bedrock wells. Assuming that rainwater did not undergo physicochemical changes before entering into groundwater, this is due to these regions experiencing similar meteorological conditions at the time regional rainwater entered groundwater.

Nonacoicus Brook samples produce the steepest slope and lowest y-intercept. Since all the samples south of the landfill were collected using either push point or a simple syringe, the majority of the fractionation is due to waters undergoing evaporation before samples were collected. The bedrock is highly fractured with one major fault that is known to transport groundwater at greater depths. The fault zone which extends from the northwest to southeast (*Figure 4*) has low hydraulic conductivity, most likely containing very aged groundwater. Since the fault zone provides access to water from remote aquifers, the bedrock groundwater may have also originated from a different location. This can explain the unique slope of the bedrock isotopic signature relative to other areas.

7.2 Meteoric Water Line

Figure 21 shows all isotopic samples from area 1 through 5 plotted with the SPATIAL interpolated MWL. Besides bedrock groundwater, the hydrology around SHL should only collect rainwater from its own watershed. This implies that all local water, should it undergo physicochemical changes, should always fractionate away from the

MWL. However, based on the isotopic analysis, a majority of the samples do not begin fractionation at the MWL. This either indicates an unrelated physicochemical change to the water before entering into groundwater or that the SPATIAL meteoric water line can possibly be unreliable. The change in meteoric water can be due to local elevational variability and meteorological turbulence that is undetected by the SPATIAL interpolation.

7.3 $\delta D/\delta^{18}O$ vs. As Concentration

Possible reasons for finding lighter isotopes in groundwater containing high As concentration can be due to insoluble arsenic "selectively" reacting with the groundwater. Under oxic conditions, aqueous As is dominated by arsenate oxyanions ($H_2As(V)O_4^-$ or $HAs(V)O_4^{2-}$ based on pH conditions). Under reducing conditions (lack of oxygen in groundwater), arsenite species ($H_3As(III)O_3^0$) or arsenious acid, predominates due to a reductive dissolution which causes a degradation of dissolved organic carbon in and around the landfill plume, removing oxygen from the water. During this transition, the lighter isotopic molecules of hydrogen and oxygen, due to having a weaker bond with other molecules, can "selectively" react with the insoluble As first to mobilize the arsenic into groundwater. This selective reaction, which populates the groundwater with isotopically lighter molecules, would later be seen in groundwater that contains higher concentration of As.

However, based on the hydrogeochemical analysis on an As contaminated region like SHL, there is no significant trend between high As concentration and the fractionation of stable isotopes of hydrogen and oxygen, both laterally (*Figure 25*a-d) and with depth (*Figure 27*a-l). Furthermore, when comparing the trends found in *Figure 25*a-d to the figure Hackley et al. (1996) created (*Figure 11*), the general trend does not

seem to correlate with previous studied geochemical processes mentioned in the figure. This may be an indication that most fractionation that is occurring around the region is undergoing geochemical changes that do not include hydrogen and oxygen in its reaction. It is also possible that sample fractionation for each site simply reflects meteorological activity and evaporation; not due to one or multiple chemical processes in groundwater. An exception to this conclusion would be a select number of vertical profiles that show changes in locations with high As concentration (discussed below).

7.3.1 Vertical profiles

The available vertical profiles of SHL wells show very little to no trends between isotopic signature and As concentration (*Figure 27*a-l). The small trend in *Figure 27*b & *Figure 27*g) signify that as As concentration increases, both δD and $\delta^{18}O$ values seem to change toward heavier isotopes. Both of the vertical profiles are from the bedrock east of the landfill.

There are two possible explanations to this trend: the water could be undergoing a chemical reaction that are both mobilizing As and using lighter hydrogen and oxygen isotopes during the reaction, and/or there could be an introduction of new As contaminated water into the bedrock from remote sources. A contradicting correlation is found in the SHM-10-16 vertical profile (*Figure 27*l). These subtle changes in isotope values can be due to geochemical reactions that are unrelated to the increase in As concentration, but that preferably utilize lighter isotopes in the reaction process and either mobilize or immobilize the lighter isotopes of hydrogen and oxygen.

Since there are multiple sources that can potentially cause As mobilization (bedrock, glacial deposit, peat layer, and/or landfill), each source might be interacting differently with the groundwater. The increase in As concentration in one area may be

due to a chemical reaction that is causing a shift in isotopic composition toward heavier oxygen/hydrogen. While in another area, the increase in As concentration may be due to a different chemical reaction that is causing a shift in oxygen/hydrogen toward lighter isotopes. There are not enough connections between the physicochemical activities to confidently conclude on one certain process of mobilization.

7.4 Hydrogeochemical Analysis

There are many changes in trace metals that occur when As is mobilized into groundwater. Sulfide concentrations are inversely proportional to As concentration in groundwater since reduction of sulfate generates hydrogen sulfides. Phosphate and manganese concentrations increase since they are adsorbed into the surfaces of hydrous ferric oxides. Certain vertical profiles show these correlations in sulfides (*Figure 27*g, k, l), phosphate (*Figure 27*d, k, l), and manganese (*Figure 27*d, k, l). *Figure 27*l shows all of these processes at work. All other vertical profiles do not (or only partially) follow these processes with increasing As concentration. This indicates the presence of other chemical reactions that can potentially produce more or less trace metals. Since there is very little correlation between As concentration and isotopic signature, we cannot use the hydrogeochemical data to further investigate the isotopic trends found within SHL waters.

7.5 Fractionation behavior of oxic to anoxic water

The results of the oxic to anoxic swamp water analysis do not show an increase in deuterium population which is evident of methanogenic processes. Thus, the fractionation toward lighter δD and $\delta^{18}O$ can signify the presence of a different physicochemical process that occurs in the anoxic phase of redox (i.e. denitrification or manganese reduction) but not anoxic enough to reduce iron or initiate methanogenesis.

The process of fractionation toward heavier isotopes can also be due to evaporation, in which case there was an error in the method of setting up the Winogradsky column.

8. Summary and conclusion

The introduction of unregulated landfills, coupled with growing populations and expanding industries result in an environment where waste disposal regulations are failing to manage the spread of anthropogenic waste. This global issue is causing countries to experience higher contamination levels (including arsenic) due to waste in their groundwater and/or drinking water systems. This further incentivizes the need for international attention and study of groundwater contamination and remediation.

The landfill at Shepley's Hill contains multiple potential sources of arsenic with complex interactions of redox reactions between each potential source. This project investigated the dependency of isotope ratios on As mobilizing reactions during these redox conditions in hopes of back-tracing the contamination to the dominant source of arsenic at the SHL region. 1) A total of 114 samples were collected for the experiment. 2) Isotopic analysis (using IRMS), and 3) hydrogeochemical analysis (using IC and ICP) were done on the samples for their hydrogeochemical properties. Furthermore, 4) the local meteoric water line was investigated for a more accurate reading of the isotopic fractionations. The analyses show that despite various connections between the geochemical composition and As concentration of waters around and within the landfill, there is little to no trend visible between As concentrations and stable isotopic ratios of hydrogen and oxygen. Arsenic concentrations as high as 6000 ppb and lower than instrumental detection levels, both contain similar isotopic ratios of δD and $\delta^{18}O$; signifying that both variables are independent of each other.

Potential re-visitation of this study should be done in a more controlled environment to see if there is a correlation between As concentration and isotopic signature; possibly in a location where there is an already known As source(s) with a

direct redox process causing the As contamination. Isotopic analyses of hydrogen and oxygen juxtaposed with arsenic data has not been previously used as one of the main techniques for finding arsenic sources in landfills. Therefore, finding any potential trends in water contamination based on isotopic data may contribute to possible techniques that can be used to identify and remediate landfill contaminants in the future.

References

Appelo T. *Arsenic in groundwater: A world problem*, Netherlands: Netherlands National Committee of the IAH, 2006. Print.

Ayotte J.D., Nielson M.G., Robinson Jr. G.R., Moore R.B. (1999) Relation of arsenic, iron, and manganese in groundwater to aquifer type, bedrock lithogeochemistry, and land use in the New England coastal basins, *Water Resources Investigations report 99-4162*, Department of Interior United States Geological Survey.

Ayotte J.D., Montgomery D.L., Flanagan S.M., Robinson K.W. (2003). Arsenic in groundwater in eastern New England, *Environmental Science & Technology 37*, 2075-2083.

Ayotte J.D., Riker S.J., Proctor A.L. (2001) Variation in bedrock ground-water arsenic concentrations and implications for human-health studies in New England, Natural Arsenic in Groundwater: Science, Regulation, and Health Implications, Session No. 47.

Bagla P., Kaiser J. (1996) India's spreading health crisis draws global arsenic experts, *Science 274*, 174-175.

Barnard N.Q. (2006) A geochemical, petrologic, and hydrologic investigation of two bedrock arsenic sources, South-Central Maine, B.A. Thesis, Middlebury College, Middlebury, VT, 79pp.

Beckett W.S., Moore J.L., Keogh J.P., Bleecker M.L. (1986) Acute encephalopathy due to occupational exposure to arsenic, *British Journal of Independent Medicine 43*, 66-67.

Bergman I., Lundberg P., Nilsson M. (1999) Microbial carbon mineralization in an acid surface peat: Effects of environmental factors in laboratory incubations, *Soil Biology & Biochemistry 31*, 1867-1877.

Brackley R.A., Hansen B.P., (1977) Water resources of the Nashua and Souhegan river basins, Massachusetts, USGS Hydrologic Investigation Atlas, Department of Interior United States geological Survey.

Bolla-Wilson K., Bleecker M.L. (1987) Neuropsychological impairment following inorganic arsenic exposure, *Journal of Occupational Medicine 29*, 500-503.

Bowen G., *WaterIsotopes.org.* University of Utah. PSI Lab (ISOscapes), Copyright 2003 – 2013. <waterisotopes.org>.

Chakraborti D., Biswas B.K., Chowdhury T.R., Basu G.K., Mandal B.K., Chowdhury U.K., Mukherjee S.C., Gupta J.P., Chowdhury S.R., Rathore K.C. (1999) Arsenic groundwater contamination and sufferings of people in Rajnandgaon district, Madhya Pradesh, India, *Current Science 77*, 502-504.

Craig H. (1961a) Isotopic variations in meteoric waters, *Science 133*, 1833-1834.

Coplen T.B. (1994) Reporting of stable hydrogen, carbon, and oxygen isotopic abundances, *Pure Applied Chemistry 66*, 273-276.

Davidson T. (2003) Arsenic pathways in leachate plumes at five landfill sites in Central Massachusetts, Master's Thesis, Department of Earth and Environmental Science, BC.

Delemos J.L., Bostick B.C., Renshaw C.E., Sturup S., and Feng X.H. (2006) Landfill-stimulated iron reduction and arsenic release at the coakley superfund site (NH), *Environmental Science & Technology 40*, 67-73.

Doherty K., Hon R., Bishop M., Lyons J. (2001) Occurrence of arsenic and lead in unconsolidated soils in central Massachusetts, Northeast Meeting of GSA, Burlington, Vermont.

Doherty K., Hon R. (2002) Naturally occurring arsenic in overburden in central Massachusetts, 18th Annual International Conference on Contaminated Soils, Sediments, and Water, Amherst, Massachusetts.

Doherty K., Hon R. (2003) Redistribution of arsenic in soils by natural hydrogeologic processes, 226th American Chemical Society National Meeting, New York City, NY.

Frank G. (1976) Neurological and psychiatric disorders following acute arsine poisoning, *Journal of Neurology 213*, 59–70.

Gulens J., Champ D.R., Jackson R.E. (1973) Influence on redox environments on the mobility of arsenic in groundwater. In: Rubia, *Chemistry of Water Supply Treatment and Distribution*, Ann Arbor Science Publishers, Ann Arbor, MI, Chapter 4.

Hackley K.C., Liu C.L., Coleman D.D. (1996) Environmental Isotope Characteristics of Landfill Leachates and Gases, *Groundwater 34*, 827-836.

Harding ESE (2002) Draft Shepley's Hill Landfill supplemental groundwater investigation, Devens Reserve Forces Training Area, Devens, Massachusetts, published by Harding ESE.

Harding Lawson Associates, Inc. (2000) Draft Shepley's Hill Landfill supplemental groundwater investigation, Devens Reserve Forces training Area, Devens, Massachusetts, published by Harding ESE.

Hendry M.J., Wassenaar L.I. (1999) Implications of the distribution of δD in pore waters for groundwater flow and the timing of geologic events in a thick aquitard system, *Water Resources Research 35*, No. 2, 1751-1760.

Hopenhayn-Rich C., Biggs M.L., Fuchs A., Bergoglio R., Tello E.E., Nicolli H., Smith A.H. (1996) Bladder cancer mortality associated with arsenic in drinking water in Argentina, *Epidemiology 7*, No. 2, 117-124.

Hon R., Brandon W., Doherty K., McTigue D., Stein C., Bishop M., Lyons J., and Davidson T. (2001a) Geochemical correlations of arsenic in overburden, bedrock, and groundwater: Central Massachusetts, Spring Meeting American Geophysical Union, Boston, Massachusetts.

Hon R., Brandon W., Doherty K., McTigue D., Stein C., Davidson T. (2001b) Arsenic occurrence in regional soils and public water supplies, central Massachusetts, Groundwater Forum: Arsenic in Drinking Water, Devens, Massachusetts.

Hon R., Brandon W., Doherty K., McTigue D., Stein C., Davidson T. (2001c) Arsenic in groundwater, overburden, and bedrock, central Massachusetts, International Conference: Arsenic in Drinking Water; Columbia University, New York City, New York.

Hon R., Brandon W., McTigue D., Stein C., Davidson T. (2002a) Geochemical correlations of arsenic in overburden, bedrock, and groundwater, central Massachusetts, Conference on Arsenic in New England, Manchester, New Hampshire.

Hon R., Brandon W., Stein C., McTigue D., Davidson T. (2002b) Arsenic in Landfill Environments, 18th International Conference on Contaminated Soils, Sediments, and Water, Amherst, Massachusetts.

Hsueh Y.M., Cheng G.S., Wu M.M., Yu H.S., Kuo T.L., Chen C.J. (1995) Multiple risk factors associated with arsenic-induced skin cancer: effects of chronic liver disease and malnutritional status, *British Journal of Cancer 71*, 109-114.

International Atomic Energy Agency (1994) Environmental Isotope Data No. 1-10: World Survey of Isotope Concentration in Precipitation, *IAEA*. http://www-naweb.iaea.org/napc/ih/IHS_resources_gnip.html.

Keimowitz A.R., Simpson H.J., Stute M., Datta S., Chillrud S.N., Ross J., Tsang M. (2005) Naturally occurring arsenic: mobilization at a landfill in Maine and implications for remediation, Applied Geochemistry 20, 1985-2000.

Kirk M.F., Holm T.R., Park J., Jin Q., Sanford R.A., Fouke B.W., Bethke C.M. (2004) Bacterial sulfate reduction limits natural arsenic contamination in groundwater, *Geological Society of America 32*, 953-956.

Komnitsas K., Xenidis A., Adam K. (1995) Oxidation of pyrite and arsenopyrite in sulphidic spoils in Lavrion, *Minerals Engineering 12*, 1443-1454.

Kopera J. (2008) Bedrock geologic map of the area surrounding Shepley's Hill, town of Ayer, MA, USGS.

Korte N.E., Fernando Q. (1991) A review of arsenic (III) in groundwater, *Critical Reviews in Environmental Control 21*, 1-39.

Lipfert G., Reeve A.S., Sidle W.C., Marvinney R. (2006) Geochemical patterns of arsenic-enriched groundwater in fractured, crystalline bedrock, Northport, Maine, USA, *Applied Geochemistry 21(3)*, 528-545.

Langner P., Mikutta C., Kretzschmar R. (2011) Arsenic sequestration by organic Sulphur in peat, *Nature Geoscience 5*, 66-73.

Matusiewicz H., Slachcinski M. (2010) *In situ* vapor generation inductively coupled plasma spectrometry for determination of iodine using a triple-mode microflow ultrasonic nebulizer after alkaline solubilization, *Analytical Methods*, Issue 10, 1592-1598.

Mayo M.J., (2006) Arsenic pathways at landfills: A case study of the Shepleys Hill Landfill, Ayer, Massachusetts, Master's Thesis, *Department of Earth and Environmental Science*, BC.

McArthur J.M., Ravenscroft P., Safiulla S., Thirlwall M.F. (2001) Arsenic in groundwater: Testing pollution mechanisms for sedimentary aquifers in Bangladesh, *Water Resources Research 37*, 109-117.

Moore J.N., Ficklin W.H., Johns C. (1988) Partitioning of arsenic and metals in reducing sulfidic sediments, *Environmental Science & Technology 22*, 432-437.

Morton W.E., Caron G.A. (1989) Encephalopathy: an uncommon manifestation of workplace arsenic poisoning, *American Journal of Independent Medicine 15*, 1–5.

Mukherjee A., Fryar A.E. (2008) Deeper groundwater chemistry and geochemical modeling of the arsenic affected western Bengal basin, West Bengal, India, *Applied Geochemistry 23*, Issue 4, 863-894.

Murunga E., Zawada E.T. (2007) Environmental and occupational causes of toxic injury to the kidneys and urinary tract, *Environmental and Occupational Medicine (4th Edition)*, 800-812.

Onishi H., Sandell E.B. (1955) Geochemistry of arsenic, *Geochimica et Cosmochimica Acta 7*, 1-33.

Pandey P.K., Yadav S., Nair S., Bhui A. (2002) Arsenic contamination of the environment – A new perspective from central-east India, *Environment International 28*, 235-245.

Pearson F. (1983) Isotope techniques in the hydrological assessment of potential sites for the disposal of high-level radioactive wastes Technical report series no.228, International Atomic Energy Agency (IAEA), *Journal of Hydrology 75*, 396-398.

Peters S.C., Blum J.D., Klaue B., Karagas M.R. (1999) Arsenic occurrence in New Hampshire drinking water, *environmental Science and Technology 33*, 1328-1333.

Peters S.C., Blum J.D. (2003) The source and transport of arsenic in a bedrock aquifer, New Hampshire, USA, *Applied Geochemistry 18(11)*, 1773-1787.

Peters S.C., Blum J.D., Karagas M.R., Chamberlain C.P., Sjostrom D.J., (2006) Sources and exposure of the New Hampshire population to arsenic in public and private drinking water supplies, *Chemical Geology 228*, 72-84.

Ratnaike R.N. (2003) Acute and chronic arsenic toxicity, *Postgrad Medical Journal 79*, 391-396.

Robinson P., Goldsmith R. (1991) Stratigraphy of the Merrimack belt, central Massachusetts, in *The bedrock geology of Massachusetts*, U.S. Geological Survey Professional Paper 1366-G, pp. G1-G37.

Rodriguez V.M., Jiménez-Capdeville M.E., Giordano M. (2003) The effects of arsenic exposure on the nervous system, *Toxicology Letters 145*, 1-18.

Rothwell J.J., Taylor K.G., Ander E.L., Evans M.G., Daniels S.M., Allott T.E.H. (2009) Arsenic retention and release in ombrotrophic peatlands, *Science of the total Environment 407*, 1405-1417.

Rothwell J.J., Taylor K.G., Chenery S.R.N., Cundy A.B., Evans M.G., Allott T.E.H. (2010) Storage and behavior of As, Sb, Pb, and Cu in ombrotophic peat bogs under contrasting water table conditions, *Environmental Science & Technology 44*, 8497-8502.

Ryker S.J. (2001) Mapping arsenic in groundwater, *Geotimes 46(11)*, 34-36.

Shotyk W., Cheburkin A.K., Appleby P.G., Fankhauser A., Kramers J.D. (1996) Two thousand years of atmospheric arsenic, antimony, and lead deposition recorded in an ombrotorophic peat bog profile, Jura mountains, Switzerland, *Earth and Planetary Science Letters 145*, Issue 1-4, E1-E7.

Sills M., Peckenham J., Serrell N. (2006) Arsenic & Landfill: Protecting Water Quality, a presentation at Tremont Courtyard, Boston, Massachusetts.

Smedley P.L., Kinniburgh D.G. (2002) A review of the source, behavior and distribution of arsenic in natural waters, *Applied Geochemistry 17*, 517-568.

Smedley P.L., Knudsen J., Maiga D. (2007) Arsenic in groundwater from mineralized Proterozoic basement rock of Burkina Faso, *Applied Geochemistry 22*, Issue 5, 1074-1092.

Smith A.H., Hopenhayn-Rich C., Bates M.N., Goeden H.M., Picciotto I.H., Duggan H.M., Wood R., Kosnett M.J., Smith M.T. (1992) Cancer risks from arsenic in drinking water, *Environmental Health Perspectives 97*, 259-267.

Stuben D., Berner Z., Chandrasekharam D., Karmakar J. (2003) Arsenic enrichment in groundwater of West Bengal, India: geochemical evidence for mobilization of As under reducing conditions, *Applied Geochemistry 18*, 1417-1434.

Tedder N.W., Hon R., Frisch J., Mayo M., Billings J. (2004) Arsenic in municipal solid waste landfills leachate plumes, Central Massachusetts, Northeastern Section (39th Annual) and Southeastern Section (53rd Annual) Joint Meeting.

Thornton, I. (1994) Sources and pathways of arsenic in south-west England: health implications, *Northwood, England: Science and Technology Letters*, 61-69.

U.S. Army Environmental Center (1995) Record of decision: Shepley's Hill landfill operable unit, Fort Devens, Massachusetts, *Army Environmental Center*.

U.S. Environmental Protection Agency (EPA) (2007) Toxicity and Exposure Assessment for Children's Health (Rev), Inorganic Arsenic: TEACH Chemical Summary, EPA, 1-20.

Vuataz F.D., Goff F. (1986) Isotope Geochemistry of Thermal and Nonthermal Waters in the Valles Caldera, Jemez Mountains, Northern New Mexico, *Journal of Geophysical Research 91*, 1835-1853.

Welch A.H., Westjohn D.B., Helsel D.R., Wanty R.B. (2000) Arsenic in groundwater of the United States: occurrence and geochemistry, *Groundwater 38(4)*, 589-604.

Werner R.A., Brand W.A. (2001), Referencing strategies and techniques in stable isotope ratio analysis, *Rapid Communications in Mass Spectrometry 15*, 501–519.

Williams M., Fordyce F., Paijitprapapon A., Charoenchaisri P. (1996) Arsenic contamination in surface drainage and groundwater in part of the southeast Asian tin belt, Nakhon Si Thammarat Province, southern Thailand, *Environmental Geology 27*, 16-33.

Xie Y. (2013) Spatial distribution and pathways of arsenic in Shepley's Hill landfill, Ayer, Massachusetts, Master's Thesis, *Department of Earth and Environmental Science*, BC.

Yan X.P., Kerrich R., Hendry M.J. (2000) Distribution of arsenic(III), arsenic(V) and total inorganic arsenic in porewaters from a thick till and clay-rich aquitard sequence, Saskatchewan, Canada, *Geochimica et Cosmochimica Acta 62*, No. 15, 2637-2648.

Yang Q., Jung H.B., Culbertson C.W., Marvinney R.G., Loiselle M.C., Locke D.B., Cheek H., Thibodeau H., Zheng Y. (2009) Spatial pattern of groundwater arsenic occurrence and association with bedrock geology in Greater Augusta, Maine, USA, *Environmental Science and Technology 43*, 2714-2719.

Zheng Y., Stute M., Geen A., Gavrieli I., Dhar R., Simpson H.J., Schlosser P., Ahmed K.M. (2004) Redox control of arsenic mobilization in Bangladesh groundwater, *Applied Geochemistry 19*, 201-214.